# WORLD METEOROLOGICAL ORGANIZATION

## GLOBAL ATMOSPHERE WATCH

## WORLD DATA CENTRE FOR GREENHOUSE GASES

# WMO WDCGG DATA SUMMARY

## WDCGG No. 29

## GAW DATA

**Volume IV-Greenhouse Gases and Other Atmospheric Gases**

**PUBLISHED BY**
**JAPAN METEOROLOGICAL AGENCY**
**IN CO-OPERATION WITH**
**WORLD METEOROLOGICAL ORGANIZATION**

**MARCH 2005**

# Acknowledgements

The present issue of *Data Summary* was prepared in cooperation with the World Meteorological Organization (WMO) and is based on the efforts of contributors (Appendix: LIST OF CONTRIBUTORS) to the WMO World Data Centre for Greenhouse Gases (WDCGG). These organizations and individuals are involved in observations and research at stations and laboratories which measure greenhouse gases and other atmospheric gases within the framework of the WMO Global Atmosphere Watch (GAW), and other cooperative monitoring and research programmes. The WDCGG thanks all of the organizations and individuals that have submitted data. Some contributors may not be explicitly acknowledged in this publication owing to lack of space, but it should be noted that all of the organizations and individuals that have submitted data to the WDCGG equally contributed to this new issue of *Data Summary*.

# CONTENTS


Page

Summary ..... 1

1. Introduction ..... 3

2. Analysis ..... 4

3. Carbon Dioxide ..... 7

4. Methane ..... 15

5. Nitrous Oxide ..... 21

6. Halocarbons ..... 25

7. Surface Ozone ..... 31

8. Carbon Monoxide ..... 35

9. Nitrogen Monoxide and Nitrogen Dioxide ..... 41

10.Sulphur Dioxide ..... 45

References ..... 49

Appendices ..... 53

CALIBRATION AND STANDARD SCALES ..... 54

LIST OF OBSERVATION STATIONS ..... 62

LIST OF CONTRIBUTORS ..... 69

GLOSSARY ..... 83

LIST OF WMO/ WDCGG PUBLICATIONS ..... 85

# Summary

This issue of *Data Summary* covers the results of basic analyses of greenhouse gas concentrations reported to the WMO World Data Centre for Greenhouse Gases (WDCGG). The observations range from 1968 to 2003, and only data that reached the WDCGG by December 2004 were analyzed. This *Data Summary* includes analyses of the monthly mean concentrations of global, hemispheric and zonal greenhouse and related gases, and provides useful information on the change in concentrations of these gases.

Only monthly mean concentrations were used in the analyses so that data from many observation sites, including a large number of stations in the NOAA flask-sampling network, are included. Of course, it is also appreciated that some stations submit daily and hourly mean concentrations, which may be more appropriate for analyzing the variations on various time-scales. All the submitted data are available on the WDCGG web site (http://gaw.kishou.go.jp/wdcgg.html).

A time series of greenhouse gas concentrations, which is often produced by removing local factors that can vary in a very short time, was made by integrating the variation in concentration on different time scales. The $CO_2$ concentration can be seen on both a seasonal scale and a long-term scale. Annual growth rates are derived from the deseasonalised long-term trend.

The analytical results are summarized below for each greenhouse and related gas:

## 1. Carbon Dioxide ($CO_2$)

The level of Carbon Dioxide ($CO_2$), which of all the greenhouse gases contributes most to global warming, has been increasing since the pre-industrial period. Global mean concentrations have increased annually, and was 374 ppm as of 2002. Concentrations peak in northern high and mid-latitudes, suggesting strong net sources in these areas.

The global growth rate varies significantly interannually and was 1.6 ppm/year on average for the period 1983-2002. The high growth rates in 1983, 1987/1988, 1994/1995, 1997/1998 and 2002 are associated with the warm events of El Niño-Southern Oscillation (ENSO). The anomalously strong El Niño event in 1997/1998 brought about worldwide high increases in 1998. The exceptionally low growth rates in 1992, including negative values for northern high and mid-latitudes, were caused by low global temperatures following the eruption of Mt. Pinatubo in 1991.

Amplitudes of the seasonal cycle are clearly large in northern high and mid-latitudes and small in the Southern Hemisphere. The northern seasonal cycle mainly reflects the seasonal variation in the absorption/emission in the biosphere there, while the southern cycle reflects oceanic variations and biomass burning in addition to the influence of the biosphere. In southern low latitudes, an annual cycle cannot be seen clearly but a semiannual cycle can. This is probably due to two opposing factors—the direct influence of sources and sinks there and the propagation of the out-of-phase seasonal variation from the Northern Hemisphere.

## 2. Methane ($CH_4$)

$CH_4$ is the second most significant greenhouse gas, and its level has been increasing since the beginning of the 19th century. Global mean concentrations reflect an annual increase, and the annual averaged concentration was 1787 ppb in 2003. The annual concentrations peak in the northernmost latitudes and fall toward the southernmost latitudes, suggesting significant net sources in northern latitudes.

The global growth rate was 11 ppb/year on average for the period 1984-1990, but the rates decreased markedly from the 1980s to the 1990s. The global growth rate for 1991-2003 was 5 ppb/year. Growth rates decreased significantly in some years, including 1992, when negative values were recorded in northern high latitudes, and 1996, when growth almost stopped in many regions. However, both hemispheres experienced high growth rates in 1998, caused by an exceptionally high global mean temperature. And the global growth rates decreased to almost zero in 2000-2001.

Monthly mean concentrations have a seasonal variation with high concentrations in winter and low concentrations in summer. Unlike $CO_2$, amplitudes of the seasonal cycle are large for $CH_4$ not only in the Northern Hemisphere but also in southern high and mid-latitudes. In southern low latitudes, a distinct semi-annual component with a secondary maximum in boreal winter overlays the annual component. This is attributed to the large-scale transportation of $CH_4$ from the Northern Hemisphere.

## 3. Nitrous Oxide ($N_2O$)

Nitrous oxide ($N_2O$) is an important greenhouse gas, and its level is increasing on a global scale. Data for $N_2O$ reported to the WDCGG show that concentrations are increasing in both hemispheres. Global mean concentration was 318 ppb in 2003.

## 4. Halocarbons

Halocarbons, most of which are anthropogenic, are effective greenhouse gases and some also act as ozone-depleting compounds. Levels of some halocarbons

(CFCs, etc.) increased in the 1970s and 1980s, but have now almost ceased increasing as a result regulation of production and emission under the Montreal Protocol on Substances that Deplete the Ozone Layer and its Adjustments and Amendments.

Concentrations of CFC-11 peaked around 1992 and then started decreasing. CFC-12 increased slowly, but growth has almost stopped in recent times. CFC-113 growth stopped in the early 1990s, and over the last decade has shown a trend of decreasing slightly. Concentrations of HCFC-141b and HCFC-142b are increasing linearly. Concentrations of $CCl_4$ are decreasing slowly. Concentrations of $CH_3CCl_3$ peaked around 1992 and then clearly started to decrease.

## 5. Surface Ozone ($O_3$)

Ozone ($O_3$) plays important roles in the atmospheric environment through radiative and chemical processes. It absorbs UV radiation in the stratosphere, making a temperature profile, and circulates the atmosphere with its absorbed energy. It also absorbs IR radiation in the troposphere, and is thus one of the greenhouse gases.

Variation in the concentration of $O_3$ near the surface, so-called surface ozone, reflects various processes there. While some of the $O_3$ in the troposphere comes from the stratosphere, the rest is chemically produced there through oxidation of CO or hydrocarbons in the presence of rich $NO_x$.

Many stations at various locations measure the concentration of surface ozone. As the seasonal and interannual variations are relatively large, it is difficult to identify a global long-term trend.

## 6. Carbon Monoxide (CO)

Carbon Monoxide (CO) is not a greenhouse gas, but brings influences the concentrations of greenhouse gases by affecting hydroxyl radicals (OH). Its concentration in northern high latitudes has been increasing since the mid-19th century. The mean global concentration was 98 ppb in 2002. The concentration is high in the Northern Hemisphere and low in the Southern Hemisphere, suggesting substantial anthropogenic emissions in the Northern Hemisphere.

Although the global concentration of CO was increasing before the mid-1980s, the growth stopped or the concentration decreased after then (WMO, 1999a). There was large fluctuation in the growth rate, however, with high positive rates followed by high negative rates in northern latitudes and southern low latitudes from 1997 to 1999. The growth rates in the Northern Hemisphere increased again in 2002.

Monthly mean concentrations show a seasonal variation with large fluctuations in the Northern Hemisphere and small fluctuations in the Southern Hemisphere. This seasonal cycle is driven by industrial emissions, biomass burning, large-scale transportation, and variations in OH concentration which acts as a sink.

## 7. Nitrogen Monoxide (NO) and Nitrogen Dioxide ($NO_2$)

Nitrogen oxides ($NO_x$, i.e., NO and $NO_2$) are not greenhouse gases, but influence concentrations of important greenhouse gases by affecting OH. In the presence of $NO_x$, CO and hydrocarbons are oxidized to produce ozone ($O_3$), which affects the Earth's radiative balance as a greenhouse gas and the oxidization capacity of the atmosphere by reproducing OH.

Most of the stations reporting $NO_x$ data to the WDCGG are located in Europe. $NO_x$ has large temporal and geographic variability, and it is difficult to identify a long-term trend. In Europe, $NO_2$ concentrations are generally higher in southern regions than in northern regions.

## 8. Sulphur Dioxide ($SO_2$)

Sulphur Dioxide ($SO_2$) is not a greenhouse gas but a precursor of atmospheric sulphate ($H_2SO_4$) aerosol. Sulphate aerosol is produced by $SO_2$ oxidation through photochemical gas-to-particle conversion. $SO_2$ has been a major source of acid rain and deposition throughout industrial times.

Most of the stations reporting $SO_2$ data to the WDCGG are located in Europe. Generally, in Europe, $SO_2$ concentrations are higher in southern regions than in northern regions.

# 1. Introduction

Human activities have been shown to have major impacts on the global environment. Since the beginning of the industrial revolution, mankind has increasingly made use of land, water, minerals and other natural resources, and future population and economy growth will result in further increases in our impact on the environment. As the global climate, biogeochemical processes and natural ecosystems are closely interlinked, changes in any one of these systems may affect the others and be detrimental to humans and other organisms. Emissions of man-made gaseous and particulate matter alter the energy balance of the atmosphere, and consequently affect interactions between the atmosphere, hydrosphere, and biosphere. Nevertheless, we do not yet have a sufficient understanding of either the chemical processes that occur within the atmosphere or the interrelationships between the atmosphere, the hydrosphere, and the biosphere. This lack of understanding regarding the chemical processes of the atmosphere and the oceans is due mainly to a paucity of observation data.

The World Meteorological Organization (WMO) launched the Global Atmosphere Watch (GAW) Programme in 1989 to promote systematic and reliable observation of the global environment, including greenhouse gases ($CO_2$, $CH_4$, CFCs, $N_2O$, *etc.*) and other related gases (*e.g.*, CO, $NO_x$, and $SO_2$) in the atmosphere. In October 1990, the WMO established the World Data Centre for Greenhouse Gases (WDCGG) at the Japan Meteorological Agency (JMA) in Tokyo as one of the GAW World Central Facilities to collect, archive, and distribute data regarding greenhouse and related gases in the atmosphere and oceans. In August 2002, the WDCGG took over the role of the Data Centre for Surface Ozone from the Norwegian Institute for Air Research (NILU) and began to collect surface ozone data from a number of observation sites throughout the world participating in GAW and other scientific monitoring programmes (Appendix: LIST OF OBSERVING STATIONS).

With regard to issues involving global warming, the Kyoto Protocol, in which quantified emission limitations and reductions were agreed upon based on the United Nations Framework Convention on Climate Change, came into force in February 2005. Therefore, global observation data and related information regarding greenhouse gases are becoming increasingly important. The WDCGG is required to swifter and smoother exchange of such data.

Since its establishment, the WDCGG has provided its users with data and other information through its regular publications: *Data Report*, *Data Catalogue*, *Data Summary*, and *CD-ROM* (Appendix: LIST OF WMO WDCGG PUBLICATIONS). All data and information are now available on the WDCGG web site, which aims to improve accessibility to data, information, and products in line with the Strategy of the Implementation of the Global Atmosphere Watch Programme (2001-2007) published in June 2001 and its Addendum for the Period 2005-2007 (WMO, 2001; WMO, 2004).

This strategy also requests that GAW facilities, including World Data Centres, build a data bank that can provide good analyses in cooperation with the scientific research community. To meet this request, the WDCGG has increased its analytical activities, and made the contents of the annual *Data Summary* more comprehensive. Global and integrated analyses used to monitor global changes in concentrations of greenhouse gases have become important tasks of the WDCGG. Other important tasks include the revision and improvement of the contents of the *Data Summary* based on comments from data contributors and scientists, and to provide scientists and policy makers with more advanced analytical information. The WDCGG welcomes comments and suggestions regarding the *Data Summary* and its other publications. It is expected that the analytical information presented here will not only stimulate the use of data regarding greenhouse and other gases, but will also increase appreciation of the value of the GAW program.

The WDCGG thanks all the data contributors, including those involved in measurement at the numerous sites worldwide, for their efforts in maintaining the observation programme and for their continuous provision of data.

Mailing address:

WMO World Data Centre for Greenhouse Gases (WDCGG)
c/o Japan Meteorological Agency
1-3-4, Otemachi, Chiyoda-ku, Tokyo 100-8122, Japan

E-mail: wdcgg@hq.kishou.go.jp
Telephone: +81-3-3287-3439
Facsimile: +81-3-3211-4640
Web Site: http://gaw.kishou.go.jp/wdcgg.html

Note:

The WDCGG requests acknowledgement from data users by the appropriate citation of the contributors and data sources when they use any data or information provided by the WDCGG. Data users should refer to the GAW Station Information System (GAWSIS) at the GAW web site (http://www.wmo.ch/web/arep/gaw/gaw_home.html) or the WDCGG web site for details on the GAW Country Contacts, what measurements are being made, and the investigators responsible. The information at the GAWSIS and the World Data Centres is updated in cooperation with the WMO Secretariat.

# 2. Analysis

The WDCGG collects, archives and distributes observation data regarding concentrations of greenhouse gases, and also provides analytical results on the collected data.

This publication presents long-term trends and seasonal variations in concentrations of $CO_2$, $CH_4$ and CO derived for the global, hemispheric and zonal means. For $N_2O$ global and hemispheric long-term trends are presented. For halocarbons, surface $O_3$, $NO_x$ and $SO_2$, only time series of monthly mean concentrations are presented because only a small number of stations have reported observation data.

The following sections explain the methods used for analysis for $CO_2$, $CH_4$, CO and $N_2O$. The respective chapters should be referred to for the other parameters.

## 2-1. Site selection for global, hemispheric and zonal mean concentrations

As ground-based stations observe air at a lower boundary layer, the measured concentrations of gases, such as $CO_2$, $CH_4$ and CO, which have sources and/or sinks on the Earth's surface, may show localised characteristics in a lower boundary layer depending on weather conditions, *etc.*

These data incorporate very useful information for investigating the power of local sources and sinks. However, for global scale analysis, it is necessary to use data that can be considered representative concentrations averaged over a reasonable geographical area and in a whole boundary layer, *i.e.*, background data. Background data can usually be extracted from the total data through appropriate selection criteria, which are chosen for each site.

In this study, observation sites that were considered to offer data appropriate for the purpose were selected. In some cases, *e.g.*, where the observatory was in a marine area, even data without any selection criteria may be regarded as background data. In contrast, it could be difficult to select background data in other cases where the observatory was located in woodland or near a densely populated city.

Final site selection was performed objectively as described below, based on data in a reasonable scattered range of the total data in the same latitudinal zone. The latitudinal distribution of the annual mean concentrations normalised with respect to the South Pole, which were calculated from the monthly mean concentrations, was fitted with the loess model curve (Cleveland *et al.*, 1988). Sites with concentrations lying more than $\pm 3\sigma$ from this curve were rejected and this process was iterated until all of the remaining sites lay within $\pm 3\sigma$ from the fitted curve. The selected sites are listed in Plate 3.1 for $CO_2$, Plate 4.1for $CH_4$, and Plate 8.1 for CO with asterisks.

## 2-2. Trend analysis

The time series of greenhouse gas concentrations, which is often produced by removing local effects with very short-term variations, represents integration of variations on different time scales. The two major components of variation in $CO_2$ concentration are seasonal variations and long-term trends. Many researchers have attempted to decompose observation data into these two components by objective curve fitting (Keeling *et al.*, 1989), digital filtering (Thoning *et al.*, 1989; Nakazawa *et al.*, 1991), or both (Conway *et al.*, 1994; Dlugokencky *et al.*, 1994).

Trend analysis approximating variations in the sum of seasonal variations by Fourier harmonics and long-term trends by low-pass filtering with a cut-off frequency of 0.48 cycles/year was performed for each selected site. Refer to the previous Summary (WDCGG No. 22) for details.

## 2-3. Estimation of value for periods without data for zonal mean calculation

The number of sites used for trend analysis outlined above varied during the analysis period. Moreover, data were frequently excluded due to pauses in the observation. When the calculations are performed without considering changes in the number of the sites used in the analysis, the values, such as the zonal growth rate, fluctuate with the change in the number of available sites. These fluctuations were particularly evident in the early period when few sites were available.

However, if we select only those sites for which data are available throughout the whole analysis period, the data from many newly established sites will not be reflected in the analysis. To use as many sites as possible and to avoid gaps accompanying changes in the number of sites, the estimated values for the periods for which no data were included in the zonal mean calculations. The values were estimated by interpolation and extrapolation as follows.

First, sites requiring interpolation were selected. A provisional seasonal variation was calculated from the longest consecutive data set for each site with all the same Lanczos filters (Duchon, 1979) as described in the previous Summary. Then, linear interpolation was performed for the data from which the provisional seasonal variation was subtracted. The complete variation was then retrieved by adding the provisional seasonal variation.

Next, the sites requiring extrapolation were selected. The provisional long-term trend and the seasonal variation were calculated from the interpolated data set with the same filter. Extrapolation was then

performed for the long-term trend as its growth rate traces the zonal mean growth rate calculated from those of the other sites in the same latitudinal zone. Subsequently, the complete variation was retrieved by adding the site's own provisional seasonal variation. Here, each zone was created every 30° of latitude.

The zonal mean concentrations were calculated from the continuous data set, derived in the above procedure, by determining the arithmetic mean for the sites included in each latitudinal zone for every 20° or 30°. The zonal mean in the early stage of the analysis period may have lower accuracy than that in the latest stage. Although the data sets were partly estimated, the completeness of data was assumed to be advantageous for trend analysis of the zonal mean.

## 2-4. Calculation of global and hemispheric means

Global and hemispheric means were calculated by averaging the zonal means, taking into consideration the area ratio of each latitudinal zone.

The deseasonalised long-term trend and growth rate for the globe, both hemispheres and each latitudinal zone were calculated again with the filter from the global, hemispheric and zonal means. To derive the trend for the whole period, we assumed provisional data extending from both ends followed the linear trend for the whole period. Therefore, analyzed trends at both ends may depart from the actual values.

Here, we summarise the characteristics of global, hemispheric and zonal mean concentrations by presenting the time series of monthly mean concentrations, deseasonalised long-term trends, annual growth rates and the averaged seasonal cycle.

# 3.
# CARBON DIOXIDE
# ($CO_2$)

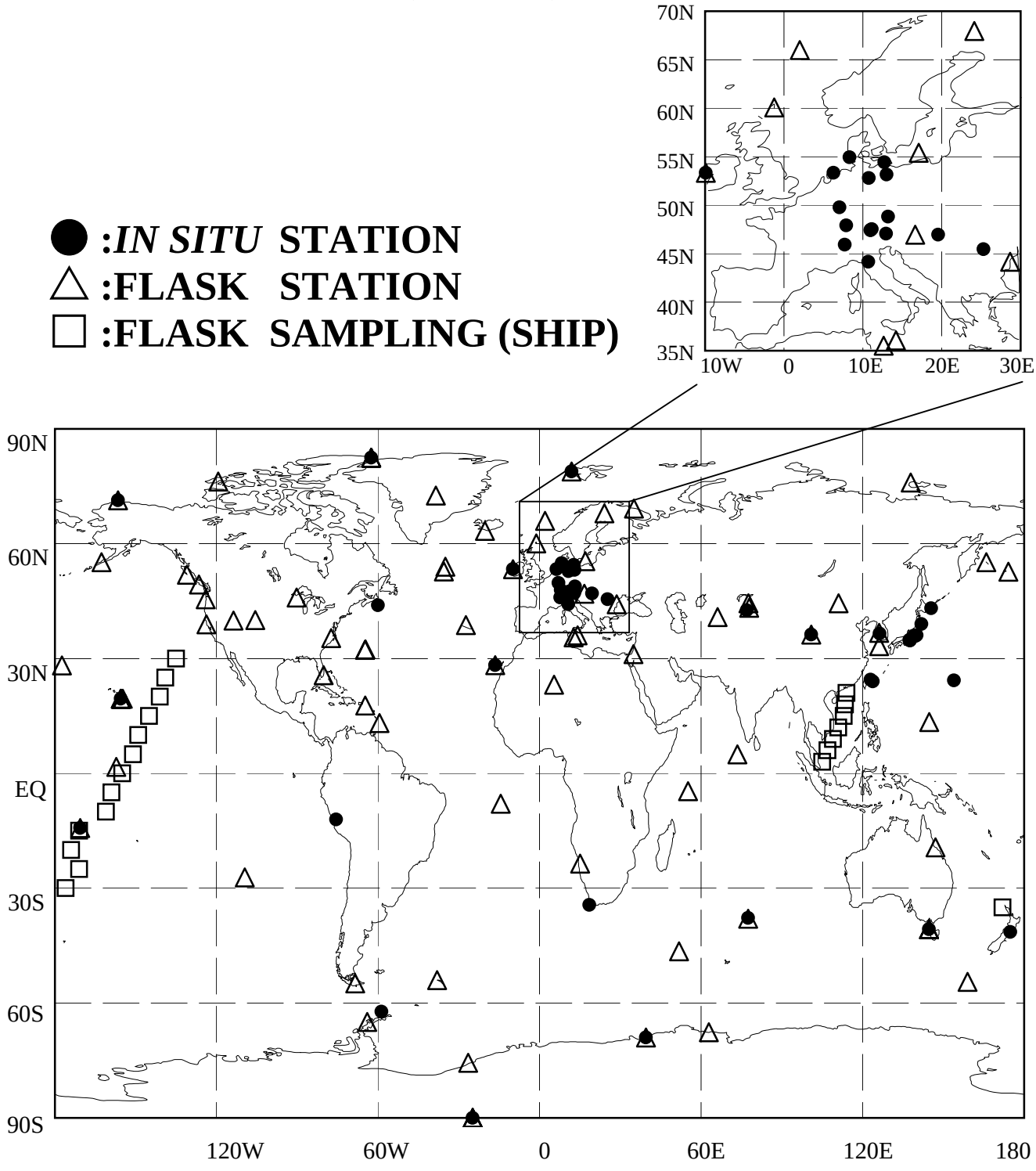

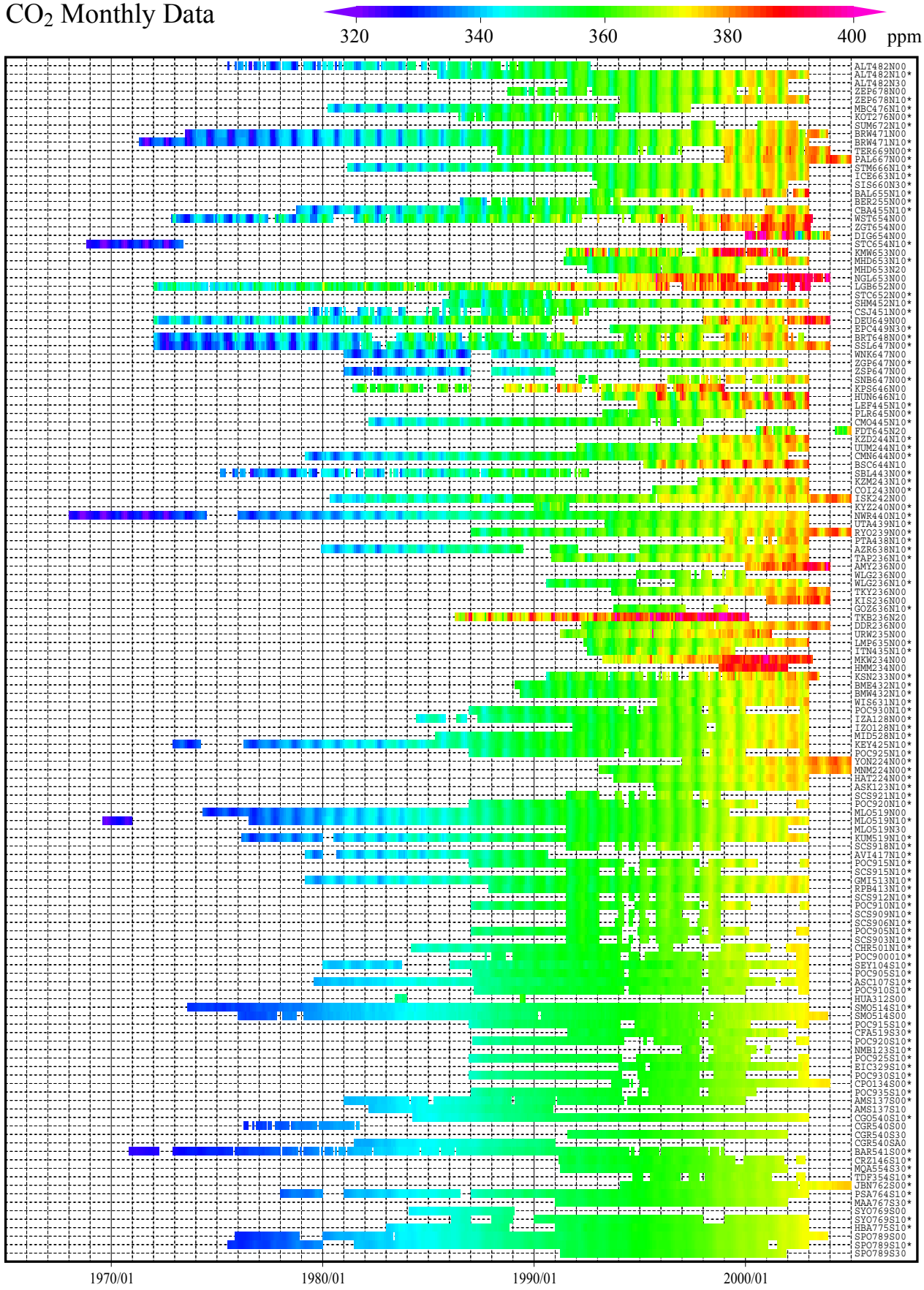


Plate 3.1 Monthly mean $CO_2$ concentrations for all sites reported to the WDCGG illustrated in colors that change with the concentration. The sites are set from north to south. Though some stations reported data at two or three different altitudes, only data at the lowest altitudes are illustrated. The monthly value at the site which has submitted only original (hourly) data before selection is calculated by the WDCGG as an arithmetic mean, and may become high for reflecting the concentration influenced in plant breathing at nighttime in the lower boundary layer. Site index with an asterisk shows the site used in the analysis shown in Plate 3.2.

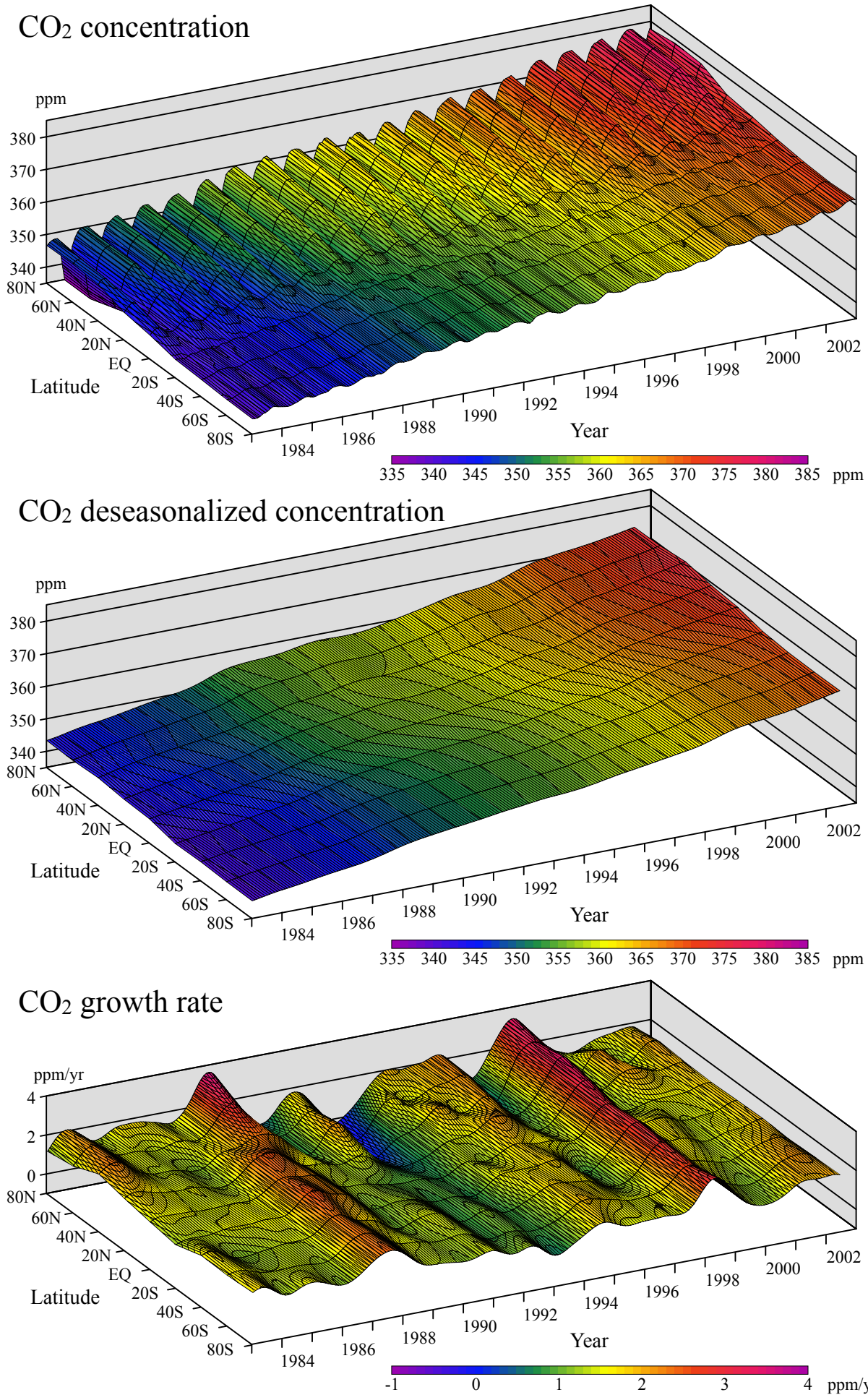


Plate 3.2 Variation of zonally averaged monthly mean $CO_2$ concentrations (top), deseasonalized concentrations (middle), and growth rates (buttom). Zonally averaged concentrations are calculated for each 20° zone. Deseasonalized concentrations and growth rates are derived as described in Chapter 2.

# 3. Carbon Dioxide ($CO_2$)

## Basic information on $CO_2$ with regard to environmental issues

Carbon dioxide ($CO_2$) is a significant greenhouse gas that has strong absorption bands in the infrared region and is the largest contributor to the greenhouse effect. $CO_2$ contributed to 60% of the radiative forcing due to the increase in well-mixed greenhouse gases after the industrial revolution (IPCC, 2001).

The balance between emission and absorption at the surface of the earth or ocean determines the concentration of $CO_2$ in the atmosphere. About 750 Gigatonnes of carbon is stored in the atmosphere as $CO_2$. This carbon in atmospheric $CO_2$ is exchanged with two other large reservoirs, the terrestrial biosphere and the ocean. The $CO_2$ is exchanged between the atmosphere and terrestrial biosphere mainly through absorption by photosynthesis and emission from plant respiration and decomposition of organic soils. These biogenic activities vary with season, resulting in large seasonal variations in $CO_2$ levels. Transport of $CO_2$ from the atmosphere to the ocean or in the opposite direction occurs according to the differences in $CO_2$ concentration, which varies with season and sea region.

The atmospheric $CO_2$ concentration has never exceeded the current level during the past 420,000 years (IPCC, 2001). The levels of anthropogenic emission of $CO_2$ have been increasing since the 18th century, and the emitted $CO_2$ has been distributed into the atmosphere, oceans and terrestrial biosphere, which serve as reservoirs of $CO_2$ in the global carbon cycle. However, the whole global carbon cycle, which is comprised mainly of $CO_2$, has not yet been revealed. About half of this anthropogenic $CO_2$ emission has increased $CO_2$ in the atmosphere and the rest has been removed by sinks, including the terrestrial biosphere and ocean uptake. However, the amount of removal depends strongly on the year (Figure 3.1).

Carbon isotopic studies have demonstrated the importance of the terrestrial biosphere and oceans as sources and sinks (Francey *et al.*, 1995; Keeling *et al.*, 1995; and Nakazawa *et al.*, 1993, 1997a). On the other hand, the atmospheric $O_2$ content is dependent mainly on $O_2$ removal by burning of fossil fuels, and $O_2$ release from the terrestrial biosphere. Therefore, the uptake of carbon by the terrestrial biosphere and the ocean can be evaluated from $O_2$ ($O_2/N_2$) measurements combined with $CO_2$ measurements (IPCC, 2001). IPCC (2001) showed that the ocean and the terrestrial biosphere respectively absorbed about 27% and 22% of $CO_2$ emitted from the burning of fossil fuel in the 1990s, while the remaining 51% contributed to the annual increase in $CO_2$ level in the atmosphere.

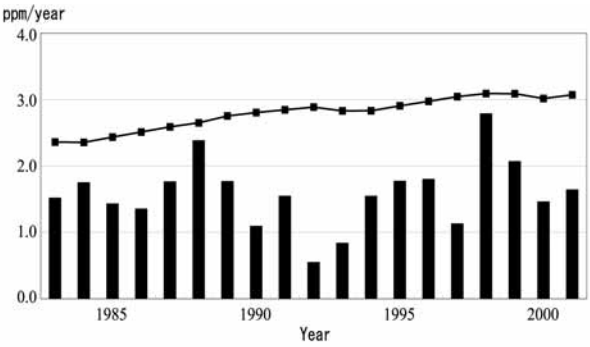


Fig. 3.1 Time series of annual mean $CO_2$ growth rates in the atmosphere calculated from observation data (column) and from anthropogenic emission data (thin line with dots). $CO_2$ emissions were calculated by CDIAC based on the United Nations Energy Statistics, and the observed growth rate was calculated by the WDCGG.

Large amounts of $CO_2$ are exchanged among these reservoirs, and the global carbon cycle is coupled with the climate system on seasonal, interannual and decadal time scales. Accurate understanding of the global carbon cycle is essential for the estimation of future $CO_2$ concentrations in the atmosphere.

The map at the beginning of this chapter shows observation sites that submitted $CO_2$ concentration data to the WDCGG by December 2004. These sites include *in situ* stations performing continuous measurement as well as flask-sampling stations, such as those in the NOAA/CMDL network. In addition to such fixed stations, mobile stations on ships and aircraft, and other stations that measure event data also report their data to the WDCGG (Appendix: LIST OF OBSERVATION STATIONS).

## Annual variations in $CO_2$ in the atmosphere

The monthly mean $CO_2$ data from all the stations that submitted to the WDCGG are shown in Plate 3.1. In this plate, concentration levels are illustrated in different colours. Global, hemispheric and zonal mean background concentrations were analysed based on selected stations (see the caption to Plate 3.1). The three-dimensional representations of latitudinal distribution of atmospheric $CO_2$ concentration, deseasonalized concentrations and the growth rate are shown in Plate 3.2. These three-dimensional representations ($CO_2$ carpets) indicate that the amplitudes of seasonal concentration variations are large in the northern mid-latitudes, but the seasonal variation is indistinct in the Southern Hemisphere; the increases in concentration occur in the Northern Hemisphere prior to the Southern Hemisphere, and propagate to the Southern Hemisphere, and the inter-

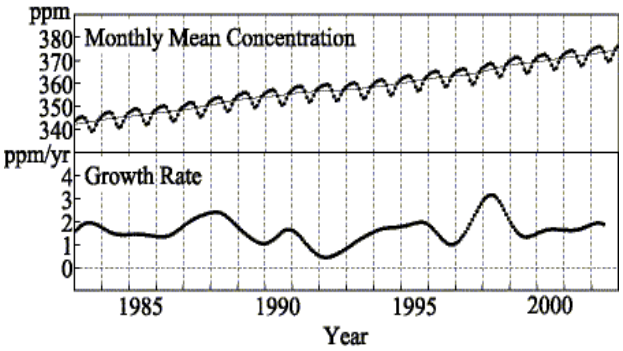


Fig. 3.2 Monthly mean concentrations (thick line and dots) and deseasonalized long-term trends (thin line) (top), and growth rate (bottom) from 1983 to 2002 for the globe.

annual variation of growth rates occurs largely in the Northern Hemisphere.

Figure 3.2 shows the global monthly mean concentrations with the long-term trends and growth rate from 1983 to 2002. Based on the results of ice core studies, the concentration of carbon dioxide in the atmosphere prior to the 18th Century (the pre-industrial period) was about 280 ppm (IPCC, 2001). The global average concentration in 2002 was 374 ppm.

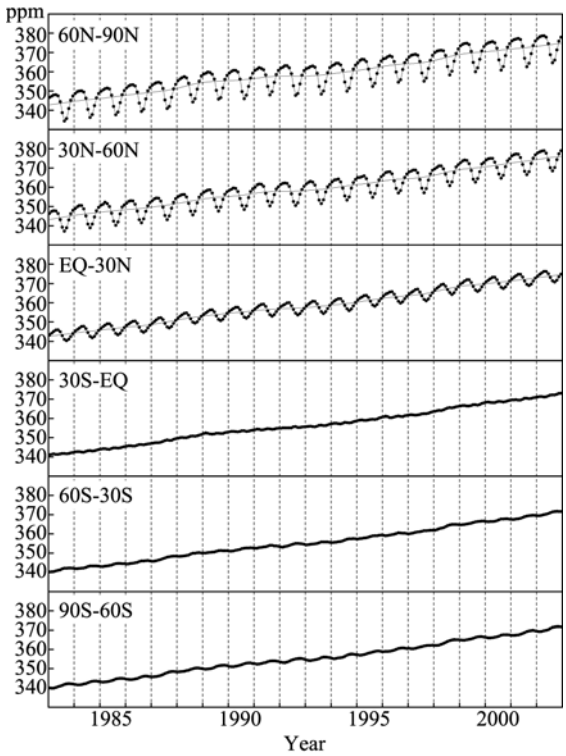


Fig. 3.3 Monthly mean concentrations (thick lines and dots) and deseasonalized long-term trends (thin lines) from 1983 to 2002 for each 30° latitudinal zone.

The mean global growth rate during this period (1983–2002) was 1.6 ppm/year. The global growth rate of $CO_2$ shows a large inter-annual variation. During the above period, the maximum and minimum global growth rates were 3.2 ppm/year in April 1998 and 0.4 ppm/year in March 1992, respectively. High growth rates exceeding 2 ppm/year were seen in 1987/1988 and 1997/1998.

Figure 3.3 shows the monthly mean concentrations and their long-term trends from 1983 to 2002 for each 30° latitudinal zone. Long-term increases in both hemispheres and seasonal variations in the Northern Hemisphere were clearly observed.

As shown in Figure 3.4, the growth rates fluctuated between –0.3 and 3.5 ppm/year, and variability in the growth rate was relatively large in northern high latitudes. All growth rates were high in 1987/1988 and 1997/1998. On the other hand, negative values were recorded in northern high latitudes in 1992.

Changes in growth rate are also known to be associated with El Niño-Southern Oscillation (ENSO). El Niño events occurred in 1982/1983, 1986-1988, 1991/1992, 1993, 1997/1998 and 2002/2003, and with the exception of 1992, growth rates were high in these years. In addition to those at the surface, the $CO_2$ growth rates at high altitudes (8-13 km) over the Pacific Ocean are also known to have a similar relationship with ENSO (Matsueda *et al.*, 2002). Ordinarily, there is an up-welling area with $CO_2$-rich ocean water in the eastern equatorial Pacific, and $CO_2$ is emitted from the ocean. However, El Niño events suppress this up-welling, which reduces $CO_2$ emission from the ocean. On the other hand, El Niño events result in high temperature anomalies in many areas globally, particularly in the Tropics, which increase $CO_2$ emission from the terrestrial biosphere by the enhanced respiration of plants and decomposition of organic matter in the soil (Keeling *et al.*, 1995). Anomalously low precipitation, particularly in the Tropics, also enhances this effect by suppressing plant photosynthesis. These oceanic and terrestrial

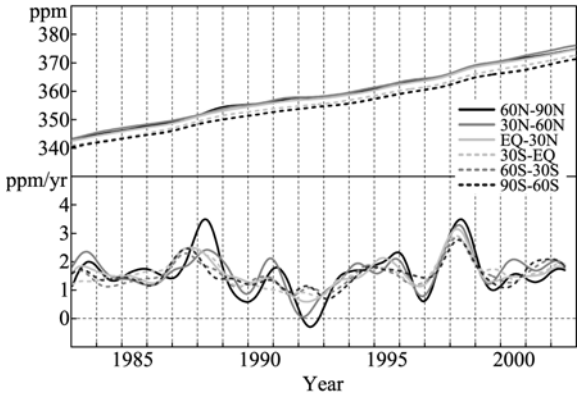


Fig. 3.4 Long-term trends (top) and growth rates (bottom) for each 30° latitudinal zone.

processes have opposite effects during El Niño events.

However, Dettinger and Ghil (1998) suggested that the former effect was limited to the eastern equatorial Pacific, while the latter had a global scale. Thus, the $CO_2$ response, which is almost synchronous with El Niño events, is due to terrestrial biosphere changes associated with temperature variations on a global scale.

Carbon isotope ($^{13}C$) studies have also shown that atmospheric $CO_2$ variations accompanying El Niño events are brought about by the flux between the terrestrial biosphere and the atmosphere, rather than between the ocean and the atmosphere (Keeling *et al.*, 1989; Nakazawa *et al.*, 1993; Morimoto *et al.*, 2000). A strong El Niño event during 1997/1998, which was one of the most severe ENSO events in the 20th Century, brought about high temperatures and low precipitation levels on a global scale during this period (JMA, 1999; WMO, 1999b), resulting in frequent wildfires and drought in Southeast Asia. Such meteorological conditions perturbed the global carbon cycle (Watanabe *et al.*, 2000), and are considered to intensify $CO_2$ emission from the terrestrial biosphere.

However, an exceptionally low $CO_2$ growth rate occurred even during the El Niño event in 1991/1992. The injection of 14-20 Mt of $SO_2$ aerosols into the stratosphere by the Mt Pinatubo eruption in June 1991, which affected the radiation budget and atmospheric circulation (Hansen *et al.*, 1992; Stenchikov *et al.*, 2002), resulted in a drop in the global temperature. The reduced $CO_2$ emission from the terrestrial respiration and from decomposition of organic matter in the soil due to anomalous low temperatures (Conway *et al.*, 1994; Lambert *et al.*, 1995; Rayner *et al.*, 1999), and enhanced $CO_2$ absorption by intensive photosynthesis due to the increase in diffuse radiation (Gu *et al.*, 2003) contributed to the low $CO_2$ growth rate despite the El Niño event (Angert *et al.*, 2004).

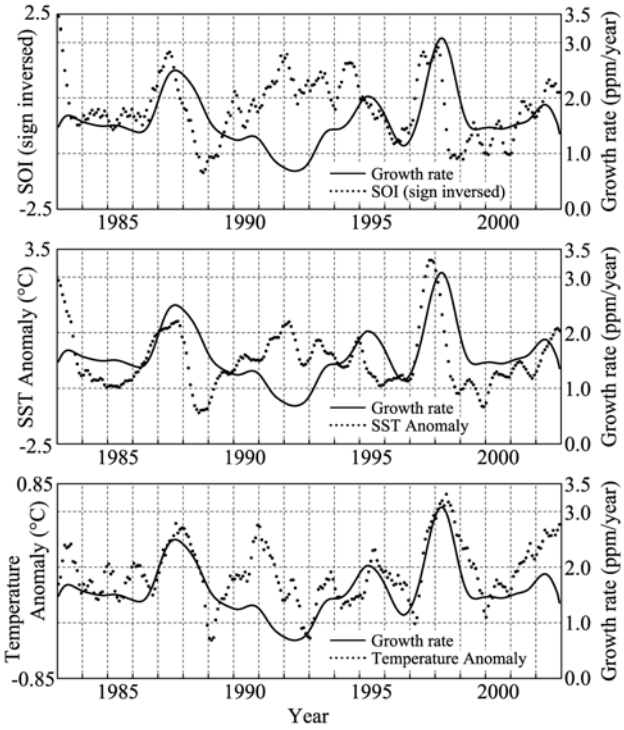


Fig. 3.5 Time series of growth rates in the Tropics (30°N-30°S) and a comparison with the Southern Oscillation Index inversed sign (top), SST anomaly in the eastern equatorial Pacific (4°N-4°S, 150°W-90°W) (middle) and temperature anomaly on land in the Tropics calculated from NCEP reanalysis data (bottom). The solid lines show the growth rates, and the dots show each element (5-month running mean).

Figure 3.5 shows a time series of $CO_2$ growth rates in the tropical area (< ±30° from 1983 to 2002), the SOI (Southern Oscillation Index), the SST anomaly in the eastern equatorial Pacific (4°N-4°S, 150°W-90°W) and the temperature anomaly on land in the Tropics calculated from NCEP (National Centers for Environmental Prediction) reanalysis data. In the figure, the SOI, the SST anomaly and the temperature anomaly are processed as a five-month running mean to display the seasonal variation. The growth rate in the Tropics showed good correspondence with the SOI and SST anomalies with a time lag except in 1992. In addition, the growth rate in the Tropics also showed good correspondence with the temperature anomaly on land in the Tropics, including 1992. These results suggested that the growth rate is related to ENSO events, but that temperature anomalies on tropical land have the closest relationship with $CO_2$ growth rate in the Tropics. These observations suggest a strong influence of the tropical biosphere on tropical $CO_2$ concentration.

## Seasonal cycle of $CO_2$ in the atmosphere

Figure 3.6 shows average seasonal cycles for each 30° latitudinal zone from which the long-term trends were subtracted.

Amplitudes of seasonal cycles are clearly large in northern high and mid-latitudes and small in the

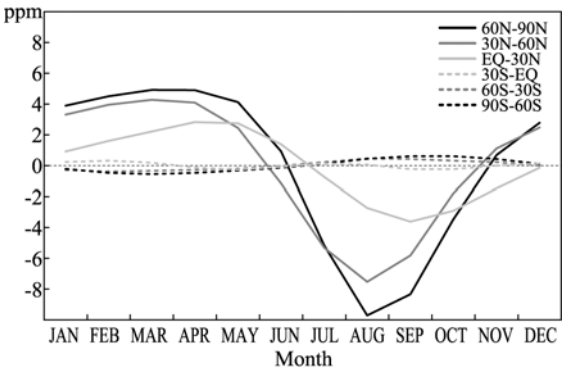


Fig. 3.6 Average seasonal cycles for each 30° latitudinal zone from which the long-term trends were subtracted.

Southern Hemisphere. Ocean uptake (Ramonet *et al.*, 1996) and biomass burning (Wittenberg *et al.*, 1998) are thought to influence the seasonal variation. However, these large seasonal cycles in the Northern Hemisphere are characterized by rapid decreases from June to August and large returns from September to December. They are the result of the activities of the terrestrial biosphere, *i.e.*, $CO_2$ absorption by photosynthesis, emission by respiration of vegetation, and decomposition of organic matter by microbes in the soil (*e.g.*, Nakazawa *et al.*, 1997b).

In northern high and low latitudes, the occurrences of their maximum concentrations are delayed by one or two months. Minimum concentrations appeared in August in northern high and mid-latitudes and in September in northern low latitudes. The peak in low latitudes is delayed because the seasonal variation in high latitudes takes some time to reach the low latitudes (Tanaka *et al.*, 1987), and the seasonal cycle of terrestrial biosphere activity at low latitudes is delayed against that in the mid-latitudes due to the courses of the wet and dry seasons (Nemry *et al.*, 1996).

In the Southern Hemisphere, the seasonal variations showed small amplitudes with a half-year delay due to small amounts of net emission and absorption by the terrestrial biosphere. The seasonal variations of northern mid-latitudes and southern mid-latitudes seemed to be superimposed in the southern low latitudes (0-30°S), while the amplitude was small, suggesting that the large seasonal variation in the Northern Hemisphere influences the Southern Hemisphere. The direct influence of sources and sinks in the Southern Hemisphere might be partially cancelled by propagation of the out-of-phase seasonal variation from the Northern Hemisphere.

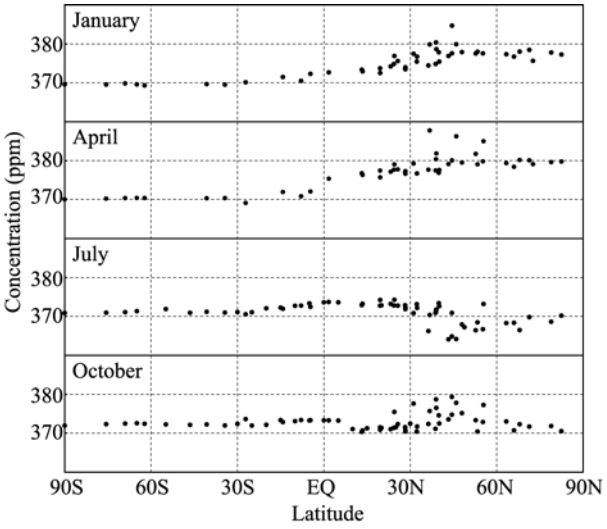


Fig. 3.7 Latitudinal distributions of monthly mean concentrations in January, April, July and October 2002.

Figure 3.7 shows the latitudinal distributions of $CO_2$ concentrations in January, April, July and October in 2002. Latitudinal gradients around 30°N were positive in January and April, and negative in July, corresponding to the large seasonal cycle in northern, mid- and high latitudes.

## Annual variation of $CO_2$ in the upper atmosphere

The Meteorological Research Institute in Japan Meteorological Agency has carried out aircraft-based measurement of trace gases, such as $CO_2$, at altitudes of 8-13 km over the western Pacific using a commercial flight between Japan and Australia in cooperation with the Japan Airlines Foundation, the Ministry of Land, Infrastructure and Transport, and Japan Airlines since 1993. The observation data are submitted to the WDCGG every year. Fig. 3.8 shows the time series of the atmospheric $CO_2$ concentrations, Deseasonalized concentrations and the growth rates in the upper air obtained by these measurements. We used continuous data obtained by linear interpolation. The trend analysis method used was the same as that described in section 2. The $CO_2$ concentrations increased with seasonal variations, similarly to those on the surface. The seasonal variations observed over the Northern Hemisphere also reflected those on the surface, but the amplitudes were smaller.

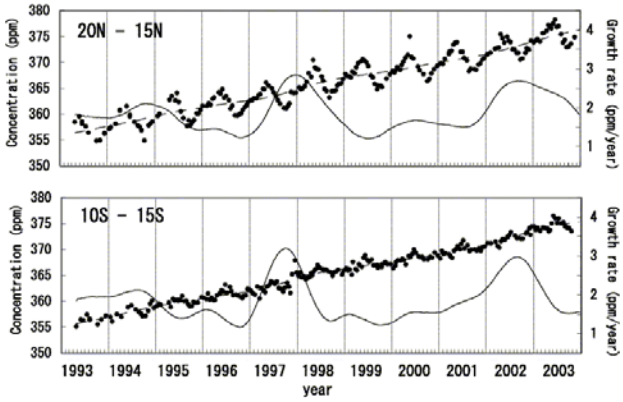


Fig. 3.8 Time series of $CO_2$ concentrations (dots), deseasonalized concentrations (dashed lines), and growth rates (solid lines) observed at latitudinal zones of 15-20°N and 10-15°S at altitudes of 8–13 km over the western Pacific.

# 4.
# METHANE
# ($CH_4$)

● :*IN SITU* STATION
△ :FLASK STATION
□ :FLASK SAMPLING (SHIP)

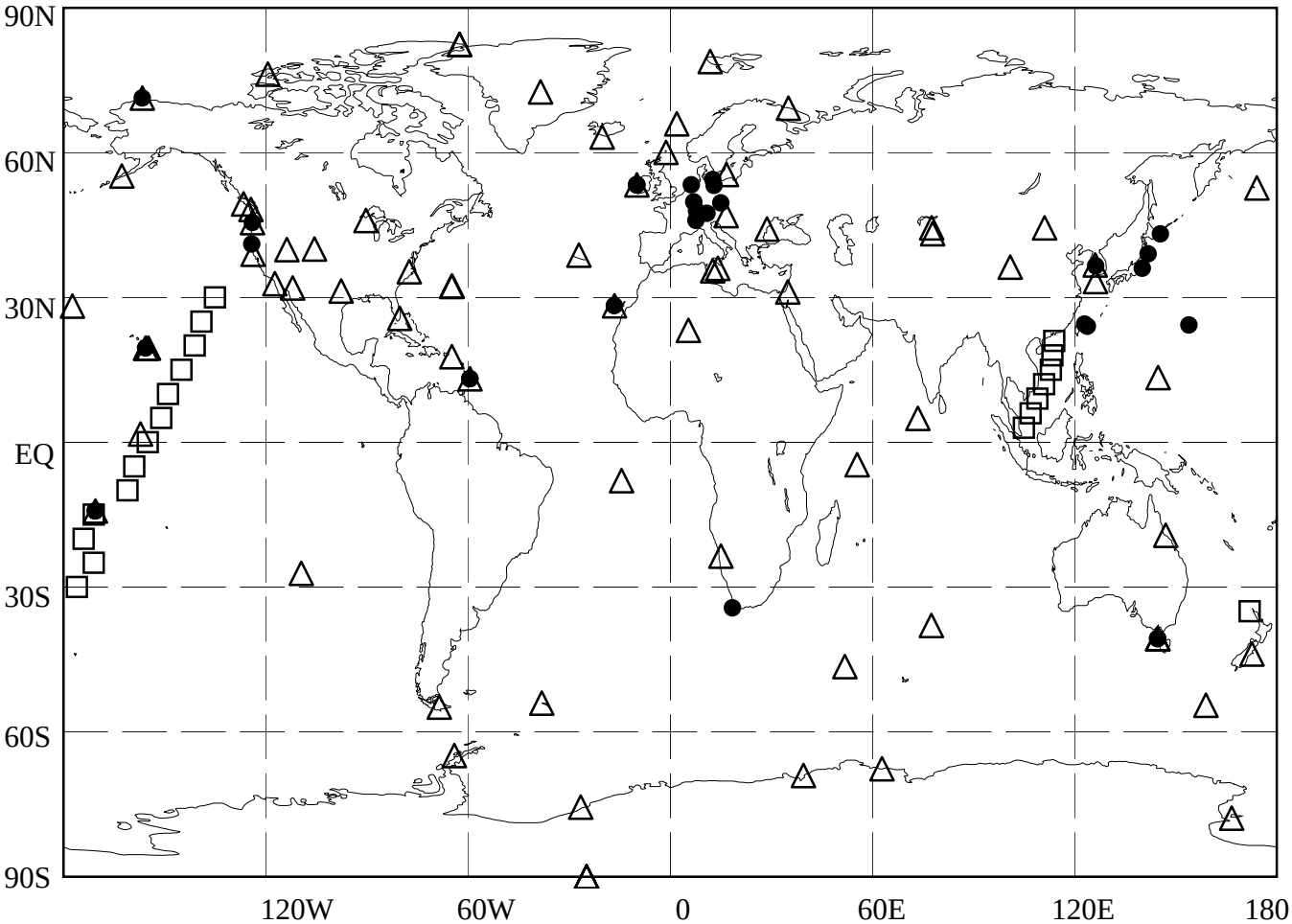

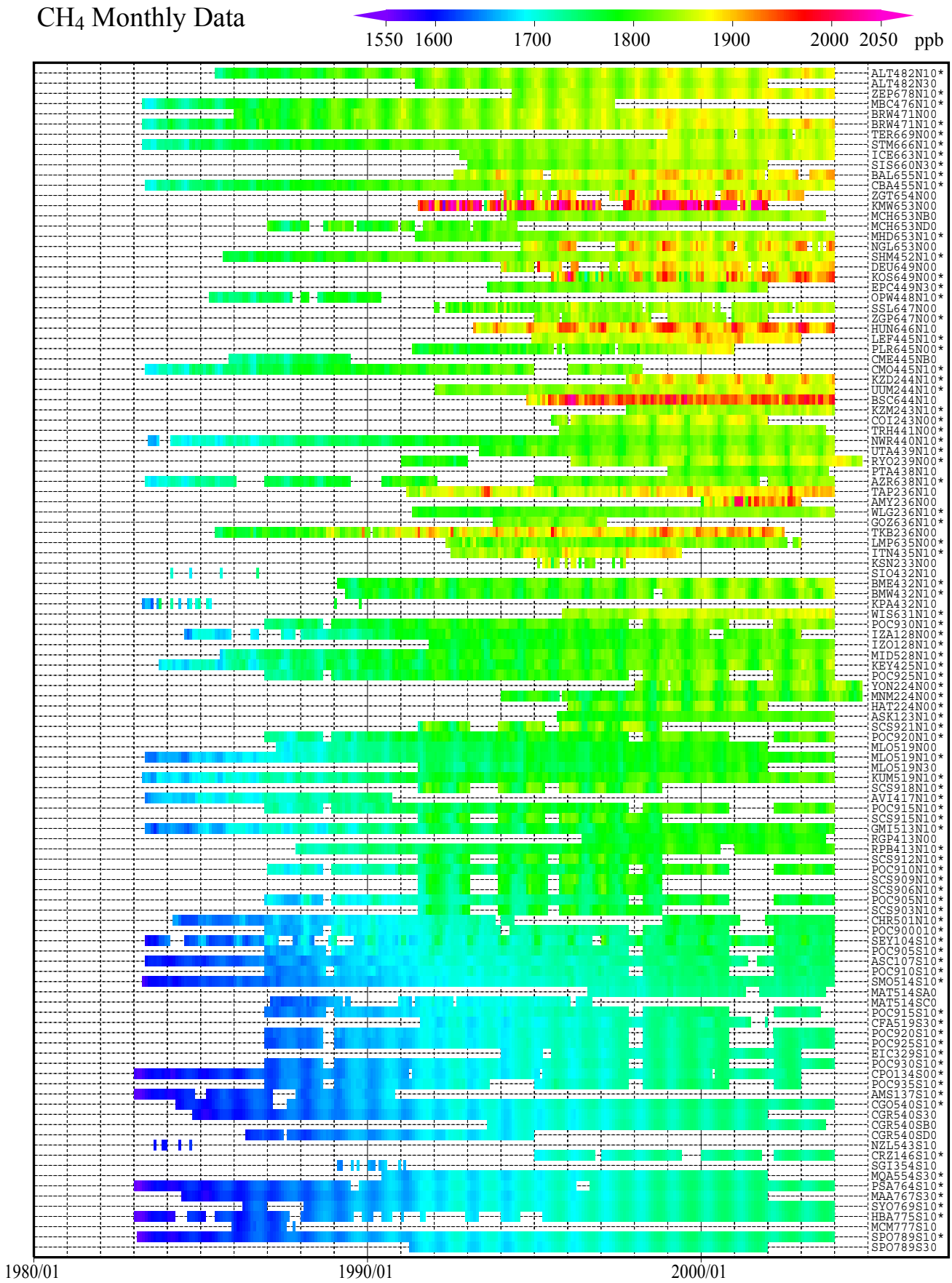


Plate 4.1 Monthly mean $CH_4$ concentrations for all sites reported to the WDCGG illustrated in colors that change with the concentration. The sites are set from north to south. Though some stations reported data at two or three different altitudes, only data at the lowest altitudes are illustrated. The monthly value at the site which has submitted only original (hourly) data before selection is calculated by the WDCGG as an arithmetic mean. Site index with an asterisk shows the site used in the analysis shown in Plate 4.2.

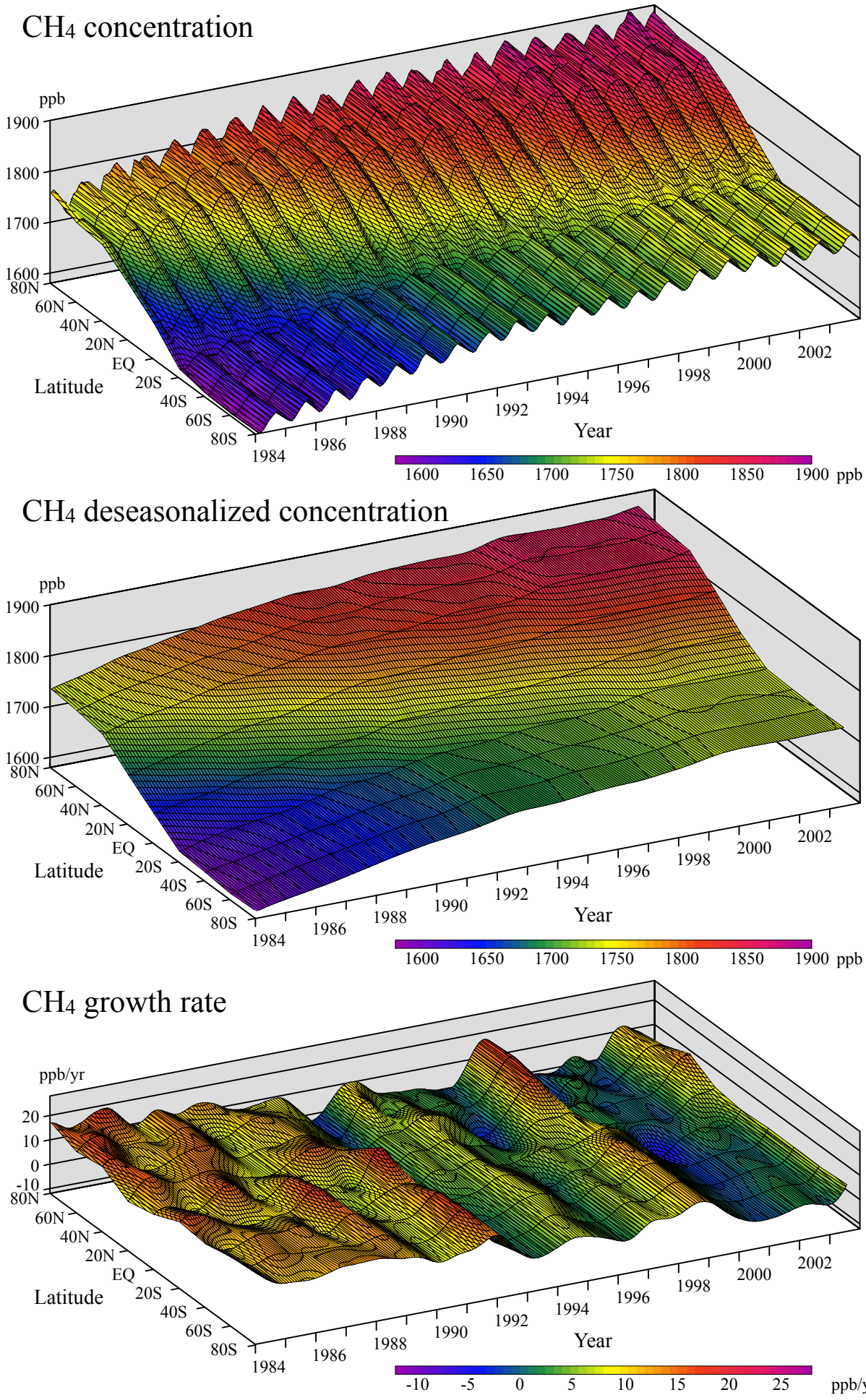


Plate 4.2 Variation of zonally averaged monthly mean $CH_4$ concentrations (top), deseasonalized concentrations (middle), and growth rates (buttom). Zonally averaged concentrations are calculated for each 20° zone. Deseasonalized concentrations and growth rates are derived as described in Chapter 2.

# 4. Methane ($CH_4$)

## Basic information on $CH_4$ with regard to environmental issues

Methane ($CH_4$) is the second most significant greenhouse gas, but is estimated to have 21 times as much radiative forcing as $CO_2$ per molecule. From 1000 to 1800 A.D., the concentration of $CH_4$ was about 700 ppb (Etheridge *et al.*, 1998). $CH_4$ contributed to 20% of the radiative forcing due to increases in levels of greenhouse gases after the industrial evolution (IPCC, 2001).

Atmospheric $CH_4$ is produced mainly by anaerobic digestion and combustion of fossil fuel, and is removed by reaction with hydroxyl radicals (OH). $CH_4$ is emitted from both natural and anthropogenic sources, including natural wetlands, oceans, landfills, rice paddies, enteric fermentation, gas drilling and biomass burning. Of the various emissions, 60-80% are estimated to have a relationship with anthropogenic activities. Particularly, the increases in energy consumption with landfills, sewage disposal, and fossil fuel use in urban cities have resulted in high concentrations of $CH_4$ in Asia (Bartlett *et al.*, 2004). $CH_4$ is destroyed by reaction with OH in the troposphere and the stratosphere, reaction with chlorine atoms and oxygen atoms in the excited $O(^1D)$ state in the stratosphere and soil absorption. $CH_4$ is one of the most important water vapour sources in the stratosphere. The atmospheric lifetime (adjustment time) of $CH_4$ was estimated to be 12 years (IPCC, 2001). However, the concentration of OH, which decomposes $CH_4$, is affected by ambient temperature and humidity. In addition, emissions from some sources are dependent on temperature. Therefore, information regarding sources and sinks of $CH_4$ must be further improved to estimate the atmospheric $CH_4$ budget.

Analyses of confined air in ice cores in Antarctica and Arctic areas showed that the present $CH_4$ concentration has not been exceeded during the past 420,000 years (IPCC, 2001). The $CH_4$ concentration before the industrial revolution was 700-800 ppb, showing a rapid increase thereafter. However, the increase was very slow in a few years.

The observation sites that submitted $CH_4$ concentration data to the WDCGG are shown on the map at the beginning of this chapter.

## Annual variation in $CH_4$ levels in the atmosphere

The monthly mean $CH_4$ data from all the stations that submitted to the WDCGG are shown in Plate 4.1. In this plate, concentration levels are illustrated in different colours. Global, hemispheric and zonal mean background concentrations were analysed based on selected stations (see the caption for Plate 4.1). The three-dimensional representations of latitudinal distribution of atmospheric $CH_4$ concentration, deseasonalized concentrations and the growth rate are shown in Plate 4.2. These three-dimensional representations ($CH_4$ carpets) indicate that the amplitudes of seasonal variation of concentration are larger in the Northern hemisphere than in the Southern Hemisphere; the increase in concentration occurs in the Northern Hemisphere prior to the Southern Hemisphere, and propagates to the Southern Hemisphere. The variation in growth rate occurs on a global scale. These features are similar to those of $CO_2$ (see Section 3). The latitudinal gradient of $CH_4$ concentration is large from the mid-latitudes in the Northern Hemisphere to the Tropics, suggesting that the major sources located in the high and middle northern latitudes and $CH_4$ are destroyed with transportation to the Tropics where OH concentrations are high.

Measurements of $CH_4$ concentrations in Antarctic and Greenland ice cores indicated that the differences between northern and southern high latitudes ranged from 24 to 58 ppb from 1000 to 1800 A.D. (Etheridge *et al.*, 1998). At present, the difference between the northern and southern high latitudes is about 150 ppb (see Fig.4.3). This increase is presumably due to increased emissions in the Northern Hemisphere, which are mainly from anthropogenic sources.

Figure 4.1 shows the monthly mean concentrations with deseasonalized long-term trends and the growth rate from 1984 to 2003 for the globe. The global mean concentration in 2003 was 1787 ppb.

The growth rate of $CH_4$ shows a large interannual

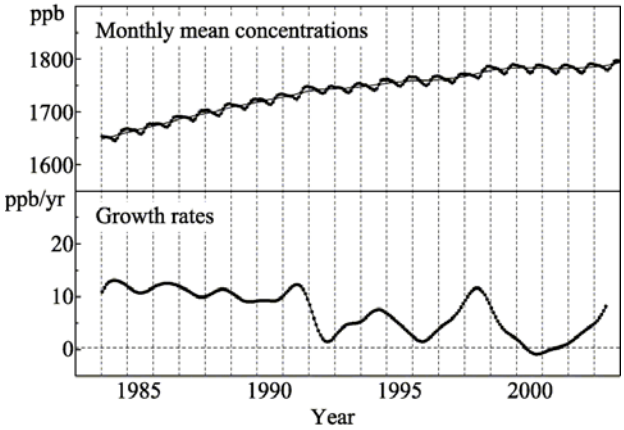


Fig. 4.1 Monthly mean concentrations (thick line), deseasonalized long-term trends (thin line) (top) and growth rates (bottom) from 1984 to 2003 for the globe.

variation. During the analysis period, global growth rates reached a maximum in June 1984 at 14 ppb/year and a minimum in October 2000 at -1 ppb/year. The global growth rate of almost zero in 2000-2001 suggested that the global $CH_4$ budget seemed to have been at a steady-state. Growth rates after the 1990s were generally lower than those during the 1980s. The global mean growth rates were 7 ppb/year for the whole period (1984-2003), 11 ppb/year for 1984-1990 and 5 ppb/year for 1991-2003. Lelieveld *et al*. (1998) noted that the decrease in global emission of $CH_4$ brought about a reduction in $CH_4$ growth rate in the 1990s. However, Dlugokencky *et al.* (1998) and Etheridge *et al.* (1998) reported that the decreased growth rates in the 1990s suggested that global $CH_4$ concentrations are approaching a steady-state where removal of $CH_4$ is balanced by emission from $CH_4$ sources.

Figure 4.2 shows the monthly mean concentrations and their deseasonalized long-term trends from 1984 to 2003 for each of the 30° latitudinal zones. The seasonal variations were small in the latitudinal zone from the equator to 30°S.

Figure 4.3 shows the deseasonalized long-term trends and growth rates for each of the 30° latitudinal zones. Deseasonalized long-term trends have the distinct feature of high concentrations in northern high and mid-latitudes and low concentrations in southern latitudes. Growth rates clearly decreased from the 1980s to 1990s for all of the latitudinal zones.

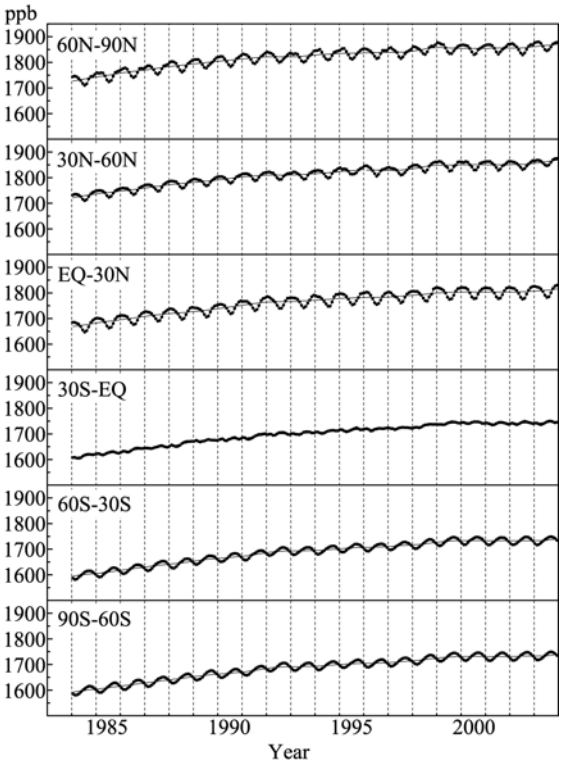


Fig. 4.2 Monthly mean concentrations (thick line) and deseasonalized long-term trends (thin line) from 1983 to 2003 for each 30° latitudinal zone.

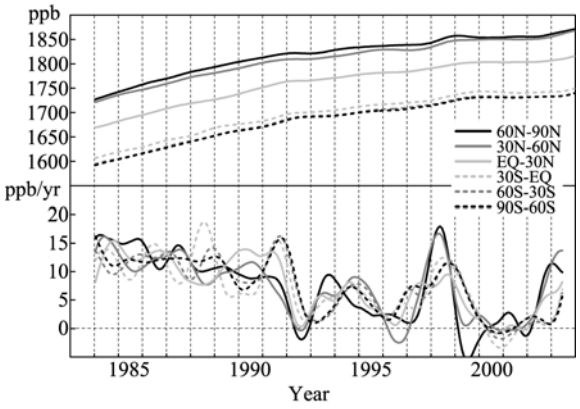


Fig. 4.3 Deseasonalized long-term trends (top) and growth rates (bottom) for each 30° latitudinal zone.

Growth rates in the Southern Hemisphere and Northern Subtropics were large in 1991 and small in 1992 and 1993 for all latitudinal zones, and took negative values in the northern high latitudes in 1992.

The large increase in 1991 may have been caused by decreased OH radical levels due to a reduction in UV radiation as a result of the eruption of Mt. Pinatubo in 1991 (Dlugokencky *et al.*, 1996). Carbon isotope observations suggested that the decrease in 1992 was probably caused by a reduction in biomass burning at low latitudes (Lowe *et al.*, 1997), and analysis of monsoon activity suggested a role of a decrease in emission from wetlands and rice paddy fields due to low temperatures and enhancement of decomposition due to dryness (Lelieveld *et al.*, 1998). The decrease in 1992 may also have been due to an increase in OH radical concentration caused by stratospheric ozone depletion after the eruption of Mt. Pinatubo in 1991 (Bekki *et al.*, 1994).

Growth rates were large in 1998 for all of the latitudinal zones. Dlugokencky *et al.* (2001) suggested that the large growth rates in 1998 were due to increased emissions from the northern high latitudinal zones and the tropical wetlands due to high temperatures and increased precipitation, and partly due to the influence of biomass burning of the boreal forest mainly in Siberia. The $CH_4$ growth rate has been almost zero since 2000, but the reasons for this observation have yet to be determined.

Fig. 4.4 shows the interannual variations in global mean growth rate and global surface temperature anomaly. Global $CH_4$ growth rates varied along with global mean temperature anomalies in the 1990s, particularly during the period from 1992-1998. High temperature anomalies result in increased $CH_4$ emission from wetlands and increased removal by increased OH radical levels (Bekki *et al.*, 1997). The relation between global growth rates and temperature anomalies showed that the former effect exceeds the latter globally. A study of the relationship between

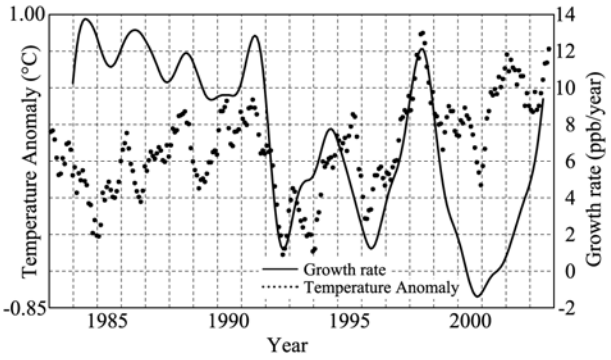


Fig. 4.4 Time series of the global mean $CH_4$ growth rates and their comparison with temperature anomalies on land from NCEP reanalysis data. The solid lines show the growth rates, and the dots show temperature anomalies (5-month running mean).

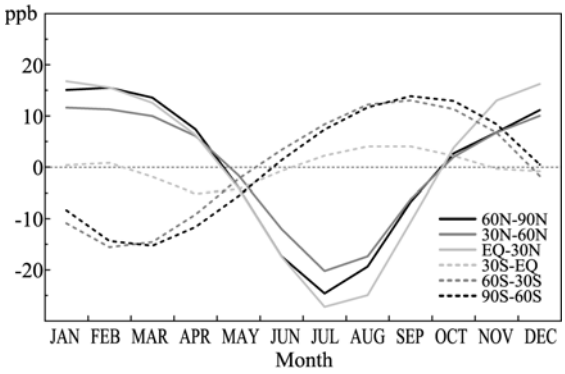


Fig. 4.5 Average seasonal cycles for each 30° latitudinal zone from which the long-term trends were subtracted.

$CH_4$ concentrations in ice cores or firn layers and global temperature anomalies also suggested that a large growth rate for the $CH_4$ concentration follows a high global mean temperature (Etheridge *et al.*, 1998). However, the global mean growth rate in the 1980s did not correspond with the global surface temperature anomaly in the same decade. This suggests that causes other than the global temperature anomaly resulted in the large increase rate in the 1980s.

## Seasonal cycle of $CH_4$ in the atmosphere

Figure 4.5 shows average seasonal cycles for each of the 30° latitudinal zones. Seasonal cycles are brought about mainly by reaction with OH, a major $CH_4$ sink in the atmosphere. The strength and timing of the emission from $CH_4$ sources, such as wetlands and biomass burning, along with transportation of $CH_4$, also affect the seasonal cycle. The amplitudes of the seasonal cycle were large in the Northern Hemisphere. Unlike $CO_2$, amplitudes were large in the Southern Hemisphere except at low latitudes. The $CH_4$ seasonal cycle showed a minimum in winter and a maximum in summer in both hemispheres. The seasonal variation of $CH_4$ is almost consistent with that of OH, which reacts chemically with $CH_4$. Southern low latitudes have a distinct semi-annual component, which is superimposed on the annual component of the seasonal cycle at southern mid-latitudes. The secondary maximum occurred in boreal winter due to the trans-hemisphere transportation of $CH_4$ from the Northern Hemisphere. This phenomenon was seen at stations located in the western Indian Ocean, *e.g.*, Mahe Island and the Seychelles, and in the western and central equatorial Pacific, *e.g.*, Cape Matatula and Samoa.

# 5.
# NITROUS OXIDE
# ($N_2O$)

● :*IN SITU* STATION
△ :FLASK STATION

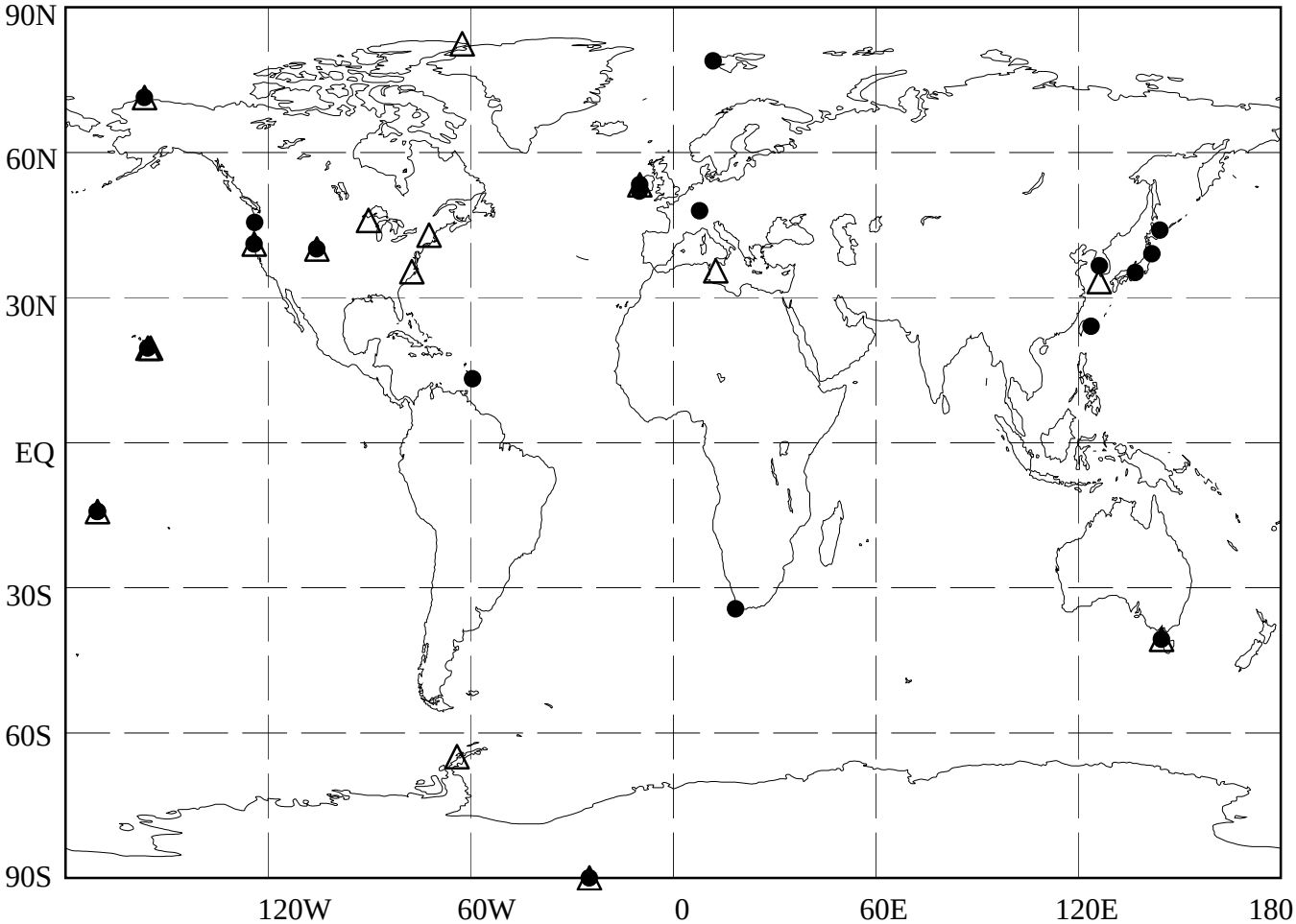

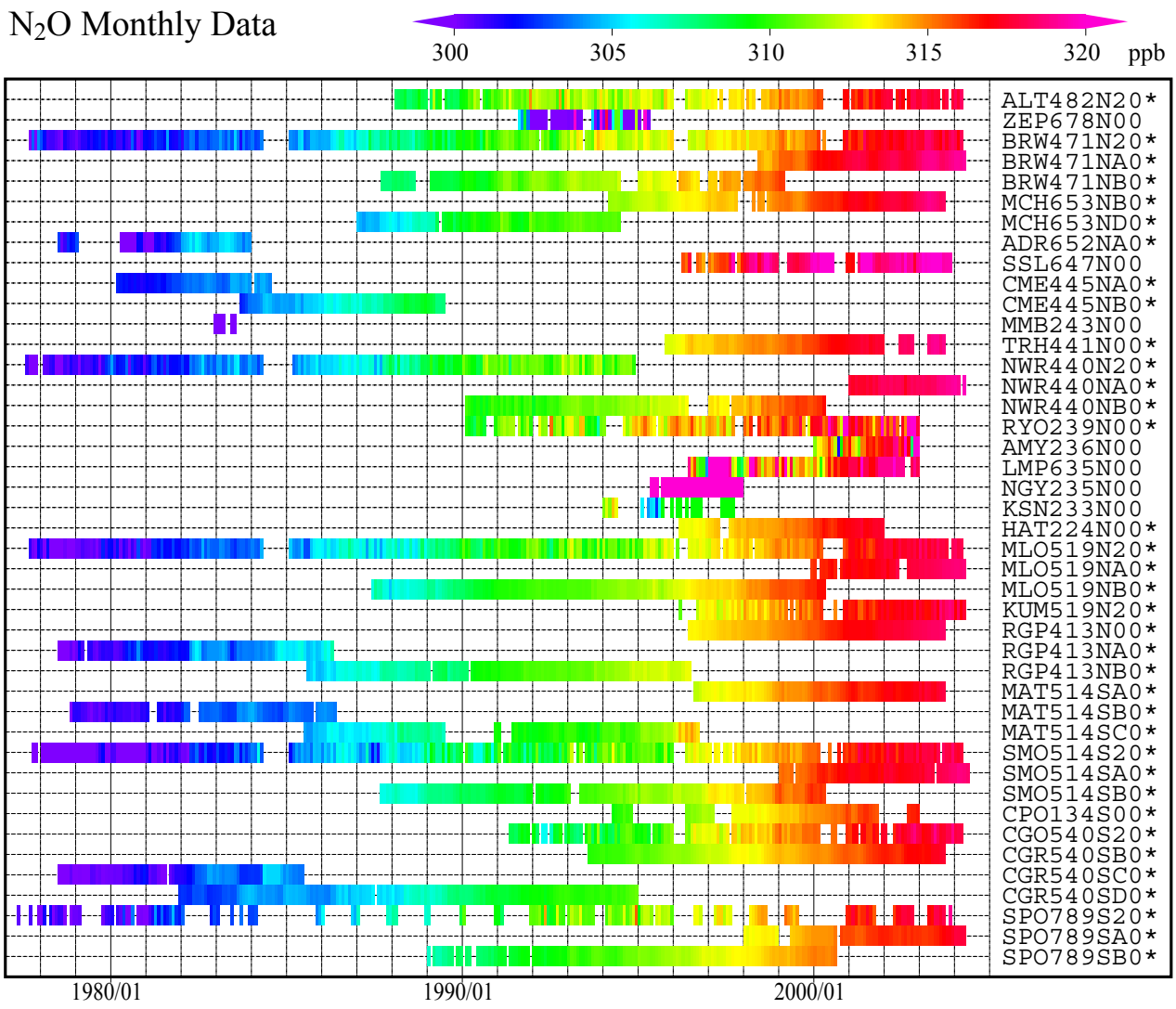


Plate 5.1 Monthly mean $N_2O$ concentrations for all sites reported to the WDCGG illustrated in colors that change with the concentration. The sites are set from north to south. Site index with an asterisk shows the site used in the analysis shown in Fig. 5.1.

# 5. Nitrous Oxide ($N_2O$)

## Basic information on $N_2O$ with regard to environmental issues

Nitrous oxide ($N_2O$), which is a relatively stable gas in the troposphere, is a greenhouse gas with an "adjustment-time" of 114 years. At present, radiative forcing of $N_2O$ is estimated at 0.15 W/m$^2$, which is 6% of the total from all of the long-lived and globally mixed greenhouse gases (IPCC, 2001). The atmospheric concentration of $N_2O$ increased steadily from about 270 ppb in pre-industrial times and is now 16% higher than in 1750 (IPCC, 2001).

$N_2O$ is emitted into the atmosphere from natural and anthropogenic sources, including the oceans, soil, combustion of fuels, biomass burning, fertiliser use and various industrial processes. One-third of the total amount of emission is considered to be from anthropogenic sources. $N_2O$ is removed from the atmosphere mainly by photo-dissociation in the stratosphere. However, even at this stage, the estimated amounts from sources and sinks have not yet been balanced.

## Annual variation of $N_2O$ in the atmosphere

The map at the beginning of this chapter shows observation sites that have submitted $N_2O$ data to the WDCGG. The monthly mean $N_2O$ data from all stations submitted to the WDCGG are shown in Plate 5.1. In this plate, concentration levels are illustrated in different colours. The time series of monthly mean concentrations are plotted in Figure 5.1 using a solid line for the stations located in the Northern Hemisphere and a faint line for those in the Southern Hemisphere. Global mean concentration was 318 ppb in 2003. The observation data in this figure did not show large fluctuations. The concentrations are increasing in both hemispheres, and the difference between both hemispheres is small.

At some stations, the average growth rate decreased considerably between 1991 and 1993, but then returned to almost the same rate as that observed during the 1980s. This was suggested to be due to a decrease in the use of nitrogen-based fertilisers, lower biogenic emissions and larger stratospheric losses due to volcanic-induced circulation changes (IPCC, 2001)

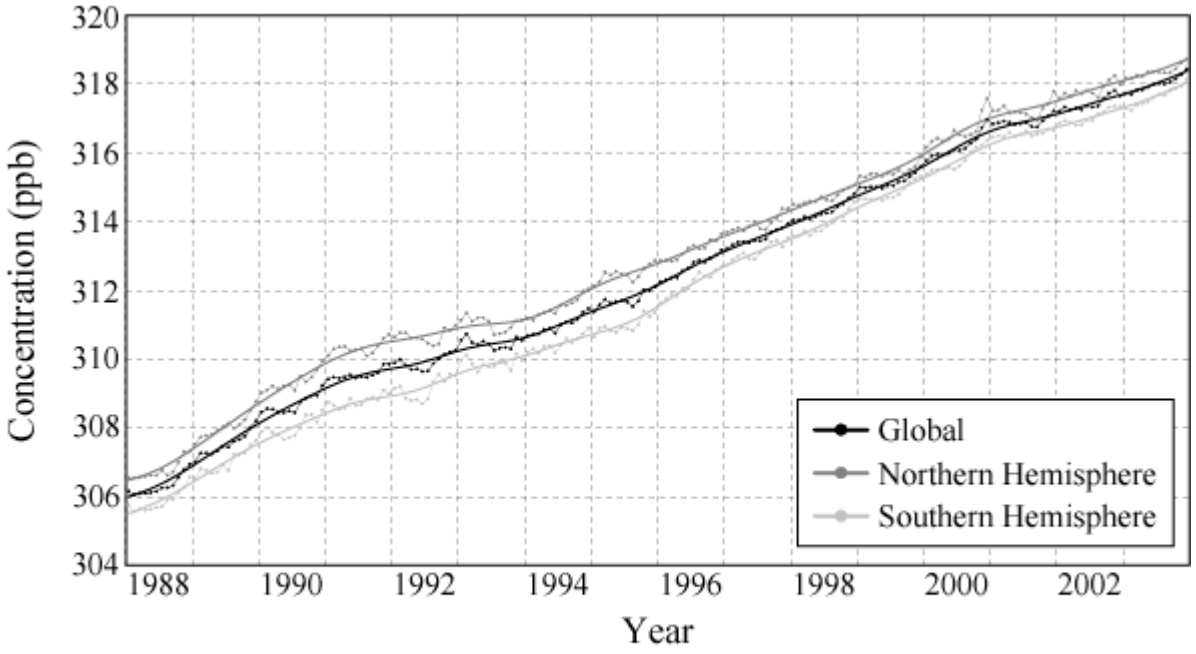


Fig. 5.1 Monthly mean concentrations (thin lines) and deseasonalized long-term trends (thick lines) from 1988 to 2003 for the globe (solid line) and both hemispheres (faint lines).

# 6.
# HALOCARBONS

● :*IN SITU* STATION
△ :FLASK STATION

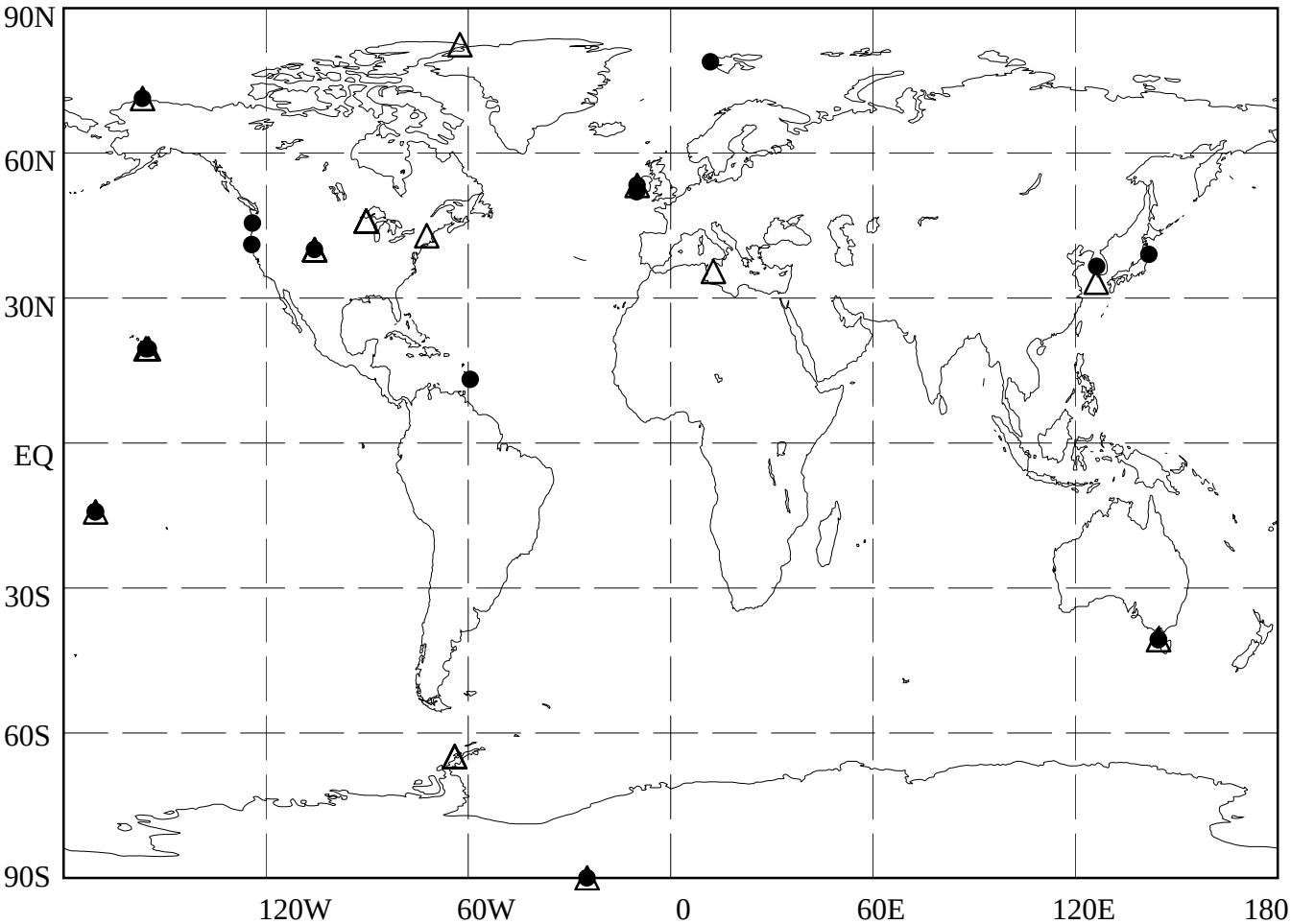

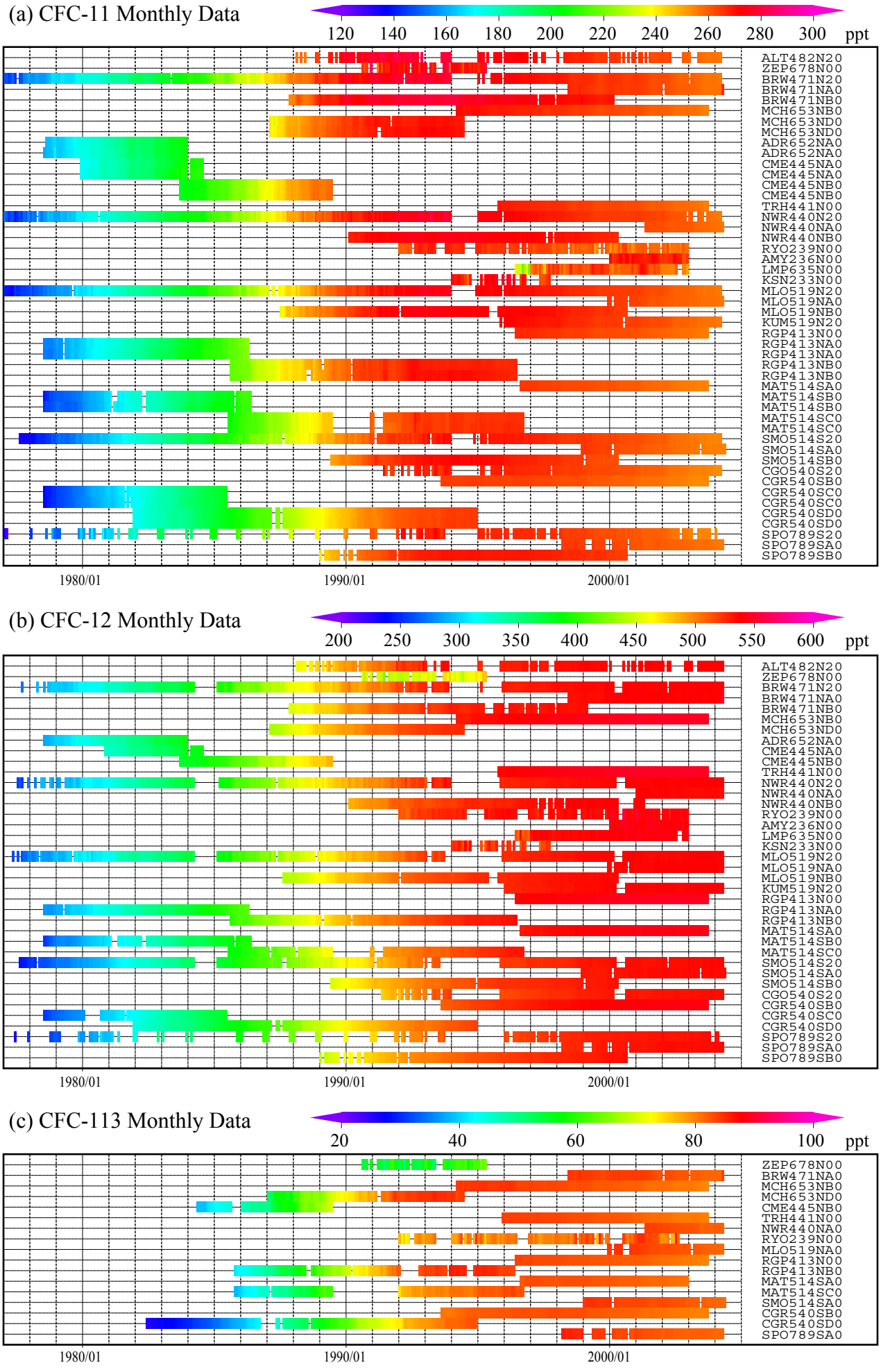


Plate 6.1 Monthly mean (a) CFC-11, (b) CFC-12, (c) CFC-113 concentrations for all sites reported to the WDCGG illustrated in colors that change with the concentration. The sites are set from north to south.

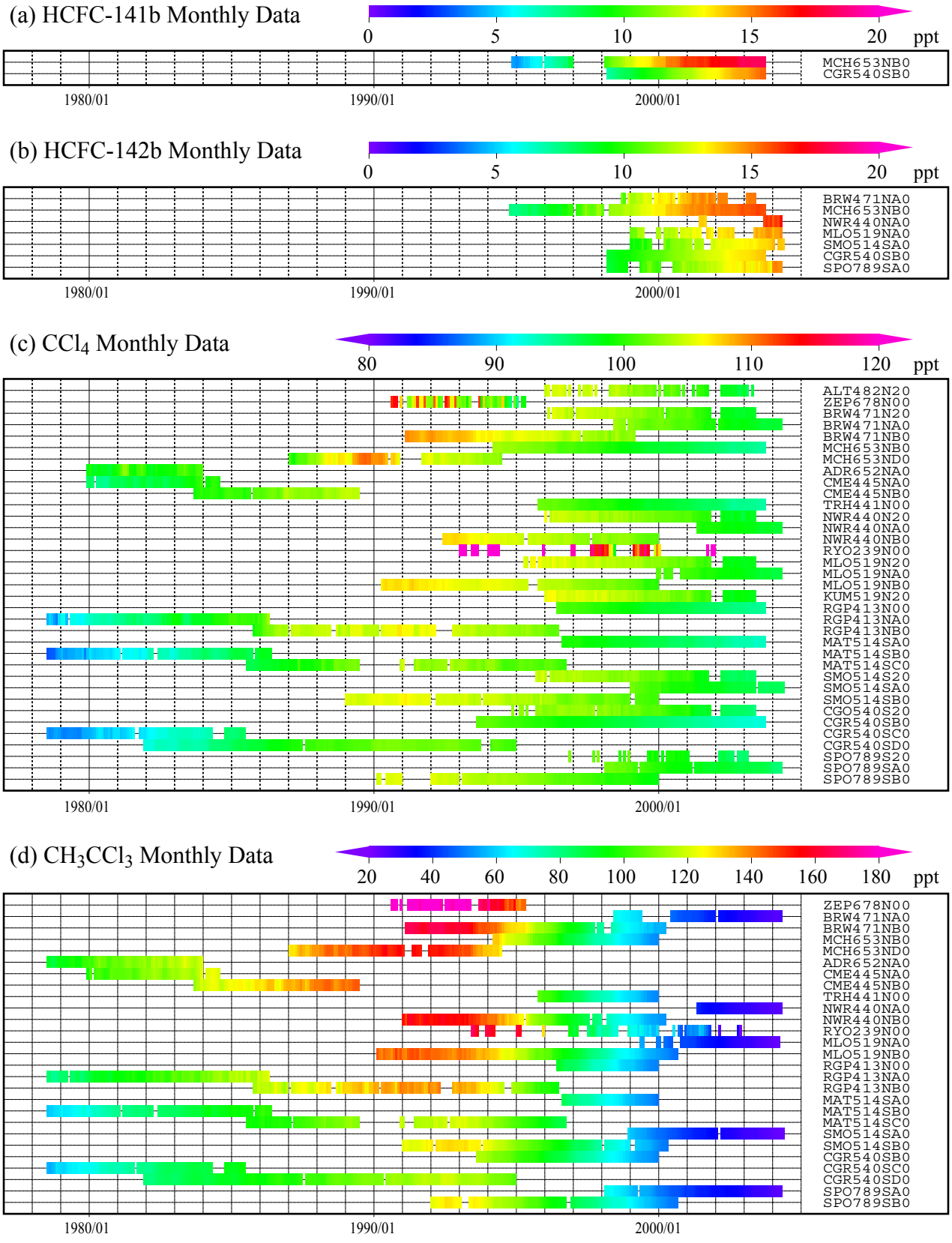


Plate 6.2 Monthly mean (a) HCFC-141b, (b) HCFC-142b, (c) $CCl_4$, (d) $CH_3CCl_3$ concentrations for all sites reported to the WDCGG illustrated in colors that change with the concentration. The sites are set from north to south.

# 6. Halocarbons (CFCs, HCFCs, $CCl_4$ and $CH_3CCl_3$)

## Basic information on halocarbons with regard to environmental issues

"Halocarbon" is a general term for carbon compounds containing one or more halogens, *i.e.*, fluorine, chlorine, bromine or iodine. Most of the halocarbons are industrial products. The chlorofluorocarbons (CFCs) are halocarbons containing fluorine and chlorine but no hydrogen, while hydrochlorofluorocarbons (HCFCs) also contain hydrogen. Carbon tetrachloride ($CCl_4$) and methyl chloroform ($CH_3CCl_3$) are produced industrially, while methyl chloride and methyl bromide are halocarbons with natural sources. Halocarbons have very low concentrations in the atmosphere, but most have large global warming potential. Thus, halocarbons contributed to 14% of radiative forcing due to increases in levels of long-lived and globally mixed greenhouse gases since the industrial revolution (IPCC, 2001).

Halocarbons are clear, odourless, and innocuous substances, which are readily gasified and liquefied and have low surface tension. Thus, they were commonly used as refrigerants, propellant and detergents for semiconductors, which resulted in a rapid increase in their atmospheric concentrations until the mid-1980s. Halocarbons containing chlorine and bromine were found to deplete the ozone layer. The Montreal Protocol on Substances that Deplete the Ozone Layer and its Adjustments and Amendments regulate the production and transportation of ozone-depleting compounds. As a result, global concentrations of CFC-11, $CCl_4$ and $CH_3CCl_3$ have begun to decrease; the global growth of CFC-113 had stopped by 1996, and that of CFC-12 has decelerated substantially.

A decrease in stratospheric ozone leads to the cooling of the lower stratosphere. However, the increase in halocarbons has a net positive radiative forcing effect on global warming because the positive direct radiative forcing of halocarbons is greater than the negative indirect radiative forcing due to ozone depletion (WMO, 1999a).

CFCs are dissociated mainly by ultraviolet radiation in the stratosphere, and their lifetimes are generally long (*e.g.*, about 50 years for CFC-11). However, HCFCs and $CH_3CCl_3$, which contain hydrogen, react with hydroxyl radicals (OH) in the troposphere and thus have relatively short lifetimes (*e.g.*, about 5 years for $CH_3CCl_3$). As the reaction with OH in the troposphere is a major sink for $CH_3CCl_3$, global measurements of $CH_3CCl_3$ provide an accurate estimate of the global concentration of OH (Prinn *et al.*, 2001).

## Annual variation of halocarbons in the atmosphere

The map at the beginning of this chapter shows observation sites that have submitted halocarbon data to the WDCGG. The monthly mean CFC-11, CFC-12, CFC-113 data from all stations submitted to the WDCGG are shown in Plate 6.1. The monthly mean HCFC-141b, HCFC-142b, $CCl_4$ and $CH_3CCl_3$ data from all stations submitted to the WDCGG are shown in Plate 6.2. Figure 6.1 shows the time series of monthly mean concentrations of CFC-11, CFC-12 and CFC-113.

Figures 6.2 and 6.3 show the corresponding data for HCFCs, and $CCl_4$ and $CH_3CCl_3$, respectively. All monthly data from each station are plotted in these figures. The absolute values of concentrations differ from station to station, suggesting that standard gases may not be traceable at each station.

Figures 6.1 and 6.3 showed significant increases in concentrations of all compounds during the 1980s in both hemispheres. Long-term trends since around 1990 for each compound are as follows:

| | |
|---|---|
| CFC-11: | Concentrations were at a maximum around 1992 in the Northern Hemisphere and about one year later in the Southern Hemisphere. They have been decreasing slowly since then. |
| CFC-12: | The growth rates have declined since around 1990 and are now nearly zero in both hemispheres. |
| CFC-113: | Concentrations were at a maximum around 1992 in the Northern Hemisphere and around 1994 in the Southern Hemisphere. Concentrations are currently almost constant or decreasing slowly in both hemispheres. |
| HCFC-141b: | Concentrations are increasing linearly. |
| HCFC-142b: | Concentrations are increasing linearly. |
| $CCl_4$: | Concentrations were at a maximum around 1991 in both hemispheres. Since then, they have been decreasing slowly. |
| $CH_3CCl_3$: | Concentrations were at a maximum around 1992 in the Northern Hemisphere and around 1993 in the Southern Hemisphere. They have been decreasing almost linearly since then. |

Comparison of the stations using identical standard gases revealed that the concentration differences between the two hemispheres were large for all compounds except HCFCs in the 1980s. However, the differences have been decreasing following each compound's concentration peak. The increases in concentrations of HCFCs are the result of their continued use as substitutes for CFCs.

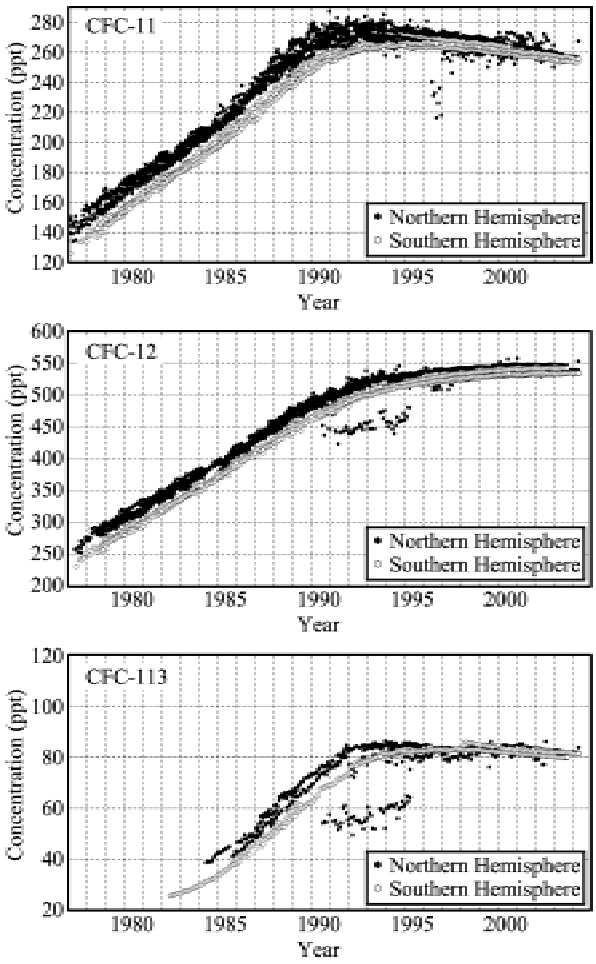


Fig. 6.1 Time series of monthly mean concentrations of (a) CFC-11, (b) CFC-12 and (c) CFC-113. Solid circles show the sites located in the Northern Hemisphere and open circles show the sites located in the Southern Hemisphere. Data at all sites reported to the WDCGG are shown.

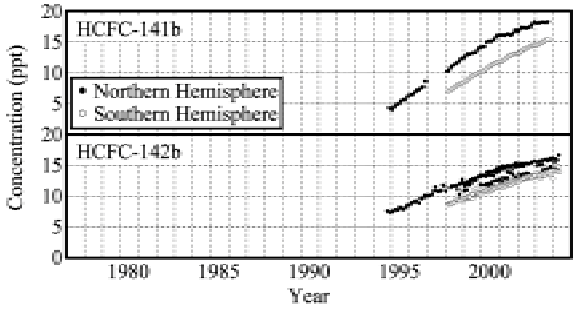


Fig. 6.2 Time series of monthly mean concentrations of HCFC-141b (upper panel) and HCFC-142b (lower panel). Solid circles show the sites located in the Northern Hemisphere and open circles show the sites located in the Southern Hemisphere. Data at all sites reported to the WDCGG are shown.

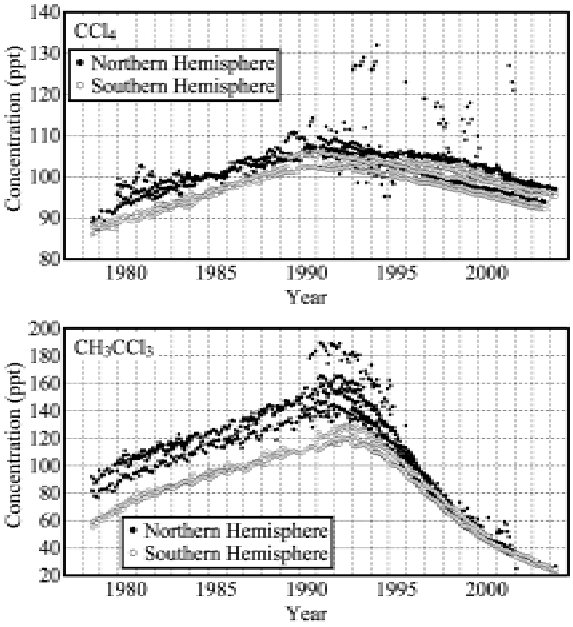


Fig. 6.3 Time series of monthly mean concentrations of (a) $CCl_4$ and (b) $CH_3CCl_3$. Solid circles show the sites located in the Northern Hemisphere and open circles show the sites located in the Southern Hemisphere. Data at all sites reported to the WDCGG are shown.

# 7.
# Surface OZONE
# ($O_3$)

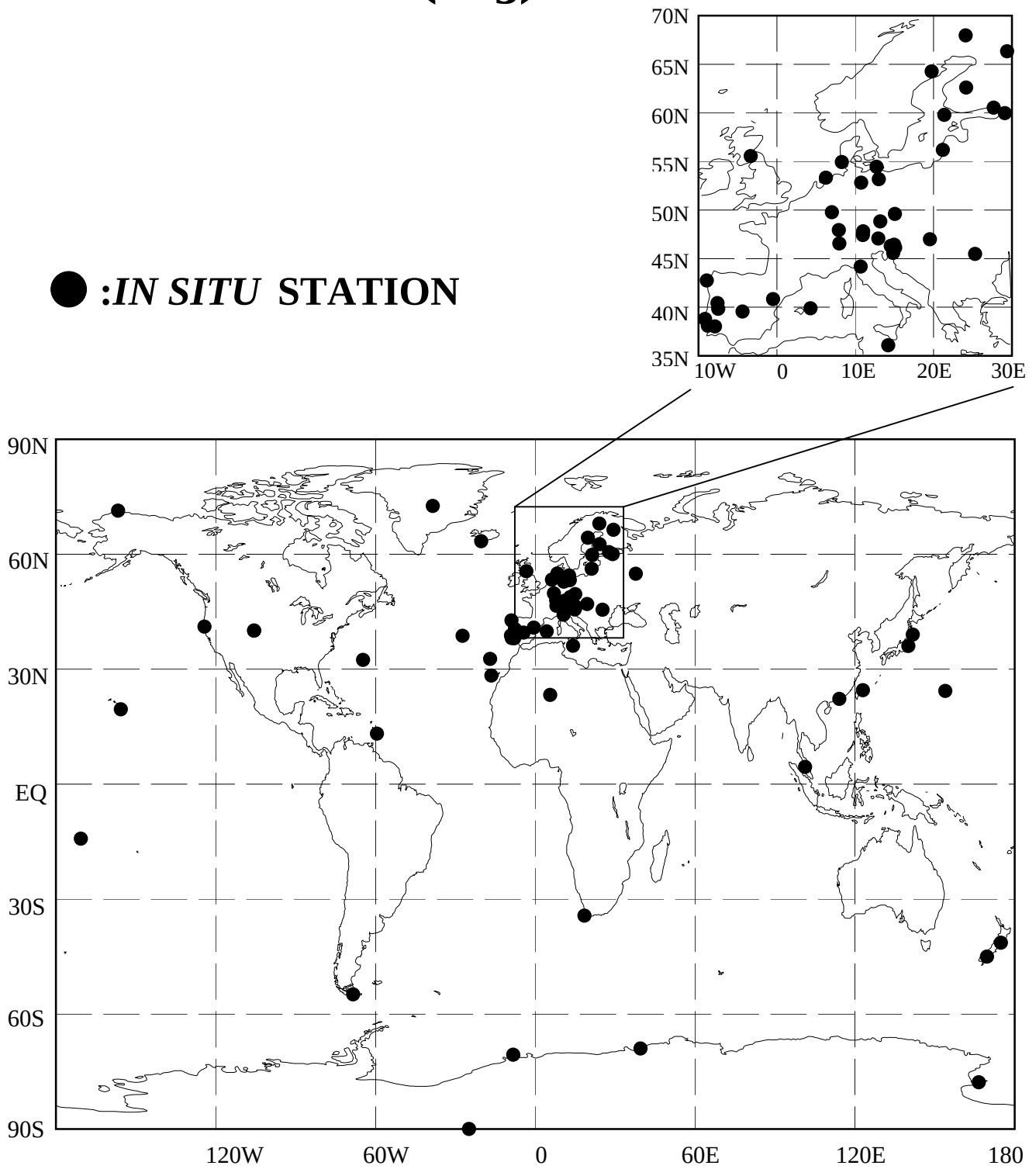

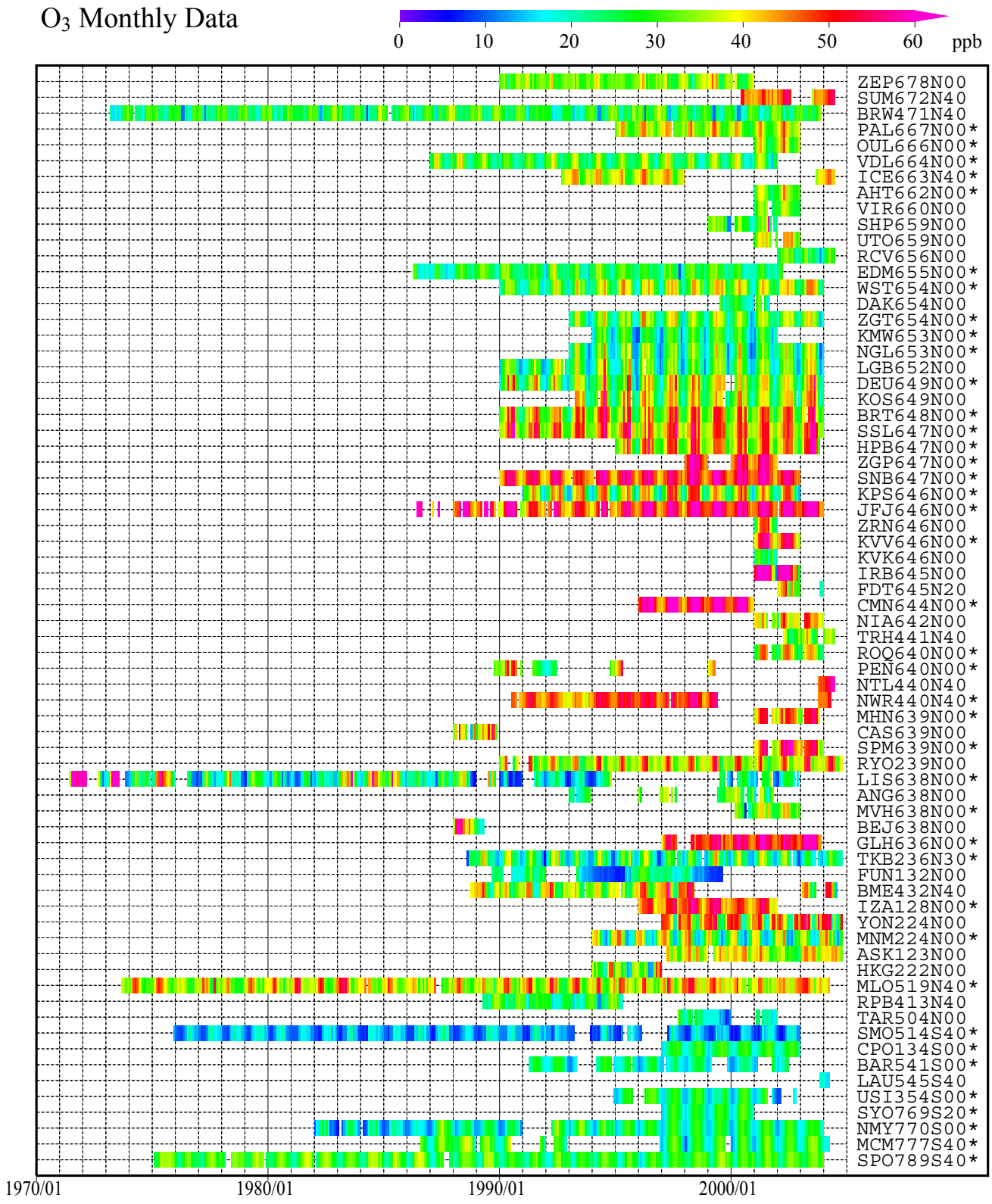


Plate 7.1 Monthly mean $O_3$ concentrations for all sites reported to the WDCGG illustrated in colors that change with the concentration. The sites are set from north to south. It is shown that an asterisk incidental to station index is one peak type in the analysis shown in Fig 7.1.

# 7. Surface Ozone ($O_3$)

## Basic information on surface ozone ($O_3$) with regard to environmental issues

Ozone ($O_3$) plays an important role in the atmospheric environment through radiative and chemical processes. $O_3$ absorbs UV radiation in the stratosphere, and this energy influences the temperature profile and circulation in the stratosphere. $O_3$ also absorbs IR radiation, and is thus one of the greenhouse gases in the troposphere. Tropospheric $O_3$ accounts for less than 10% of atmospheric $O_3$, but tropospheric $O_3$ is the third most important greenhouse gas after $CO_2$ and $CH_4$ (IPCC, 2001), and is also a chemically reactive gas producing OH radicals that control atmospheric concentrations of many greenhouse gases, such as $CH_4$ through chemical reactions. $O_3$ differs markedly from other greenhouse gases (such as $CO_2$, $CH_4$, $N_2O$ and CFCs). $O_3$ does not have direct natural sources, but is produced in the atmosphere, and its concentration ranges from around 10 ppb near the remote Earth's surface to about 10 ppm in the stratosphere. In contrast to $O_3$, $CO_2$, $CH_4$, $N_2O$ and halocarbons (*e.g.*, CFCs) are relatively uniform—hence the term "well-mixed greenhouse gases".

A variation in $O_3$ near the Earth's surface (the so-called "surface $O_3$") reflects various reactions involving $O_3$. Tropospheric $O_3$ is partly transported from the stratosphere, while the rest is produced chemically in the troposphere itself, especially near the Earth's surface where various $O_3$ precursors are emitted. At the same time, $O_3$ is destroyed mainly through chemical reactions with OH radicals and deposition at the Earth's surface.

$O_3$ is produced in the troposphere through oxidation of precursors, *i.e.*, CO or hydrocarbons in the presence of high concentrations of $NO_x$. As mentioned in following chapters, most of these substances (the so-called "$O_3$ precursors") are anthropogenic. As they are localized and their lifetimes are generally short, the distribution of surface $O_3$, produced from anthropogenic precursors, is also localized and time-variant.

Surface $O_3$ is estimated to have increased since pre-industrial times (IPCC, 2001).

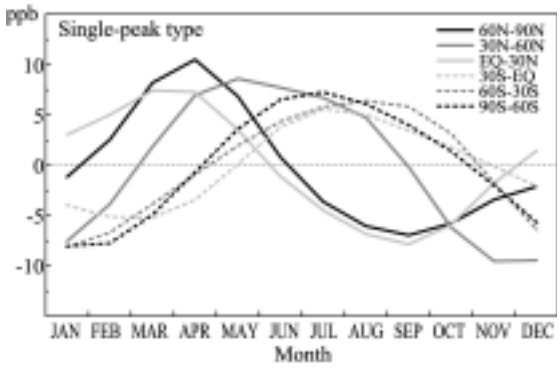


Fig. 7.1 Average seasonal cycles of single-peak type for each 30° latitudinal zone from which the long-term trends were subtracted.

## Annual variation of surface $O_3$

The World Data Centre for surface $O_3$ was transferred from NILU to JMA in August 2002. The map at the beginning of this chapter shows observation sites that have submitted $O_3$ data to the WDCGG.

The monthly mean $O_3$ data from all stations submitted to the WDCGG are shown in Plate 7.1. In the plate, concentration levels are illustrated by different colours. Please note that the data on surface $O_3$ is reported in two units, *i.e.*, mixing ratio (ppb) and weight per volume ($\mu g/m^3$) at 25°C. Weights per volume ($\mu g/m^3$) are converted to mixing ratios (ppb) as follows:

$$X_p\,[ppb] = (R * T / M / P_0) * 10 * X_g\,[\mu g/m^3]$$

where R is the molar gas constant (8.31451 [J/K/mol]),
T is the absolute temperature reported by an individual station,
M is the molecular weight of $O_3$ (47.9982), and
$P_0$ is the standard pressure (1013.25 [hPa]).

The concentration of surface $O_3$ varies from station to station, many of which are located in Europe. Moreover, the seasonal and interannual variation is relatively large at most stations and so it is difficult to identify a general long-term trend in surface $O_3$ concentrations.

Figures 7.1 and 7.2 show average seasonal cycles from which the long-term trends were subtracted for each 30° latitudinal zone of a single- or multi-peak type. The seasonal cycles for each site can be divided into two types: a single-peak type that has a maximum monthly mean, and a multi-peak type that has more than one annual maximum. One single-peak type, the Southern Hemisphere site, is not shown in Figure 7.1. The maximum concentration of the single-peak type appears in April in northern high and low latitudes and in May in northern mid-latitudes. The delayed peak in the mid-latitudes may be attributed to the air pollution in Europe given that most mid-latitude stations are located on this continent. Relatively high spring maximum concentrations were observed at Sonnblick, Niwot Ridge, Assekrem and Mauna Loa, all of which are located at high altitudes (higher than

2700 m).

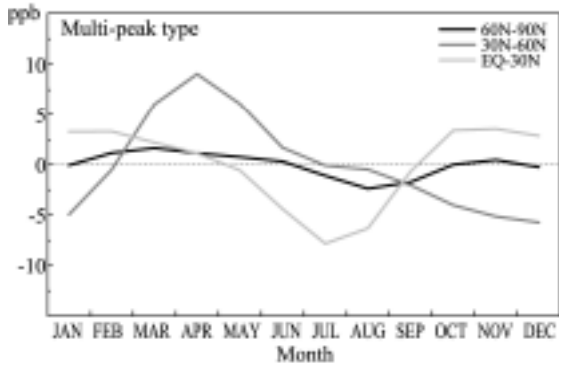


Fig. 7.2 Average seasonal cycles of multi-peak type for each 30° latitudinal zone from which the long-term trends were subtracted.

# 8.
# CARBON MONOXIDE (CO)

● :*IN SITU* STATION
△ :FLASK STATION
□ :FLASK SAMPLING (SHIP)

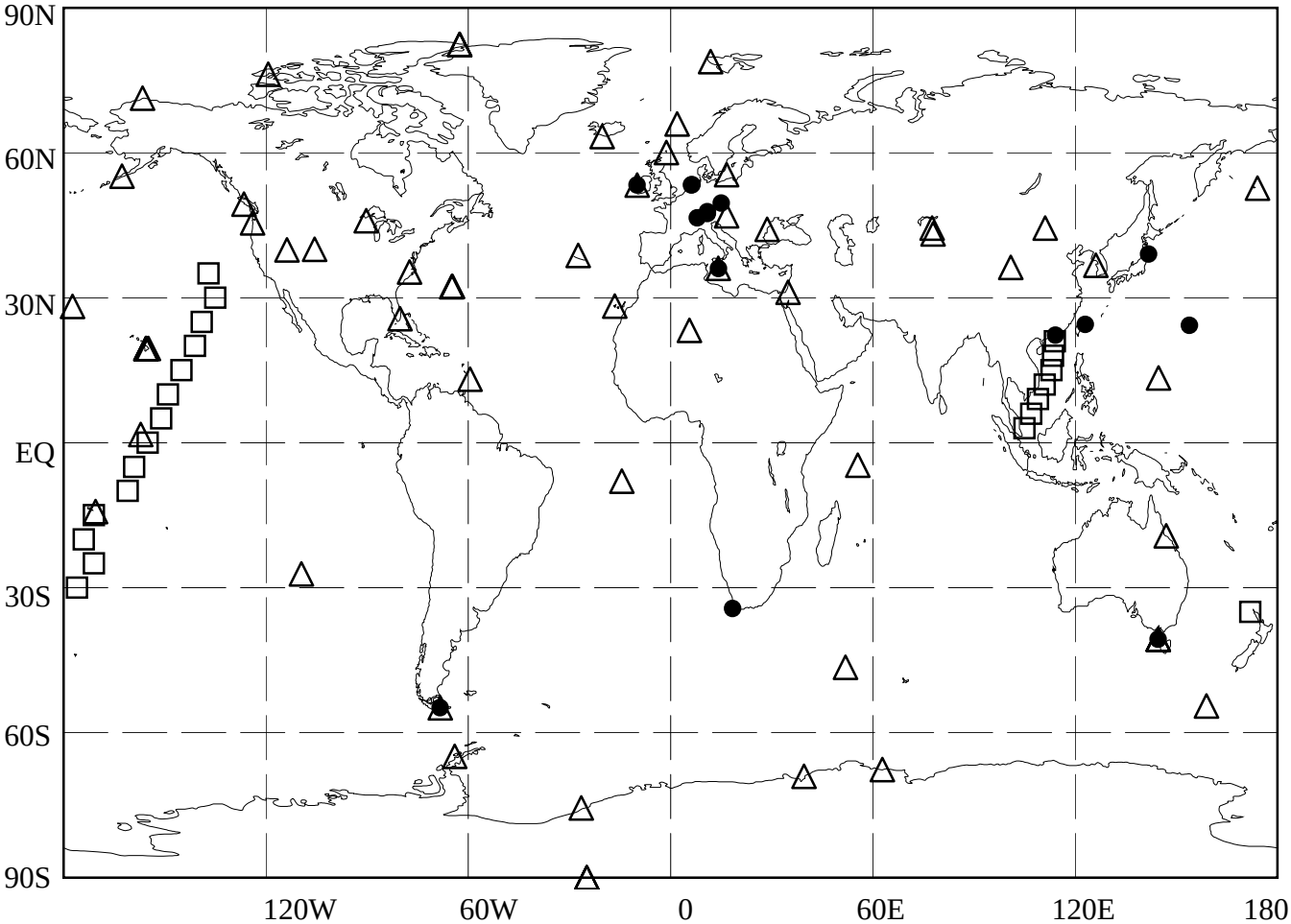

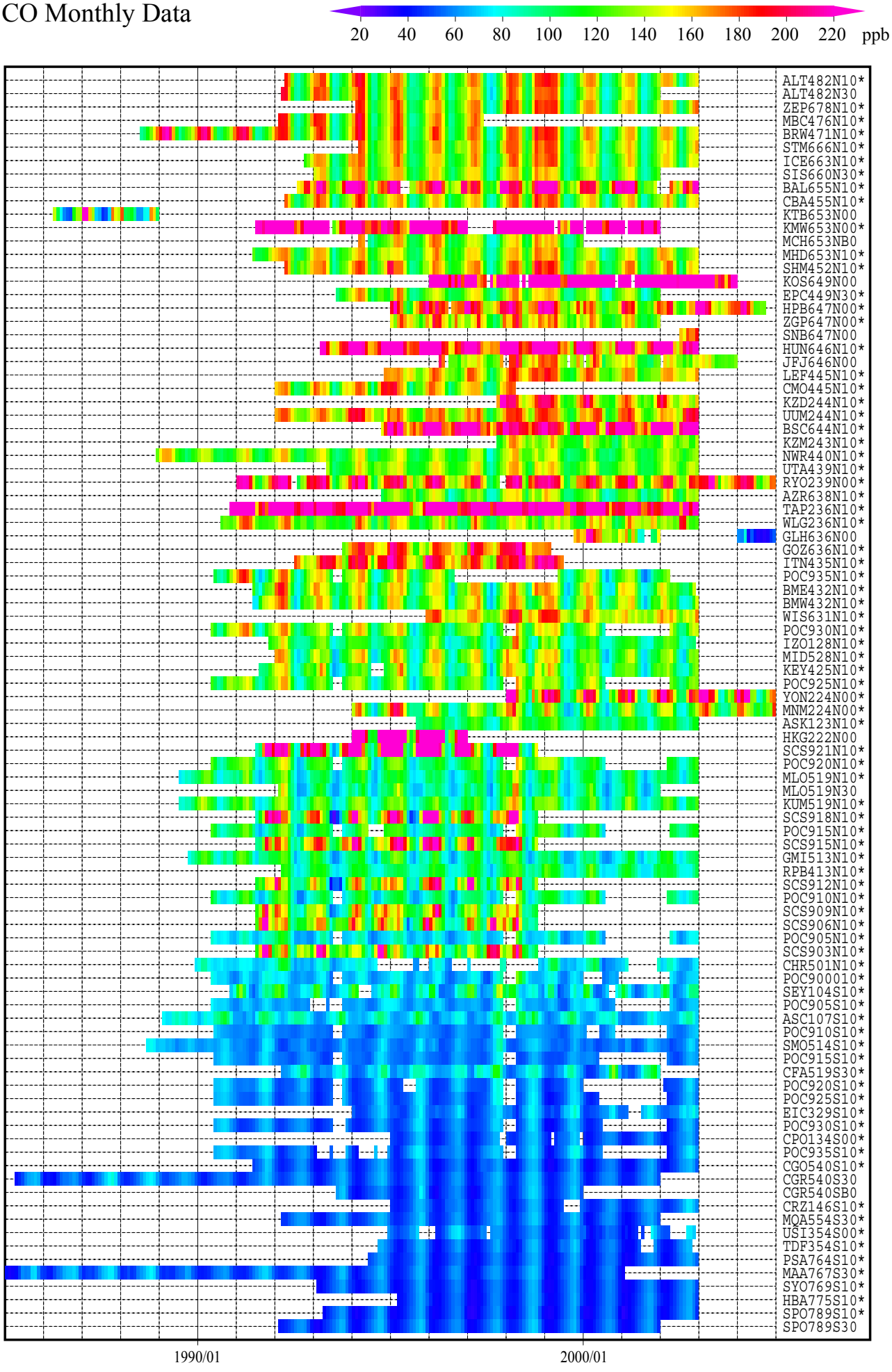


Plate 8.1 Monthly mean concentrations of CO for all stations reported to the WDCGG. The stations are set from north to south. Station index with an asterisk shows the station used in the analysis shown in Plate 8.2.

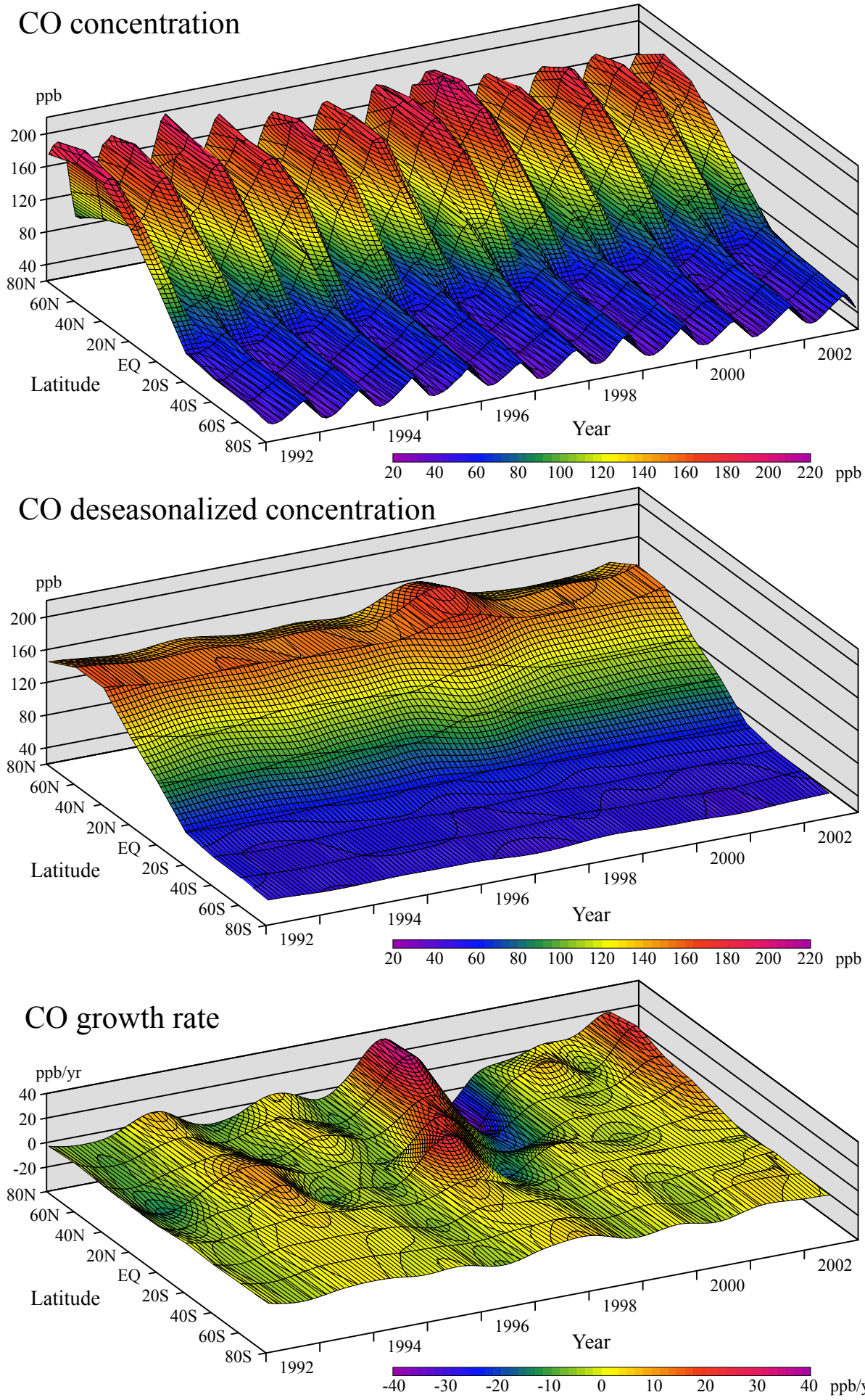


Plate 8.2 Variation of zonally averaged monthly mean CO concentrations (top), deseasonalized concentrations (middle), and growth rates (buttom). Zonally averaged concentrations are calculated for each 20° zone. Deseasonalized concentrations and growth rates are derived as described in Chapter 2.

# 8. Carbon Monoxide (CO)

## Basic information on CO with regard to environmental issues

Carbon monoxide (CO) is not a significant greenhouse gas as it absorbs little infrared radiation from the Earth. However, it does have an influence on oxidisation in the atmosphere through interaction with hydroxyl radicals (OH), which also react with methane, halocarbons and tropospheric ozone. The eventual indirect influence of current CO emission on radiative forcing has been estimated to be greater than the direct influence of $N_2O$ (Daniel and Solomon, 1998). In addition, CO is identified in IPCC (2001) as an important indirect greenhouse gas.

Most of the significant sources and sinks of CO have been identified, but there are large uncertainties in the CO budget. Sources of atmospheric CO include fossil fuel combustion and biomass burning along with the oxidisation of both natural and anthropogenic methane and non-methane hydrocarbons (NMHC). Major sinks are primarily reaction with OH and surface deposition. The measurement of carbon isotopic partitioning in CO should provide constraints for reducing these uncertainties. Issues of calibration and the consistency of measurements between laboratories still remain a concern. CO measurements in ice cores have indicated that the CO concentration of about 50 ppb has not changed markedly during the last two millennia over central Antarctica and that it increased to 110 ppb in 1950 in Greenland (Haan and Raynaud, 1998).

## Annual variation of CO in the atmosphere

The map at the beginning of this chapter shows observation sites that have submitted CO data to the WDCGG. The time series of monthly mean CO data from all the stations that submitted to WDCGG are shown in Plate 8.1. Concentration levels are illustrated by different colours. Global, hemispheric and zonal mean concentrations were calculated based on selected stations (see the caption for Plate 8.2).

The three-dimensional representations of latitudinal distribution of atmospheric CO concentration, deseasonalized concentrations and growth rate are shown in Plate 8.2. The concentrations are clearly dependent on latitude and exhibit seasonal variations.

Please note that the CO data are reported in various units, *i.e.*, ppb, $\mu g/m^3$-25°C, $\mu g/m^3$-20°C and $mg/m^3$-25°C. All units are converted to ppb as follows:

$$X_p\,[ppb] = (R * T / M / P_0) * 10 * X_g\,[\mu g/m^3]$$
$$X_p\,[ppb] = (R * T / M / P_0) * 10^4 * X_g\,[mg/m^3]$$

where R is the molar gas constant (8.31451 [J/K/mol]),
T is the absolute temperature reported by an individual station,
M is the molecular weight of CO (28.0101), and
$P_0$ is the standard pressure (1013.25 [hPa]).

Global monthly mean concentrations, their deseasonalized long-term trends and growth rates are shown in Figure 8.1.

Clear seasonal variations were seen. WMO (1999a) reported that the increasing trend in CO concentration of slightly less than 1% per year before the mid-1980s appears to have been reversed in the late 1980s, but the significant long-term global trend is not seen after 1991. Growth rates were high in 1993/1994, 1997/1998 and 2002, and low in 1992 and 1998/1999. The global annual mean concentration was about 98 ppb in 2002.

Figure 8.2 shows the monthly mean concentrations and their deseasonalized long-term trends for each 30° latitudinal zone. A seasonal variation is seen in both hemispheres. In the Northern Hemisphere, the concentration is higher in the winter season. Amplitudes of the seasonal cycle are larger in the Northern Hemisphere than in the Southern Hemisphere.

Figure 8.3 shows the deseasonalized long-term trends and growth rates for each 30° latitudinal zone. Deseasonalized long-term trends clearly showed that concentrations are highest in the northern mid-latitudes, suggesting intense anthropogenic CO sources in these regions. CO concentrations are generally higher in northern than in southern regions. A negative growth rate was seen in 1992 in all latitudes. Novelli *et al.* (1998) reported a clear decline in CO concentrations from late 1991 through mid-1993, with a subsequent recovery from mid-1993 through mid-1994. The

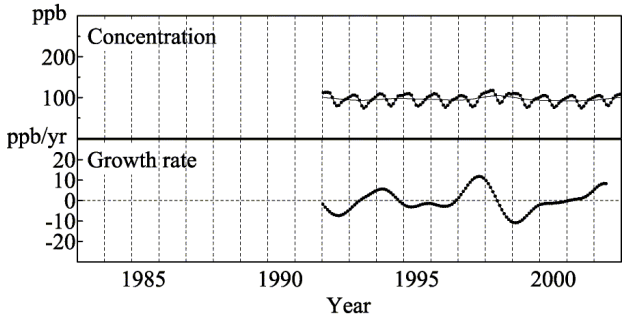


Fig. 8.1 Global monthly mean concentrations (thick line and dots) and deseasonalized long-term trends (thin line) (top) and the growth rate (bottom) from 1992 to 2002.

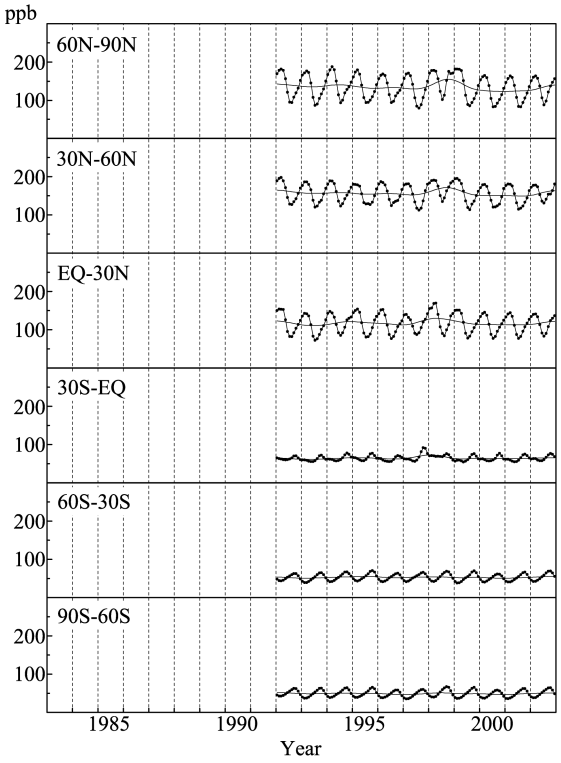


Fig. 8.2 Monthly mean CO concentrations (thick lines and dots) and deseasonalized long-term trends (thin lines) from 1992 to 2002 for each 30° latitudinal zone.

decline in CO concentrations almost coincides with the decrease in growth rate of $CH_4$ concentration, which can be ascribed to the variations in their common sink. Enhanced stratospheric ozone depletion due to the increase in volcanic aerosols from the eruption of Mt. Pinatubo in 1991 may have increased the concentration of OH, which reacts with both CO and $CH_4$ (Dlugokencky *et al.*, 1996). Increases in CO concentrations were observed from 1997 to 1998 in northern latitudes and southern low latitudes. This increase was attributed to the severe biomass burning around Indonesia in late 1997 and that around Siberia between summer and autumn 1998 (Novelli *et al.*, 1998). Duncan *et al.* (2003) also suggested that CO emission in 1997 and 1998 was 19-32% greater than that in 1999. The concentrations returned to normal levels after 1999, but the growth rates in the Northern Hemisphere increased again substantially in 2002.

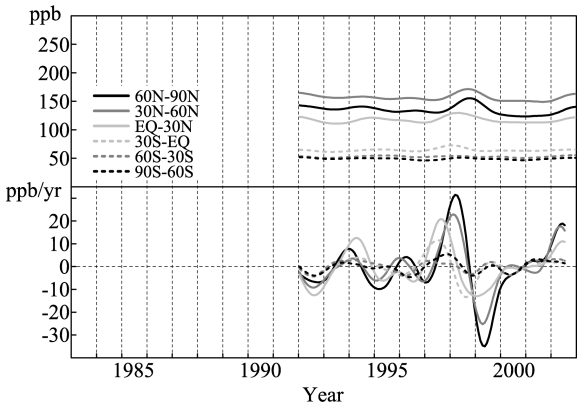


Fig. 8.3 Deseasonalized long-term trends (top) and growth rates (bottom) for each 30° latitudinal zone.

## Seasonal cycle of CO in the atmosphere

Figure 8.4 shows the average seasonal cycles for each 30° latitudinal zone from which the long-term trends were subtracted. The seasonal cycle of CO is mainly driven by seasonal variations in OH concentration, which acts as a CO sink. Furthermore, emission and oxidation as CO sources and the large-scale transportation of CO are additional factors, although the seasonality of emission and oxidation is relatively weak compared with that of the OH concentration. This seasonality and the roughly 2-month lifetime of CO produce a sharp decrease in early summer and a relatively gradual increase in autumn. Semi-annual features evident in the southern low latitudes may be attributed to the cross-equatorial transportation of CO from the Northern Hemisphere.

Direct CO emission also brings about intense seasonal variation on some occasions. Novelli *et al.* (1998) showed with a model of a box representing the well-mixed northern layer and a box representing the southern boundary layer that seasonal cycles are strongly affected by changes in emission from biomass burning in both hemispheres. Using observation data for the upper troposphere, Matsueda *et al.* (1998) showed that high CO concentrations in southern low latitudes from October to November were enhanced by tropical biomass burning.

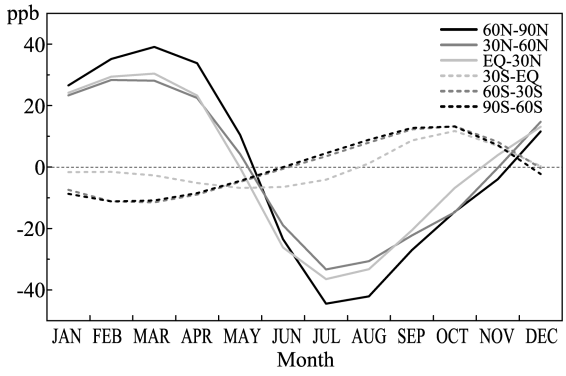


Fig. 8.4 Average seasonal cycles for each 30° latitudinal zone from which the long-term trends were subtracted.

# 9.
# NITROGEN MONOXIDE (NO)
# and
# NITROGEN DIOXIDE ($NO_2$)

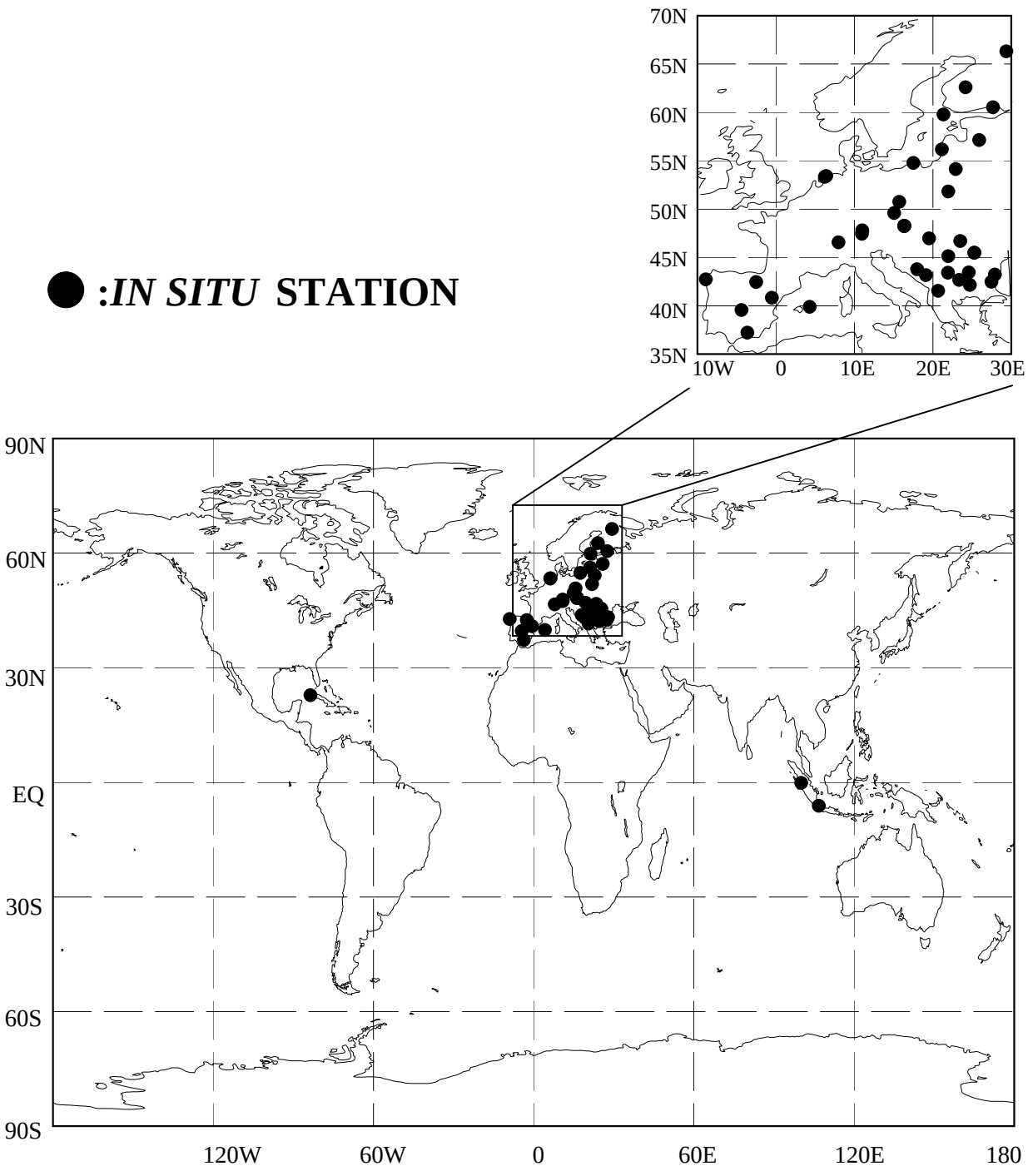

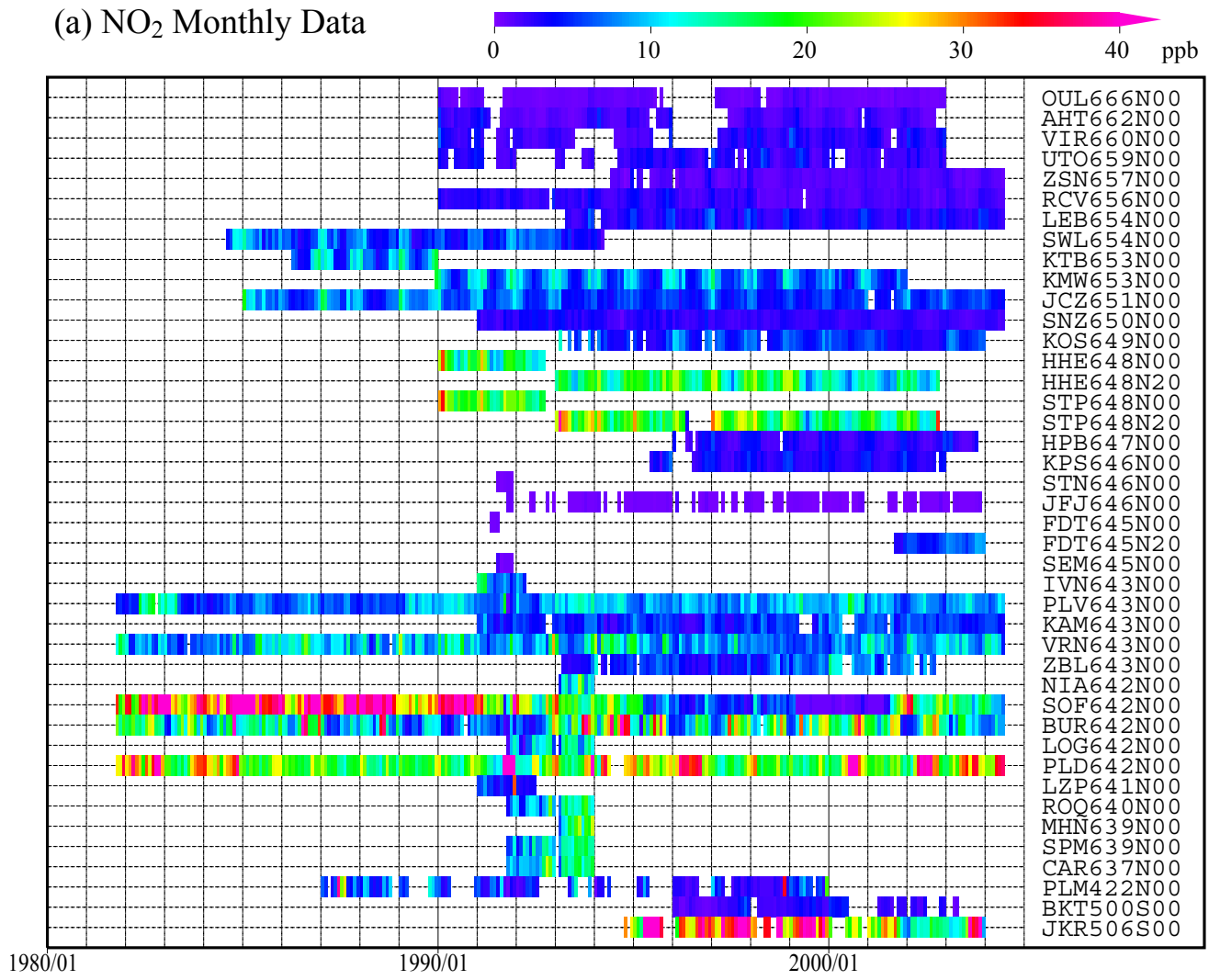


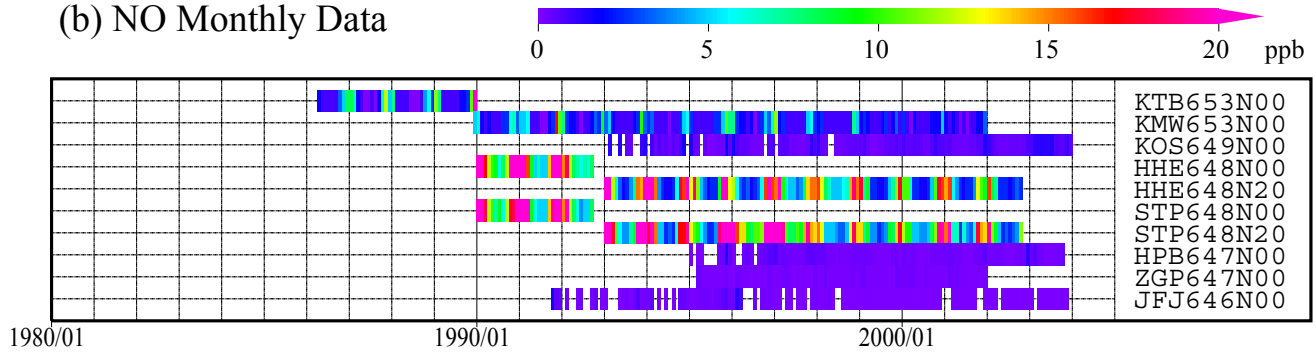


Plate 9.1 Monthly mean (a) $NO_2$ and (b) NO concentrations for all sites reported to the WDCGG illustrated in colors that change with the concentration. The sites are set from north to south.

# 9. Nitrogen Monoxide (NO) and Nitrogen Dioxide ($NO_2$)

## Basic information on NO and $NO_2$ with regard to environmental issues

Nitrogen oxides ($NO_x$, *i.e.*, NO and $NO_2$) are not greenhouse gases, but affect hydroxyl radicals (OH), which control concentrations of methane ($CH_4$), carbon monoxide (CO) and hydrochlorofluorocarbons (HCFCs). In the presence of $NO_x$, CO and hydrocarbons are oxidised to produce ozone ($O_3$) in the troposphere, which is a greenhouse gas. Thus, $NO_x$ can influence the Earth's radiative balance and, by generating OH, alter the oxidisation capacity of the atmosphere.

Sources of $NO_x$ include fossil fuel combustion, biomass burning, lightning and soil (IPCC, 2001). The dominant sink of $NO_x$ in the atmosphere is its conversion into nitric acid ($HNO_3$) and peroxyacetylnitrate (PAN), which are eventually removed by dry or wet deposition. In some cases, $NO_x$ are removed from the atmosphere directly by dry deposition. Anthropogenic emission of $NO_x$ is currently one of the major causes of acid rain and deposition. $NO_x$ concentrations show large variability in both space and time because of the species' short lifetimes and uneven source distribution .

## Annual variation of NO and $NO_2$

Observation stations that submitted data for $NO_2$ and NO to the WDCGG are shown on the map at the beginning of this chapter. Most of the contributing stations are located in Europe.

The time series of monthly mean NO and $NO_2$ data from all stations submitted to the WDCGG are shown in Plate 9.1. In this plate, concentration levels are illustrated in different colours. Please note that the data for $NO_x$ are reported in various units, *i.e.*, ppb, $\mu g/m^3$-25°C, $\mu g/m^3$-20°C, $\mu gN/m^3$-25°C and $mg/m^3$-25°C.

All units are converted to ppb as follows:

$X_p$ [ppb] = (R * T / M / $P_0$) * 10 * $X_g$ [$\mu g/m^3$]
$X_p$ [ppb] = (R * T / M / $P_0$) * $10^4$ * $X_g$ [$mg/m^3$]
$X_p$ [ppb] = (R * T / $M_N$ / $P_0$) * 10 * $X_g$ [$\mu gN/m^3$]

where R is the molar gas constant (8.31451 [J/K/mol]),
T is the absolute temperature reported by an individual station,
M is the molecular weight of NO (30.00614) or $NO_2$ (46.00554),
$M_N$ is the atomic weight of N (14.00674), and
$P_0$ is the standard pressure (1013.25 [hPa]).

As their sources are localised and their lifetimes are short, the distributions of NO and $NO_2$ are also localised and vary over time. Due to the high temporal variability of $NO_2$ concentrations for each observation site, it was difficult to identify a long-term trend. A number of stations located in southern Europe showed higher concentrations, and some stations exhibited a winter enhancement of $NO_2$.

As the number of observation sites for NO is quite small, it is difficult to identify increasing or decreasing trends for NO concentrations.

# 10.
# SULPHUR DIOXIDE
# ($SO_2$)

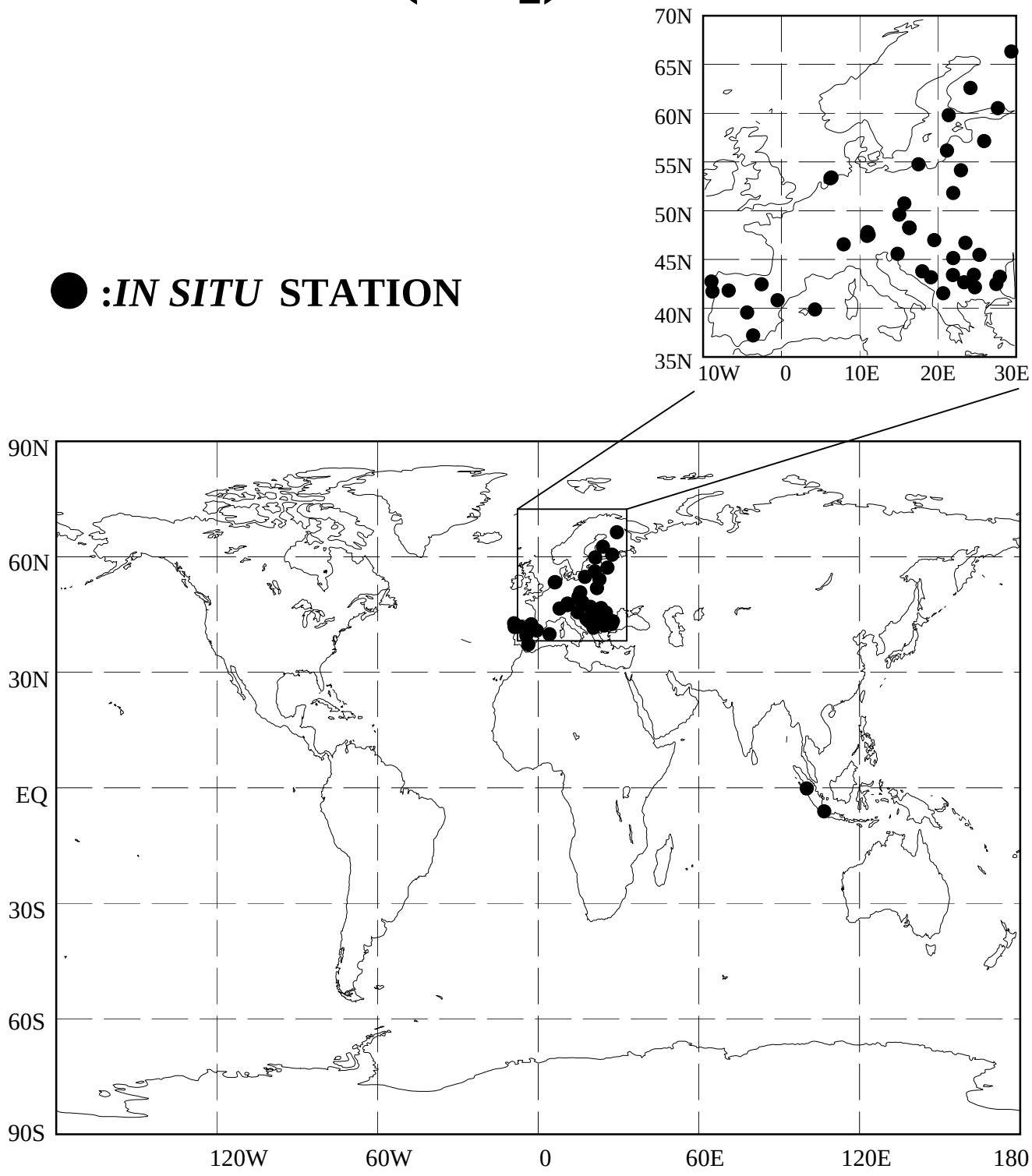

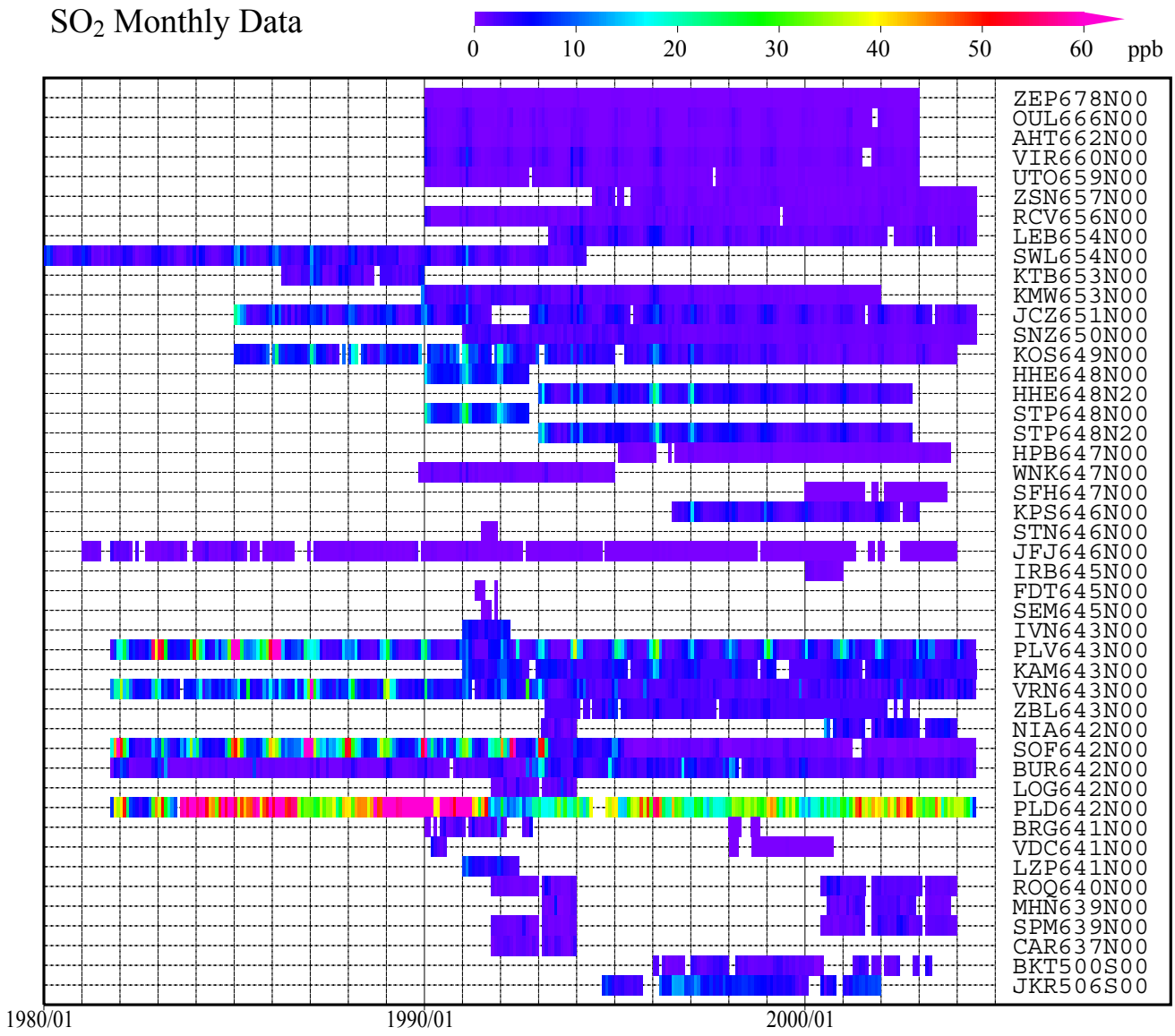


Plate 10.1 Monthly mean $SO_2$ concentrations for all sites reported to the WDCGG illustrated in colors that change with the concentration. The sites are set from north to south.

# 10. Sulphur Dioxide ($SO_2$)

## Basic information on $SO_2$ with regard to environmental issues

Sulphur dioxide ($SO_2$) is not a greenhouse gas, but is a precursor of atmospheric sulphuric acid ($H_2SO_4$) or sulphate aerosol. $SO_2$ is oxidised by hydroxyl radicals (OH) to form sulphuric acid, which then produces aerosols through photochemical gas-to-particle conversion. While the $SO_2$ reaction with OH is much slower than with $NO_2$, $SO_2$ dissolves readily in suspended liquid droplets in the atmosphere.

Sources of $SO_2$ include fossil fuel combustion by industry, biomass burning, volcanoes and the oxidation of dimethylsulphide (DMS) from the oceans (IPCC, 2001). Major $SO_2$ sinks are oxidation by OH and deposition onto wet surfaces. Anthropogenic $SO_2$ has caused acid rain and deposition throughout the industrial era. $SO_2$ concentrations show large variations in both space and time because of the species' short lifetime and uneven anthropogenic source distribution.

## Annual variation of $SO_2$

The map at the beginning of this chapter shows observation sites that have submitted $SO_2$ data to the WDCGG. Most of the contributing stations are located in Europe.

The monthly mean $SO_2$ data from all stations submitted to the WDCGG are shown in Plate 10.1. In this plate, concentration levels are illustrated in different colours. Please note that the data for $SO_2$ are reported in various units, *i.e.*, ppb, $\mu g/m^3$, $mg/m^3$ and $\mu gS/m^3$.

All units are converted to ppb as follows:

$X_p\ [ppb] = (R * T / M / P_0) * 10 * X_g\ [\mu g/m^3]$
$X_p\ [ppb] = (R * T / M / P_0) * 10^4 * X_g\ [mg/m^3]$
$X_p\ [ppb] = (R * T / M_S / P_0) * 10 * X_g\ [\mu gS/m^3]$

where R is the molar gas constant (8.31451 [J/K/mol]),
T is the absolute temperature reported by an individual station,
M is the molecular weight of $SO_2$ (64.0648),
$M_S$ is the atomic weight of S (32.066), and
$P_0$ is the standard pressure (1013.25 [hPa]).

Certain stations in southern Europe showed higher concentrations. However, it was difficult to identify an increasing or decreasing trend for $SO_2$ concentrations.

# REFERENCES

# References


Angert A., S. Biraud, C. Bonfils, W. Buermann, I. Fung, $CO_2$ seasonality indicates origins of post-Pinatubo sink, *Geophys. Res. Lett.*, **31**, L11103, doi:10.1029/2004GL019760, 2004.

Bartlett, B. B., G. W. Sache, T. Slate, C. Haward, and D. D. Blake, Large-scale distribution of $CH_4$ in the western Pacific: Sources and transport from the Asian continent, *J. Geophys. Res.*, **108 (D20),** 8807, doi:10.1029/2002JD003076, 2003.

Bekki, S., K. S. Law, and J. A. Pyle, Effects of ozone depletion on atmospheric $CH_4$ and CO concentrations, *Nature*, **371**, 595-597, 1994.

Bekki, S., K. S. Law, Sensitivity of atmospheric $CH_4$ growth rate to global temperature change observed from 1980 to 1992, *Tellus*, **49B**, 409-416, 1997.

Ciais, P., P. P. Tans, M. Trolier, J. W. C. White, and R. J. Francey, A large northern hemisphere terrestrial $CO_2$ sink indicated by the $^{13}C/^{12}C$ ratio of atmospheric $CO_2$, *Science*, **269**, 1098-1102, 1995.

Cleveland, W. S., S. J. Devlin, Locally weighted regression: an approach to regression analysis by local fitting, *J. Amer. Statist. Assn.*, **83**, 596-610, 1988.

Conway, T. J., P. P. Tans, L. S. Waterman, K. W. Thoning, D. R. Kitzis, K. A. Masarie, and N. Zhang, Evidence for interannual variability of the carbon cycle from the National Oceanic and Atmospheric Administration/Climate Monitoring and Diagnostics Laboratory global air sampling network, *J. Geophys. Res.*, **99**, 22831-22855, 1994.

Daniel, J. S. and S. Solomon, On the climate forcing of carbon monoxide. *J. Geophys. Res.*, **103(D11)**, 13249-13260, 1998.

Dettinger, M. D. and M. Ghill, Seasonal and interannual variations of atmospheric $CO_2$ and climate, *Tellus*, **50B**, 1-24, 1998.

Dlugokencky, E. J., L. P. Steele, P. M. Lang, and K. A. Masarie, The grouth rate and distribution of atmospheric methane, *J. Geophys. Res.*, **99**, 17021-17043, 1994.

Dlugokencky, E. J., E. G. Dutton, P. C. Novelli, P. P. Tans, K. A. Masarie, K. O. Lantz, and S. Mardronich, Changes in $CH_4$ and CO growth rates after the eruption of Mt. Pinatubo and their link with changes in tropical tropospheric UV flux, *Geophys. Res. Lett.*, **23**, 2761-2764, 1996.

Dlugokencky, E. J., K. A. Masarie, P. M. Lang, and P. P. Tans, Continuing decline in the growth rate of the atmospheric methane burden, *Nature*, **393**, 447-450, 1998.

Dlugokencky, E. J., B. P. Walter, K. A. Masarie, P. M. Lang and E .S. Kasischke, Measurements of an anomalous global methane increase during 1998, *Geophys. Res. Lett.*, **28**, 499-502, 2001.

Duchon, C. E., Lanczos filtering in one and two dimensions, *J. Appl. Meteor.*, **18**, 1016-1022, 1979.

Duncan, B. N., I. Bey, M. Chin, L. J. Mickley, T. D. Fairlie, R. V. Martin, and H. Matsueda, Indonesian wildfires of 1997: Impact on tropospheric chemistry , *J. Geophys. Res.*, **108 (D15)**, 4458, doi:10.1029/2002JD003195, 2003.

Etherridge, D. M., L. P. Steele, R. J. Francey, and R. L. Langenfelds, Atmospheric methane between 1000 A.D. and present: Evidence of anthropogenic emissions and climatic variability, *J. Geophys. Res.*, **103**, 15979-15993, 1998.

Francey, R. J., P. P. Tans, C. E. Allison, I. G. Enting, J. W. C. White, and M. Trolier, Changes in oceanic and terrestrial carbon uptake since 1982, *Nature*, **373**, 326-330, 1995.

Gu, L., D. D. Baldocchi, S. C. Wofsy, J. W. Munger, J. J. Michalsky, S. P. Urbanski , and T. A. Bonden, Response of a deciduous forest to the Mount Pinatubo eruption enhanced photosysthesis, *Science*, **299**, 2035-2038, 2003.

Haan, D. and D. Raynaud, Ice core record of CO variations during the last two millennia: atmospheric implications and chemical interactions within the Greenland ice, *Tellus*, **50B**, 253-262, 1998.

Hansen, J., A.Lacis, R. Ruedy, and M. Sato, Potential Clim. Impact of Mount-Pinatubo Eruption, *Geophys. Res. Lett.*, **19(2)**, 215-218, 1992.

IPCC, Climate Change 2001: The Science Basis, Contribution of Working Group I to the Third Assessment Report of the Intergovernmental Panel on Climate Change, Cambridge University Press, Cambridge, United Kingdom and New York, NY, USA, 881pp, 2001.

JMA, Climate change monitoring report 1998, Japan Meteorological Agency, Tokyo, Japan, 49 pp, 1999.

Keeling, C. D., R. B. Bacastow, A. F. Carter, S. C. Piper, T. P. Whorf, M. Heimann, W. G. Mook, and H. Roeloffzen, A three-dimensional model of atmospheric $CO_2$ transport based on observed winds: 1. Analysis of observational data, in aspects of climate variability in the Pacific and the Western Americas, edited by D. H. Peterson, *Geophysical Monograph* **55**, 165-236, American Geophysical Union,

Washington, D.C, 1989.

Keeling, C. D., T. P. Whorf, M. Wahlen, and J. van der Plicht, Interannual extremes in the rate of rise of atmospheric carbon dioxide since 1980, *Nature*, **375**, 666-670, 1995.

Lambert, G. , P. Monfray, B. Ardouin, G. Bonsang,, A.Gaudry, V. Kazan and G. Polian, Year-to-year changes in atmospheric $CO_2$, *Tells*, **47B**, 35-55,1995.

Lelieveld, J., P. J. Crutzen, and F. J. Dentener: Changing concentration, lifetime and climate forcing of atmospheric methane, *Tellus*, **50B**, 128-150, 1998.

Lowe, D. C., M. R. Manning, G. W. Brailsford, and A. M. Bromley, The 1991-1992 atmospheric methane anomaly: Southern hemisphere $^{13}C$ decrease and growth rate fluctuations, *Geophys. Res. Lett.*, **24**, 857-860, 1997.

Morimoto, S., T. Nakazawa, K. Higuchi, and S. Aoki, Latitudinal distribution of atmospheric $CO_2$ sources nad sinks inferred by $\delta\ ^{13}C$ measurements from 1985 to 1991. *J. Geophys. Res*., **105(D19)**, 24,315-24,326, 2000,

Matsueda, H., H. Inoue, Y. Sawa, Y. Tsutsumi, and M. Ishii, Carbon monoxide in the upper troposphere over the western Pacific between 1993 and 1996, *J. Geophys. Res.*, **103**, 19093-19110, 1998.

Matsueda, H., S. Taguchi, H.Y. Inoue, and M. Ishii, A large impact of tropical biomass burning on CO and $CO_2$ in the upper troposphere. Science in China (Series C), **45**, 116-125, 2002.

Nakazawa, T., K. Miyashita, S. Aoki, and M. Tanaka, Temporal and spatial variations of upper tropospheric and lower stratospheric carbon dioxide, *Tellus*, **43B**, 106-117, 1991.

Nakazawa, T., S. Morimoto, S. Aoki and M. Tanaka, Time and space variations of the carbon isotopic ratio of tropospheric carbon dioxide over Japan, *Tellus*, **45B**, 258-274, 1993.

Nakazawa, T., S. Morimoto, S. Aoki and M. Tanaka, Temporal and spatial variations of the carbon isotopic ratio of atmospheric carbon dioxide in the western Pacific region, *J. Geophys. Res.*, **102**, 1271-1285, 1997a.

Nakazawa, T., S. Murayama, M. Toi, M. Ishizawa, K. Otonashi, S. Aoki and S. Yamamoto, Temporal variations of $CO_2$ concentration and its carbon and oxygen isotopic ratios in a temperate forest in the central part of the main island of Japan, *Tellus*, **49B**, 364-381, 1997b.

Nemry, B., L. Francois, P. Warnant, F. Robinet, and J.C. Gerard, The seasonality of the $CO_2$ exchange between the atmosphere and the land biosphere: A study with a global mechanistic vegetation model, *J. Geophys. Res.*, **101**, 7111-7125, 1996.

Novelli, P. C., K. A. Masarie, and P. M. Lang, Distributions and recent changes of carbon monoxide in the lower troposphere, *J. Geophys. Res.*, **103**, 19015-19033, 1998.

Prinn, R. G., J. Huang, R. F. Weiss, D. M. Cunnold, P. J. Fraser, P. G. Simmonds, A. McCulloch, C. Harth, P. Salameh, S. O'Doherty, R. H. J. Wang, L. Porter, B. R. Miller, Evidence for substantial variations of atmospheric hydroxyl radicals in the past two decades, *Science*, **292**, 1882-1888, 2001.

Rayner, P. J., I. G. Enting, R. J. Francey and R. Langenfelds, Reconstructing the recent carbon cycle from atmospheric $CO_2$,$\delta^{13}C$ and $O_2/N_2$ observations, *Tellus*, **51B**, 213-232, 1999.

Ramonet, M. and P. Monfray, $CO_2$ baseline concept in 3-D atmospheric transport models, *Tellus*, **48B**, 502-520, 1996.

Stenchikov, G., A.Robock, V. Ramaswamy, M. D. Schwarzkopf, K. Hamilton, and S. Ramachandran, Arctic Oscillation response to the 1991 Mount Pinatubo eruption: Effects of volcanic aerosols and ozone depletion, J. Geophys. Res., 107(D24), 4803, doi:10.1029/2002JD002090., 2002.

Tanaka, M., T. Nakazawa, S. Aoki, Seasonal and meridional variations of atmospheric carbon dioxide in the lower troposphere of the northern and southern hemispheres, *Tellus*, **39B**, 29-41, 1987.

Thoning, K. W., P. P. Tans, and W. D. Komhyr, Atmospheric carbon dioxide at Mauna Loa observatory, 2. Analysis of the NOAA GMCC data, 1974-1985, *J. Geophys. Res.*, **94**, 8549-8565, 1989.

Watanabe, F., O. Uchino, Y. Joo, M. Aono, K. Higashijima, Y. Hirano, K. Tsuboi, and K. Suda, Interannual variation of grouth rate of atmospheric carbon dioxide concentration observed at the JMA's three monitoring stations: Large increase in concentration of atmospheric carbon dioxide in 1998, J. Meteor. Soc. Japan, **78**, 673-682, 2000.

Wittenberg, U., M. Heimann, G. Esser, A.D. Mcguire, and W. Sauf, On the influence of biomass burning on the seasonal $CO_2$ signal as observed at monitoring stations, *Global Biogeochem. Cycles*, **12**, 531-544, 1998.

WMO, Scientific assessment of ozone depletion: 1998. WMO global ozone research and monitoring project - Report No. 44, World Meteorological Organization, Geneva, 1999a.

WMO, WMO statement on the status of the global climate in 1998, WMO- No.896, World Meteorological Organization, Geneva, 1999b.

WMO, World Data Centre for Greenhouse Gases (WDCGG) Data Summary, WDCGG No. 22,

84pp, 2000.
WMO, Strategy for the Implementation of the Global Atmosphere Watch Programme (2001-2007), WMO/GAW - Report No. 142, 62pp, 2001.
WMO, World Data Centre for Greenhouse Gases (WDCGG) Data Summary, WDCGG No. 28, 98pp, 2004.

# APPENDICES

# Appendix A Calibration and Standard Scales

**1. Calibration System in the GAW programme**

Under the Global Atmosphere Watch (GAW) programme, World Calibration Centres (WCCs) are responsible for maintaining calibration standards for certain species, establishing instrument calibrations and providing training to the stations. A Reference Standard is designated for each species to be used for all GAW measurements of that species. Table 1 lists the organizations that serve as WCCs and maintain Reference Standards for GAW [*WMO*, 2001].

**Table 1. Overview of the GAW Reference Standards and World Calibration Centres for Greenhouse and Other Related Gases (as of December 2000). The World Calibration Centres Have Assumed Global Responsibilities, Except Where Indicated (Am, Americas; E/A, Europe and Africa; A/O, Asia and the South-West Pacific)**

| Species | Reference Standard | World Calibration Centre |
|---|---|---|
| Carbon Dioxide ($CO_2$) | CMDL | CMDL |
| Methane ($CH_4$) | CMDL (currently being established) | EMPA (Am, E/A) JMA (A/O) |
| Nitrous Oxide ($N_2O$) | CMDL | IFU |
| Chlorofluorocarbons (CFCs) | | |
| Surface Ozone ($O_3$) | NIST | EMPA |
| Carbon Monoxide (CO) | CMDL | EMPA |
| Volatile Organic Compounds (VOCs) | | IFU |
| Sulphur Dioxide ($SO_2$) | | |
| Nitrogen Oxides ($NO_x$) | | |

**2. Carbon Dioxide ($CO_2$)**

In 1995, Climate Monitoring and Diagnostics Laboratory (CMDL) took over the role of CCL from the Scripps Institution of Oceanography (SIO) in San Diego, California, USA. NOAA CMDL, Boulder, Colorado, USA has been designated by WMO as the Central Calibration Laboratory (CCL) responsible for maintenance of the GAW Reference Standard for $CO_2$. As the World Calibration Centre (WCC) for $CO_2$, CMDL maintains a high-precision manometric system for absolute calibration of $CO_2$ as the reference used for GAW measurements throughout the world [*Zhao et al.*, 1997]. It is recommended that the standards of the GAW measurement laboratories be calibrated every two years at the CCL (WMO, 2003).

Under the WMO calibration system, there have been several calibration scales for $CO_2$ data, *e.g.*, SIO-based X74, X85, X87 and X93 scales and the CMDL-based WMO Mole Fraction Scale partially based on the past SIO scales. The CMDL and SIO are working to resolve the possible small differences between their scales. The CCL will adopt the WMO X2002 scale, reflecting historical manometric calibrations of the WMO CCL set of 15 cylinders and the possible small differences between SIO and CMDL calibrations [*CMDL*, 2002].

To assess the differences in standard scales among $CO_2$ measuring laboratories, CMDL organizes intercomparisons or Round Robin experiments endorsed by WMO every few years. Many laboratories participated in the experiments organized in 1991-1992, 1996-1997 and 1999-2000. Table 2 shows the results of the experiments performed in 1996-1997 in which the concentrations measured by various laboratories are compared with the concentrations measured by NOAA/CMDL [*Peterson et al.*, 1999]. In addition, many laboratories compare their standards bilaterally or multilaterally among themselves.

Table 3 lists laboratories contributing $CO_2$ measurement data to WDCGG with standard scales of reported data and history of participation in the WMO intercomparison experiments.

**Table 2. Round Robin Results for Carbon Dioxide Concentration. Differences Between the Concentrations Measured by Various Laboratories and the Concentration Measured by NOAA (Laboratory minus NOAA, ppm)**

| Laboratory | Analysis Date | Concentration Difference (ppm) | | |
|---|---|---|---|---|
| | | Low | Medium | High |

| | | 340-350 ppm | 350-360 ppm | 370-380 ppm |
|---|---|---|---|---|
| NIWA | 1996-02 | 0.02 | 0.10 | 0.20 |
| CSIRO | 1996-05 | -0.07 | -0.02 | -0.02 |
| AES | 1997-06 | -0.04 | 0.00 | -0.02 |
| CMA | 1995-12 | -0.07 | -0.01 | -0.02 |
| Tohoku Univ. | 1996-06 | -0.01 | 0.04 | 0.02 |
| NIES | 1996-08 | -0.02 | 0.09 | 0.12 |
| MRI | 1996-12 | 0.04 | 0.07 | 0.14 |
| JMA | 1997-01 | 0.07 | 0.31 | 0.30 |
| SNU | 1997-03 | 0.24 | 0.13 | 0.29 |
| CFR | 1996-01 | 0.10 | 0.08 | 0.16 |
| IMS | 1996-03 | 0.04 | 0.06 | 0.07 |
| ENEA | 1996-04 | -0.29 | -0.06 | 0.19 |
| UBA | 1996-07 | 0.00 | -0.02 | 0.11 |
| HMS | 1996-12 | -1.22 | -1.04 | -0.80 |

**Table 3. Status of Standard Scales and Calibration/Intercomparison for Carbon Dioxide at Laboratories Contributing to the WDCGG as of October 2002.**

| Laboratory | WDCGG Site Index | Calibration Scale | Most Recent Calibration | WMO Intercomparison |
|---|---|---|---|---|
| Aichi | MKW234N0 | WMO | JMA | |
| CAMS | WLG236N0 | WMO | 1994-01 at SIO | 96/97, 99/00 |
| CESI | PLR645N00 | WMO | 2001-12 at CMDL | 99/00 |
| CMDL | BRW471N0, MLO519N0, SPO789S0, SMO514S0, CMDL flask network* | WMO | 2002-07 at CMDL | 91/92, 96/97, 99/00 |
| CNR | JBN762S0 | WMO | ENEA | |
| CSIRO | CGR540S0, CSIRO flask network** | WMO | 2001-11 at CMDL | 91/92, 96/97, 99/00 |
| ENEA | LMP635N0 | WMO | 2000-08 at CMDL | 91/92, 96/97, 99/00 |
| Heidelberg | | WMO | 1998-10 at CMDL | 96/97, 99/00 |
| HMS | KPS646N0 | WMO | 2000-05 at CMDL | 91/92, 96/97, 99/00 |
| IFU | WNK647N0, ZSP647N00 | SIO 1974 | | 99/00 |
| IGP | HUA312S0 | X81 | | |
| IMS | CMN644N0 | WMO | 1998-10 at CMDL | 91/92, 96/97 |
| INM | IZA128N0 | WMO | 2002-03 at CMDL | 91/92, 96/97, 99/00 |
| NIWA | BAR541S0 | WMO | 1995-11 at SIO | 91/92, 96/97, 99/00 |
| METRI/SNU | KSN233N0 | WMO | 2001-09 | 96/97 |
| JMA | MNM224N0, RYO239N0, YON224N0, ALG99990, EOM99990, RYF99990 | WMO | 2002-03 at CMDL | 91/92, 96/97, 99/00 |
| KMA | AMY236N0 | | | |
| KSNU | ISK242N0 | | MGO | |
| LSCE | AMS137S0, MCH653N0 | WMO | 2002-02 at CMDL | 91/92, 96/97, 99/00 |
| MGO | BER255N0, KOT276N0, KYZ240N0, STC652N0, TER669N0 | X97 | 1991 at SIO | |
| MISU/NILU | ZEP678N0 | WMO | 1996-07 at CMDL | 96/97, 99/00 |
| MRI | TKB236N0, INS9999A, HKH99990, KIY99990, NTU99990, RFM99990, WLT99990 | MRI 1997 | | 91/92, 96/97, 99/00 |

| | | | | |
|---|---|---|---|---|
| MSC | ALT482N0, CSJ451N0, SBL443N0 | WMO | 2001-12 at CMDL | 91/92, 96/97, 99/00 |
| NIES | COI243N0, HAT224N0 | NIES 95 | 2001-09 at CMDL | 96/97, 99/00 |
| NIMH | FDT645N20 | | SIAD SpA, Italy | |
| NIST | | NIST | | 91/92, 96/97, 99/00 |
| RIVM | KMW653N0 | NIST | | |
| Saitama | DDR236N0, URW235N0 | WMO | JMA | |
| SAWS | CPO134S0 | WMO | 1997-06 at CMDL | 99/00 |
| Shizuoka | HMM234N0 | | Nippon Sanso | |
| SIO | | SIO | | 91/92, 96/97, 99/00 |
| Tohoku Univ. | SYO769S0 | Tohoku | | 91/92, 96/97, 99/00 |
| UBA | BRT648N0, DEU649N0, NGL653N0, SSL647N0, LGB652N0, WST654N0, ZGT654N0, ZGP647N0 | WMO | 1998-10 at CMDL | 91/92, 96/97, 99/00 |
| ZAMG | SNB647N00 | WMO | UBA | |

* CMDL flask network: ALT482N10, AMS137S10, ASC107S10, ASK123N10, BAL655N10, BRW471N10, SGI354S10, BSC644N10, NMB123S10, CGO540S10, KUM519N10, CHR501N10, CBA455N10, CRZ146S10, GOZ636N10, EIC329S10, ITN435N10, GMI513N10, HBA775S10, HUN646N10, ICE663N10, KEY425N10, MHD653N10, SEY104S10, MLO519N10, MBC476N10, WLG236N10, NWR440N10, ZEP678N10, STC654N10, STM666N10, POC9XXX10, PSA764S10, LEF445N10, RPB413N10, MID528N10, WIS631N10, SHM452N10, SCS9XXX10, SPO789S10, BMW432N10, AVI417N10, BME432N10, SYO769S10, TAP236N10, AZR638N10, TDF354S10, SMO514S10, UUM244N10, UTA439N10

** CSIRO flask network: AIA999930, ALT482N30, CFA519S30, CGR540S30, EPC449N30, MQA554S30, MLO519N30, MAA767N30, SIS660N30, SPO789S30

### 3. Methane ($CH_4$)

There is no Reference Standard for methane designated in the framework of the GAW programme [*Aoki et al.*, 1992; *Dlugokencky et al.*, 1994; *Prinn et al.*, 2000]. The GAW programmes have established two World Calibration Centres (WCCs) for methane: the Swiss Federal Laboratory for Materials Testing and Research (EMPA), Dübendorf, Switzerland and the Japan Meteorological Agency (JMA), Tokyo, Japan [*WMO*, 2001].

Many laboratories maintain their own set of standard gases and perform intercomparisons of the concentrations with other laboratories bilaterally or multilaterally. To improve traceability of methane data measured in different laboratories, several organizations have taken the initiative in calibrating standard gases and organising intercomparison experiments; for example, the CMDL offers calibration, the JMA organizes Round Robin experiments mainly among Asian countries, and EMPA visits GAW Global Stations to audit measurement equipment.

Table 4 summarizes the status of methane standard scales at the laboratories contributing to the WDCGG and lists multiplying conversion factors applied for the analysis in the present issue of *Data Summary* to make the data on different scales more intercomparable on an interim basis pending the designation of the GAW Reference Standard for methane. The CMDL scale is lower than an absolute gravimetric scale [*Aoki et al.*, 1992] by ~1.5% [*Dlugokencky et al.*, 1994] and lower than the AES (MSC) scale by a factor of 1.0151 [*Worthy et al.*, 1998]. The CSIRO scale can be converted to the Tohoku University standard by multiplying by 1.01069 [*Prinn et al.*, 1999].

**Table 4. Status of Methane Standard Scales at Laboratories Contributing to the WDCGG with Conversion Factors Used in the Present Issue of *Data Summary*.**

| Laboratory | WDCGG Site Index | Calibration Scale | Conversion Factor |
|---|---|---|---|
| AGAGE | CGR540SX, MAT514SX, CME445NX, MCH653NX, RGP413NX, TRH441N0 | Tohoku | 1* |
| CESI | PLR645N00 | CMDL | 1.0151 |
| CHMI | KOS649N0 | NIST | 1* |
| CMDL | BRW471N0, MLO519N0, CMDL flask network** | CMDL | 1.0151 |
| CSIRO | CSIRO flask network*** | CSIRO 94 | 1.0119 |

| | | | |
|---|---|---|---|
| ENEA | LMP635N0 | ENEA | 1* |
| INM | IZA128N0 | CMDL | 1.0151 |
| JMA | MNM224N0, RYO239N0, YON224N0, RYF99990, RYF9999A | JMA | 1* |
| METRI/SNU | KSN233N0 | CMDL | 1.0151 |
| MRI | EOM99990, INS9999A, MRI9999A, TKB236N0 | MRI | 1* |
| NIES | COI243N0, HAT224N0 | NIES | 1* |
| RIVM | KMW653N0 | NIST | 1* |
| SAWS | CPO134S0 | CMDL | 1.0151 |
| Tohoku Univ. | MZH770S0, GRL666N0 | Tohoku | 1* |
| UBA | ZGP647N0 | CMDL | 1.0151 |

* In analysis for *Data Summary*, no conversion is applied because the differences in scales among these laboratories are considered to be negligible.

** CMDL flask network: ALT482N10, AMS137S10, ASC107S10, ASK123N10, BAL655N10, BRW471N10, SGI354S10, BSC644N10, CGO540S10, KUM519N10, CHR501N10, CBA455N10, CRZ146S10, GOZ636N10, EIC329S10, ITN435N10, GMI513N10, HBA775S10, HUN646N10, ICE663N10, KEY425N10, MHD653N10, SEY104S10, MLO519N10, MBC476N10, WLG236N10, NWR440N10, ZEP678N10, STM666N10, POC9XXX10, PSA764S10, LEF445N10, RPB413N10, MID528N10, WIS631N10, SHM452N10, SCS9XXX10, SPO789S10, BMW432N10, AVI417N10, BME432N10, SYO769S10, TAP236N10, AZR638N10, TDF354S10, SMO514S10, UUM244N10, UTA439N10, CMO445N10, IZO128N10, KPA432N10, KZD244N10, KZM243N10, MCM777S10, NMB123S10, NZL543S10, OPW448N10, SIO432N10, SUM672N10

*** CSIRO flask network: AIA999930, ALT482N30, CFA519S30, CGR540S30, EPC449N30, MQA554S30, MLO519N30, MAA767N30, SIS660N30, SPO789S30

## 4. Nitrous Oxide ($N_2O$)

The Halocarbons and other Atmospheric Trace Species (HATS) Group of the Climate Monitoring and Diagnostics Laboratory (CMDL), NOAA, USA, maintains a set of standards for $N_2O$ [*Hall et al.*, 2001, *Hall et al.*, 2002]. These standards have been designated as Reference Standards of the GAW programme. The HATS Group analyses the standards of laboratories, including the Meteorological Service of Canada (MSC) and the Australian Commonwealth Scientific and Industrial Research Organisation (CSIRO). The Fraunhofer Institut für Atmosphärische Umweltforschung (IFU) in Garmisch-Partenkirchen, Germany, serves as the GAW World Calibration Centre (WCC).

The NOAA CMDL $N_2O$ calibration scale agrees to within 0.3% of that predicted using NIST Standard Reference Materials (at 300 and 330 ppb). According to a results of the Nitrous Oxide and Halocarbons Intercalibration Experiment (NOHALICE) implemented under the International Global Atmospheric Chemistry (IGAC) programme, the difference between the scales of AGAGE (SIO-98) and NOAA/CMDL is 1% or less [*Prinn et al.*, 2000].

**Table 5. Status of $N_2O$ Standard Scales at Laboratories Contributing to the WDCGG.**

| Laboratory | WDCGG Site Index | Calibration Scale |
|---|---|---|
| AGAGE | ADR652NA, CGR540SX, MAT514SX, CME445NX, MCH653NX, RGP413NX, TRH441N0 | SIO 1998 |
| CMDL | BRW471NX, MLO519NX, NWR440NX, SPO789SX, SMO514SX | CMDL 2000 |
| ENEA | LMP635N0 | CMDL 2000 |
| JMA | RYO239N0 | JMA |
| KMA | AMY236N0 | |
| METRI | KSN233N0 | SIO |
| MISU | ZEP678N0 | |
| NIES | HAT224N0 | NIES |

## 5. Surface Ozone ($O_3$)

The National Institute of Standards and Technology (NIST) has developed and deployed Standard Reference Photometers (SRPs) in the USA and other countries. The GAW has designated the SRP #2

maintained at NIST as the Reference Standard for the GAW programme. The Swiss Federal Laboratory for Materials Testing and Research (EMPA) maintains NIST SRP #15 as the reference for the activities for the GAW World Calibration Centre for Surface Ozone [*Hofer et al.,* 1998]. The traceability and uncertainty of surface ozone within the GAW network were reported by Klausen *et al.,* (2003). Regional Calibration Centres have been established at the Czech Hydrometeorological Institute (CHMI) in Prague, Czech Republic, and Servicio Meteorológico Nacional (SMN) in Buenos Aires, Argentina [*WMO,* 2001]. The former maintains the SRP #17 directly purchased by NIST.

**Table 6. Status of Surface Ozone Standard Scales at Laboratories Contributing to the WDCGG.**

| Laboratory | WDCGG Site Index | Calibration Scale | Audit EMPA-WCC |
|---|---|---|---|
| AWI/DWD | NMY770S0 | | |
| BMG | (Bukit Kototabang) | WMO (NIST & EMPA) | 1999, 2001 |
| CAMS | (Mt. Waliguan) | WMO (NIST & EMPA) | 2000 |
| CMDL | BRW471N4, ICE663N4, MLO519N4, NWR440N4, RPB413N4, SPO789S4, BME432N4, SUM672N4, SMO514S4 | CMDL | |
| DEFRA | EDM655N0 | | |
| DWD | (Hohenpeissenberg) | WMO (NIST & EMPA) | 1997 |
| EAS | KVK646N0, KVV646N0, ZRN646N0 | | |
| EMPA | (Jungfraujoch) | WMO (NIST & EMPA) | 1999 |
| HKPU | HKG222N0 | | |
| IM | MVH638N0 | | |
| INM | IZA128N0 | WMO (NIST & EMPA) | 1996, 1998, 2000 |
| INMET | (Arembepe) | WMO (NIST & EMPA) | 2001 |
| IVL | VDL664N0 | | |
| JMA | RYO239N0, MNM224N0, YON224N0, SYO769S20 | JMA | |
| JMA/AO | TKB236N3 | | |
| KMD | (Mt. Kenya) | WMO (NIST & EMPA) | 2000, 2002 |
| LHMA | RCV656N0 | | |
| NILU | (Ny Ålesund/Mt. Zeppelin) | WMO (NIST & EMPA) | 1997, 2001 |
| NUI | (Mace Head) | WMO (NIST & EMPA) | 1996, 1998, 2002 |
| ONM | ASK123N0 | | |
| RIVM | KMW653N0 | | |
| SAWS | (Cape Point) | WMO (NIST & EMPA) | 1997, 1998, 2002 |
| SMN | (Ushuaia) | WMO (NIST & EMPA) | 1998 |
| UBA | (Zugspitze) | WMO (NIST & EMPA) | 1996, 1997, 2001 |
| UBA Austria | SNB647N0 | WMO (NIST & EMPA) | 1998 |
| UM | GLH636N0 | | |

## 6. Carbon Monoxide (CO)

The Swiss Federal Laboratory for Materials Testing and Research (EMPA) serves as the World Calibration Centre (WCC) under GAW based on its secondary standards calibrated against the standard at NOAA/CMDL designated as the Reference Standard for GAW.

**Table 7. Status of Carbon Monoxide Standard Scales at Laboratories Contributing to the WDCGG.**

| Laboratory | WDCGG Site Index | Calibration Scale | Audit EMPA-WCC |
|---|---|---|---|
| AGAGE | CGR540SX, MCH653NX | SIO 98 | |
| CAMS | (Mt. Waliguan) | WMO (CMDL & EMPA) | 2000 |
| CHMI | KOS649N0 | Observer | |

| | | | |
|---|---|---|---|
| CMDL | CMDL flask network* | WMO (CMDL & EMPA) | |
| CSIRO | CSIRO flask network** | WMO (CMDL & EMPA) | |
| DWD | HPB647N0 | WMO (CMDL & EMPA) | |
| EMPA | JFJ646N0 | WMO (CMDL & EMPA) | 1999 |
| HKPU | HKG222N0 | Observer | |
| INM | (Izaña) | WMO (CMDL & EMPA) | 2000 |
| JMA | RYO239N0, MNM224N0, YON224N0 | JMA | |
| NILU | (Ny Ålesund/Mt. Zeppelin) | WMO (CMDL & EMPA) | 2001 |
| NUI | (Mace Head) | WMO (CMDL & EMPA) | 1998, 2002 |
| RIVM | KTB653N0, KMW653N0 | National | |
| SAWS | (Cape Point) | WMO (CMDL & EMPA) | 1998, 2002 |
| SMN | (Ushuaia) | WMO (CMDL & EMPA) | 1998 |
| UBA | ZGP647N0 | WMO (CMDL & EMPA) | 2001 |
| UBA Austria | (Sonnblick) | WMO (CMDL & EMPA) | 1998 |

* CMDL flask network: ALT482N10, ASC107S10, ASK123N10, BAL655N10, BRW471N10, BSC644N10, CGO540S10, KUM519N10, CHR501N10, CBA455N10, CRZ146S10, GOZ636N10, EIC329S10, ITN435N10, GMI513N10, HUN646N10, ICE663N10, KEY425N10, MHD653N10, SEY104S10, MLO519N10, MBC476N10, WLG236N10, NWR440N10, ZEP678N10, POC9XXX10, PSA764S10, LEF445N10, RPB413N10, MID528N10, SHM452N10, SCS9XXX10, SPO789S10, BMW432N10, BME432N10, SYO769S10, TAP236N10, AZR638N10, SMO514S10, UUM244N10, UTA439N10, CMO445N10, IZO128N10, KPA432N10, KZD244N10, KZM243N10, MCM777S10, NZL543S10, OPW448N10, SIO432N10

** CSIRO flask network: AIA999930, ALT482N30, CFA519S30, CGR540S30, EPC449N30, MQA554S30, MLO519N30, MAA767N30, SIS660N30, SPO789S30

**Acronyms and Abbreviations:**

| | |
|---|---|
| AES: | Meteorological Service of Canada (formerly Atmospheric Environment Service) |
| Aichi: | Aichi Prefecture, Japan |
| AGAGE: | Advanced Global Atmospheric Gases Experiment |
| AWI: | Alfred Wegener Institute, Germany |
| BMG: | Bureau of Meteorology and Geophysics, Indonesia |
| CAMS: | Chinese Academy of Meteorological Sciences, China |
| CESI: | Italian Electrical Experimental Center, Italy |
| CFR: | Laboratoire des Sciences du Climat et de l'Environnement, CEA-CNRS, France |
| CHMI: | Czech Hydrometeorological Institute, Prague, Czech Republic |
| CMA: | Chinese Academy of Meteorological Sciences, China Meteorological Administration |
| CMDL: | Climate Monitoring and Diagnostics Laboratory, NOAA, USA |
| CNR: | Istituto di Fisica dell'Atmosfera, Consiglio Nazionale delle Ricerche, Italy |
| CSIRO: | Commonwealth Scientific and Industrial Research Organisation, Australia |
| DEFRA: | Department for Environment, Food and Rural Affairs, London, United Kingdom |
| DWD: | Deutscher Wetterdienst, Germany |
| EAS: | Environmental Agency of Slovenia |
| EMPA | Swiss Federal Laboratories for Materials Research and Testing, Dübendorf, Switzerland |
| ENEA: | Italian National Agency for New Technology, Energy and the Environment, Italy |
| HKPU: | Hong Kong Polytechnik University, Hong Kong, China |
| HMS: | Hungarian Meteorological Service, Hungary |
| IFU | Fraunhofer Institut für Atmosphärische Umweltforschung, Garmich-Partenkirchen, Germany |
| IGP: | Instituto Geofísico del Perú |
| IM: | Instituto de Meteorologia, Portugal |
| IMS: | Centro Aeronautico di Montagna, Italian Air Force Meteorological Service, Italy |
| INM: | Instituto Nacional de Meteorología, Spain |
| INMET: | Instituto Nacional de Meteorologia, Brazil |
| IVL: | Swedish Environmental Research Institute, Göteborg, Sweden |
| JMA: | Japan Meteorological Agency, Tokyo, Japan |
| JMA/AO: | Aerological Observatory, Japan Meteorological Agency, Tsukuba, Japan |
| KMA: | Korea Meteorological Administration, Republic of Korea |
| KMD: | Kenya Meteorological Department, Kenya |

| | |
|---|---|
| KSNU: | Kyrgyz State National University, Kyrgyzstan |
| LHMA: | Latvian Hydrometeorological Agency, Latvia |
| LSCE: | Laboratoire des Sciences du Climat et de l'Environnement, CEA-CNRS, France |
| METRI: | Meteorological Research Institute, KMA, Republic of Korea |
| MISU: | Department of Meteorology, Stockholm University, Sweden |
| MGO: | Main Geophysical Observatory, Russian Federation |
| MRI: | Meteorological Research Institute, Japan Meteorological Agency, Japan |
| MSC: | Meteorological Service of Canada |
| NIES: | National Institute for Environmental Studies, Japan |
| NILU: | Norwegian Institute for Air Research, Norway |
| NIMH: | Institutul National de Meteorologie, Hidrologie si Gospodarirea Apelor, Romania |
| NIST | National Institute of Standards and Technology, Gaithersburg MD, USA |
| NIWA: | National Institute of Water and Atmospheric Research, New Zealand |
| NUI: | National University of Ireland, Galway, Ireland |
| ONM: | Office National de la Météorologie, Algeria |
| RIVM: | National Institute of Public Health and the Environment, Bilthoven, Netherlands |
| Saitama: | Saitama Prefecture, Japan |
| SAWS: | South African Weather Service, South Africa |
| Shizuoka: | Shizuoka University, Japan |
| SIO: | Scripps Institution of Oceanography, USA |
| SMN: | Servicio Meteorológico Nacional, Argentina |
| SNU: | Seoul National University, Republic of Korea |
| Tohoku Univ.: | Tohoku University, Japan |
| UBA: | Umweltbundesamt (Federal Environmental Agency), Germany |
| UBA Austria: | Umweltbundesamt (Federal Environmental Agency), Austria |
| UHEI-IUP: | Institut für Umweltphysik, Universität Heidelberg, Germany |
| UM: | University of Malta |
| ZAMG: | Central Institute of Meteorology and Geodynamics, Austria |

**References**


Aoki, S., T. Nakazawa, S. Murayama and S. Kawaguchi, Measurements of atmospheric methane at the Japanese Antarctic station, Syowa, *Tellus, Ser. B, 44*, 273-281, 1992.

CMDL, Climate Monitoring and Diagnostics Laboratory Summary Report No.26 2000-2001, 2002.

Dlugokencky, E. J., L. P. Steele, P. M. Lang, and K. A. Masarie, The growth rate and distribution of atmospheric methane, *J. Geophys. Res., 99*, 17021-17043, 1994.

Hall, B. D. (ed.), J. W. Elkins, J. H. Butler, S. A. Montzka, T. M. Thompson, L. Del Negro, G. S. Dutton, D. F. Hurst, D. B. King, E. S. Kline, L. Lock, D. Mactaggart, D. Mondeel, F. L. Moore, J. D. Nance, E. A. Ray, and P. A. Romashkin, Halocarbons and Other Atmospheric Gases, Section 5 in Climate Monitoring and Diagnostics Laboratory, Summary Report N. 25, 1998-1999, R. S. Schnell, D. B. King, R. M. Rosson (eds.), NOAA-CMDL, Boulder, CO., USA, 2001.

Hall, B. D. (ed.), J. H. Butler, A. D. Clarke, G. S. Dutton, J. W. Elkins, D. F. Hurst, D. B. King, E. S. Kline, J. Lind, L. Lock, D. Mondeel, F. L. Moore, S. A. Montzka, J. D. Nance, E. A. Ray, P. A. Romashkin, and T. M. Thompson, Halocarbons and Other Atmospheric Gases, Section 5 in Climate Monitoring and Diagnostics Laboratory, Summary Report N. 26, 2000-2001, D. B. King, R. C. Schnell, C. Sweet, R. M. Rosson (eds.), NOAA-CMDL, Boulder, CO., USA, 2002.

Hofer, P., B. Buchmann and A. Herzog, Traceability, Uncertainty and Assessment Criteria of Surface Ozone Measurements, *EMPA-WCC Report 98/5*, 20 pp, 1998.

Klausen, J., C. Zellweger, B. Buchmann, and P. Hofer, Uncertainty and bias of surface ozone measurements at selected Global Atmosphere Watch sites, *J. Geophys. Res., 108*(D19), 4622, doi:10.1029/2003JD003710, 2003.

Peterson, J., P. Tans, and D. Kitzis, "$CO_2$ Round-Robin Reference Gas Intercomparison" in Report of the Ninth WMO Meeting of Experts on Carbon Dioxide Concentration and Related Tracer Measurement Techniques, Aspendale, Vic. Australia, 1 - 4 September 1997, edited by R. Francey, WMO/GAW Report No. 132, 1999.

Prinn, R. G., R. Zander, D. M. Cunnold, J. W. Elkins, A. Engel, P. J. Fraser, M. R. Gunson, M. K. W. Ko, E. Mahieu, P. M. Midgley, J. M. Russell III, C. M.

Volk, and R. F. Weiss, Long-lived ozone-related compounds, in Scientific Measurement of Ozone Depletion: 1998, Global Ozone Res. and Monit. Proj. Rep. 44, pp. 1.1-1.54, World Meteorol. Org., Geneva, 1999.

Prinn, R. G., R. F. Weiss, P. J. Fraser, P. G. Simmonds, D. M. Cunnold, F. N. Alyea, S. O'Doherty, P. Salameh, B. R. Miller, J. Huang, R. H. J. Wang, D. E. Hartley, C. Harth, L. P. Steele, G. Sturrock, P. M. Midgley, and A. McCulloch, A history of chemically and radiatively important gases in air deduced from ALE/GAGE/AGAGE, *J. Geophys. Res., 105*, 17751-17792, 2000.

WMO, Strategy for the Implementation of the Global Atmosphere Watch Programme (2001-2007), WMO/GAW Report No. 142, 62pp, 2001.

WMO, Report of the Eleventh WMO/IAEA Meeting of Experts on Carbon Dioxide Concentration and Related Tracer Measurement Techniques, Global Atmosphere Watch Report Series No.148, 2003.

Worthy, D. E. J., I. Levin, N. B. A. Trivett, A. J. Kuhlmann, J. F. Hopper and M. K. Ernst, Seven years of continuous methane observations at a remote boreal site in Ontario, Canada, *J. Geophys. Res., 103,* 15995-16007, 1998.

Zhao, C. L., P. P. Tans, and K. W. Thoning, A high precision manometric system for absolute calibrations of $CO_2$ in dry air, *J. Geophys. Res., 10*2, 5885-5894, 1997.

# LIST OF OBSERVING STATIONS

| Station | Country/Territory | Index Number | Location Latitude (° ') | Location Longitude (° ') | Altitude (m) | Parameter |
|---|---|---|---|---|---|---|
| **REGION I (Africa)** | | | | | | |
| Amsterdam Island | France | AMS137S00 | 37 48 S | 77 32 E | 65 | $CO_2$ |
| Amsterdam Island | France | AMS137S10 | 37 57 S | 77 32 E | 150 | $CO_2$, $CH_4$ |
| Ascension Island | United Kingdom | ASC107S10 | 7 55 S | 14 25 W | 54 | $CO_2$, $CH_4$, CO, $H_2$, $^{13}CO_2$, $C^{18}O_2$ |
| Assekrem | Algeria | ASK123N00 | 23 16 N | 5 38 E | 2710 | $O_3$ |
| Assekrem | Algeria | ASK123N10 | 23 11 N | 5 25 E | 2728 | $CO_2$, $CH_4$, CO, $H_2$, $^{13}CO_2$, $C^{18}O_2$ |
| Cape Point | South Africa | CPO134S00 | 34 21 S | 18 29 E | 230 | $CO_2$, $CH_4$, $O_3$, CO, $N_2O$ |
| Crozet | France | CRZ146S10 | 46 27 S | 51 51 E | 120 | $CO_2$, $CH_4$, CO, $H_2$, $^{13}CO_2$, $C^{18}O_2$ |
| Funchal | Portugal | FUN132N00 | 32 39 N | 16 53 W | 58 | $O_3$ |
| Gobabeb | Namibia | NMB123S10 | 23 35 S | 15 02 E | 408 | $CO_2$, $CH_4$, $^{13}CO_2$ |
| Izaña | Spain | IZA128N00 | 28 18 N | 16 30 W | 2367 | $CO_2$, $CH_4$, $O_3$ |
| Mahe Island | Seychelles | SEY104S10 | 4 40 S | 55 10 E | 3 | $CO_2$, $CH_4$, CO, $H_2$, $^{13}CO_2$, $C^{18}O_2$ |
| Tenerife | Spain | IZO128N10 | 28 18 N | 16 29 W | 2360 | $CO_2$, $CH_4$, CO, $H_2$, $^{13}CO_2$, $C^{18}O_2$ |
| **REGION II (Asia)** | | | | | | |
| Anmyeon-do | Rep. of Korea | AMY236N00 | 36 32 N | 126 19 E | 47 | $CO_2$, $CH_4$, $N_2O$, CFCs |
| Bering Island | Russian Federation | BER255N00 | 55 12 N | 165 59 E | 13 | $CO_2$ |
| Cape Ochi-ishi | Japan | COI243N00 | 43 09 N | 145 30 E | 45 | $CO_2$, $CH_4$ |
| Gosan | Rep. of Korea | KSN233N00 | 33 17 N | 126 10 E | 72 | $CO_2$, $CH_4$, $N_2O$, CFCs |
| Hamamatsu | Japan | HMM234N00 | 34 43 N | 137 43 E | 35 | $CO_2$ |
| Hateruma | Japan | HAT224N00 | 24 03 N | 123 48 E | 10 | $CO_2$, $CH_4$, $N_2O$ |
| Hok Tsui | Hong Kong, China | HKG222N00 | 22 13 N | 114 15 E | 60 | CO, $O_3$ |
| Issyk-Kul | Kyrgyzstan | ISK242N00 | 42 37 N | 76 59 E | 1640 | $CO_2$, $O_3$, $CH_4$ |
| Kaashidhoo | Maldives | KCO204N10 | 4 58 N | 73 28 E | 1 | $CO_2$, $CH_4$, $^{13}CO_2$ |
| Kisai | Japan | KIS236N00 | 36 05 N | 139 33 E | 13 | $CO_2$ |
| Kotelny Island | Russian Federation | KOT276N00 | 76 00 N | 137 52 E | 5 | $CO_2$ |
| Kyzylcha | Uzbekistan | KYZ240N00 | 40 52 N | 66 09 E | 340 | $CO_2$ |
| Memanbetsu | Japan | MMB243N00 | 43 55 N | 144 12 E | 32.9 | $N_2O$ |
| Mikawa-Ichinomiya | Japan | MKW234N00 | 34 51 N | 137 26 E | 50 | $CO_2$ |
| Minamitorishima | Japan | MNM224N00 | 24 18 N | 153 58 E | 8 | $CO_2$, $CH_4$, CO, $O_3$ |
| Mt. Dodaira | Japan | DDR236N00 | 36 00 N | 139 11 E | 840 | $CO_2$ |
| Mt. Waliguan | China | WLG236N00 | 36 17 N | 100 54 E | 3810 | $CO_2$ |
| Mt. Waliguan | China | WLG236N10 | 36 17 N | 100 54 E | 3810 | $CO_2$, $CH_4$, CO, $H_2$, $^{13}CO_2$, $C^{18}O_2$ |
| Nagoya | Japan | NGY235N00 | 35 09 N | 136 58 E | 35 | $N_2O$ |
| Plateau Assy | Kazakhstan | KZM243N10 | 43 15 N | 77 53 E | 2519 | $CO_2$, $CH_4$, CO, $H_2$, $^{13}CO_2$ |
| Ryori | Japan | RYO239N00 | 39 02 N | 141 49 E | 260 | $CO_2$, $CH_4$, $N_2O$, CFCs, $CCl_4$, $CH_3CCl_3$, CO, $O_3$ |
| Sary Taukum | Kazakhstan | KZD244N10 | 44 27 N | 77 34 E | 412 | $CO_2$, $CH_4$, CO, $H_2$, $^{13}CO_2$ |
| Tae-ahn Peninsula | Rep. of Korea | TAP236N10 | 36 44 N | 126 08 E | 20 | $CO_2$, $CH_4$, CO, $H_2$, $^{13}CO_2$, $C^{18}O_2$ |
| Takayama | Japan | TKY236N00 | 36 08 N | 137 25 E | 1420 | $CO_2$ |
| Tsukuba | Japan | TKB236N00 | 36 03 N | 140 08 E | 26 | $CH_4$ |
| Tsukuba | Japan | TKB236N20 | 36 03 N | 140 08 E | 26 | $CO_2$ |
| Tsukuba | Japan | TKB236N30 | 36 03 N | 140 08 E | 25 | $O_3$ |
| Ulaan Uul | Mongolia | UUM244N10 | 44 27 N | 111 06 E | 914 | $CO_2$, $CH_4$, CO, $H_2$, $^{13}CO_2$, $C^{18}O_2$ |
| Urawa | Japan | URW235N00 | 35 52 N | 139 36 E | 10 | $CO_2$ |
| Yonagunijima | Japan | YON224N00 | 24 28 N | 123 01 E | 30 | $CO_2$, $CH_4$, CO, $O_3$ |
| **REGION III (South America)** | | | | | | |
| Arembepe | Brazil | ABP312S00 | 12 46 S | 38 10 W | 0 | |
| Bird Island | United Kingdom | SGI354S10 | 54 00 S | 38 03 W | 30 | $CO_2$, $CH_4$ |
| Easter Island | Chile | EIC329S10 | 27 09 S | 109 27 W | 50 | $CO_2$, $CH_4$, CO, $H_2$, $^{13}CO_2$, $C^{18}O_2$ |

# LIST OF OBSERVING STATIONS (continued)

| Station | Country/Territory | Index Number | Location Latitude (° ') | Location Longitude (° ') | Altitude (m) | Parameter |
|---|---|---|---|---|---|---|
| Huancayo | Peru | HUA312S00 | 12 04 S | 75 32 W | 3313 | $CO_2$ |
| Tierra del Fuego | Argentina | TDF354S10 | 54 52 S | 68 29 W | 20 | $CO_2$, $CH_4$, CO, $H_2$, $^{13}CO_2$, $C^{18}O_2$ |
| Ushuaia | Argentina | USI354S00 | 54 51 S | 68 19 W | 18 | $O_3$, CO |
| **REGION IV (North and Central America)** | | | | | | |
| Alert | Canada | ALT482N00 | 82 27 N | 62 31 W | 210 | $CO_2$ |
| Alert | Canada | ALT482N10 | 82 27 N | 62 31 W | 210 | $CO_2$, $CH_4$, CO, $H_2$, $^{13}CO_2$, $C^{18}O_2$ |
| Alert | Canada | ALT482N20 | 82 27 N | 62 31 W | 210 | CFCs, HCFCs, $CH_3CCl_3$, $C_2Cl_4$, $CH_2Cl_2$, $SF_6$, $N_2O$ |
| Alert | Canada | ALT482N30 | 82 27 N | 62 31 W | 210 | $CO_2$, $CH_4$, CO, $H_2$ |
| Alert | Canada | ALT482NX0 | 82 27 N | 62 31 W | 210 | HFCs |
| Algoma | Canada | ALG447N00 | 47 02 N | 84 23 W | 411 | $O_3$ |
| Barrow | U. S. A. | BRW471N00 | 71 19 N | 156 36 W | 8 | $CO_2$, $CH_4$ |
| Barrow | U. S. A. | BRW471N10 | 71 19 N | 156 36 W | 11 | $CO_2$, $CH_4$, CO, $H_2$, $^{13}CO_2$, $^{13}CH_4$, $C^{18}O_2$ |
| Barrow | U. S. A. | BRW471N20 | 71 19 N | 156 36 W | 8 | CFCs, HCFCs, $CH_3CCl_3$, $C_2Cl_4$, $CH_2Cl_2$, $SF_6$, $N_2O$ |
| Barrow | U. S. A. | BRW471N40 | 71 19 N | 156 36 W | 8 | $O_3$ |
| Barrow | U. S. A. | BRW471NX0 | 71 19 N | 156 36 W | 8 | $N_2O$, CFCs, HFCs, $CCl_4$, $CH_3CCl_3$, $SF_6$, HCFCs |
| Bratt's Lake | Canada | BRA450N00 | 50 12 N | 104 12 W | 588 | $O_3$ |
| Cape Meares | U. S. A. | CME445NX0 | 45 29 N | 123 58 W | 30 | $CH_4$, $N_2O$, CFCs, $CCl_4$, $CH_3CCl_3$ |
| Cape Meares | U. S. A. | CMO445N10 | 45 29 N | 123 58 W | 30 | $CO_2$, $CH_4$, CO, $H_2$, $^{13}CO_2$, $C^{18}O_2$ |
| Cape St. James | Canada | CSJ451N00 | 51 56 N | 131 01 W | 89 | $CO_2$ |
| Chalk River | Canada | CHA446N00 | 46 04 N | 77 24 W | 184 | $O_3$ |
| Chapais | Canada | CPS449N00 | 49 49 N | 74 59 W | 381 | $O_3$ |
| Cold Bay | U. S. A. | CBA455N10 | 55 12 N | 162 43 W | 25 | $CO_2$, $CH_4$, CO, $H_2$, $^{13}CO_2$, $C^{18}O_2$ |
| Egbert | Canada | EGB444N00 | 44 14 N | 79 47 W | 253 | $O_3$ |
| Estevan Point | Canada | EPC449N30 | 49 23 N | 126 32 W | 39 | $CO_2$, $CH_4$, CO, $H_2$ |
| Esther | Canada | EST451N00 | 51 40 N | 110 12 W | 707 | $O_3$ |
| Experimental Lakes Area | Canada | ELA449N00 | 49 40 N | 93 43 W | 369 | $O_3$ |
| Grifton | U. S. A. | ITN435N10 | 35 21 N | 77 23 W | 9 | $CO_2$, $CH_4$, CO, $H_2$, $^{13}CO_2$, $C^{18}O_2$ |
| Grifton | U. S. A. | ITN435N20 | 35 21 N | 77 23 W | 9 | CFCs, $SF_6$, $N_2O$ |
| Harvard Forest | U. S. A. | HFM442N20 | 42 54 N | 72 18 W | 340 | CFCs, HCFCs, $CH_3CCl_3$, $SF_6$, $N_2O$ |
| Harvard Forest | U. S. A. | HFM442NX0 | 42 54 N | 72 18 W | 340 | HFCs |
| Kejimkujik | Canada | KEJ444N00 | 44 26 N | 65 12 W | 127 | $O_3$ |
| Key Biscayne | U. S. A. | KEY425N10 | 25 40 N | 80 12 W | 3 | $CO_2$, $CH_4$, CO, $H_2$, $^{13}CO_2$, $C^{18}O_2$ |
| Kitt Peak | U. S. A. | KPA432N10 | 32 N | 112 W | 2083 | $CH_4$ |
| La Jolla | U. S. A. | SIO432N10 | 32 50 N | 117 16 W | 14 | $CH_4$ |
| La Palma | Cuba | PLM422N00 | 22 45 N | 83 32 W | 47 | $NO_2$ |
| Longwoods | Canada | LON442N00 | 42 53 N | 81 29 W | 239 | $O_3$ |
| Moody | U. S. A. | WKT431N10 | 31 19 N | 97 20 W | 723 | $CH_4$ |
| Mould Bay | Canada | MBC476N10 | 76 15 N | 119 21 W | 58 | $CO_2$, $CH_4$, CO, $H_2$, $^{13}CO_2$, $C^{18}O_2$ |
| Niwot Ridge | U. S. A. | NWR440N10 | 40 03 N | 105 35 W | 3475 | $CO_2$, $CH_4$, CO, $H_2$, $^{13}CO_2$, $^{13}CH_4$, $C^{18}O_2$ |
| Niwot Ridge | U. S. A. | NWR440N20 | 40 03 N | 105 35 W | 3475 | CFCs, HCFCs, HFCs, $CH_3CCl_3$, $C_2Cl_4$, $CH_2Cl_2$, $SF_6$, $N_2O$ |
| Niwot Ridge | U. S. A. | NWR440N40 | 40 02 N | 105 32 W | 3022 | $O_3$ |
| Niwot Ridge | U. S. A. | NWR440NX0 | 40 03 N | 105 35 W | 3475 | $N_2O$, CFCs, HFCs, $CCl_4$, $CH_3CCl_3$, $SF_6$, HCFCs |
| Niwot Ridge (Saddle) | U. S. A. | NTL440N40 | 40 03 N | 105 35 W | 3538 | $O_3$ |

# LIST OF OBSERVING STATIONS (continued)

| Station | Country/Territory | Index Number | Location Latitude (° ') | Location Longitude (° ') | Altitude (m) | Parameter |
|---|---|---|---|---|---|---|
| Niwot Ridge C-1 | U. S. A. | NWC440N20 | 40 00 N | 105 36 W | 3475 | HFCs |
| Olympic Peninsula | U. S. A. | OPW448N10 | 48 15 N | 124 25 W | 488 | $CH_4$, $H_2$ |
| Park Falls | U. S. A. | LEF445N10 | 45 56 N | 90 16 W | 472 | $CO_2$, $CH_4$, CO, $H_2$, $^{13}CO_2$, $C^{18}O_2$ |
| Park Falls | U. S. A. | LEF445N20 | 45 56 N | 90 16 W | 868 | CFCs, $CH_3CCl_3$, HCFCs, $SF_6$, $N_2O$ |
| Park Falls | U. S. A. | LEF445NX0 | 45 56 N | 90 16 W | 868 | HFCs |
| Point Arena | U. S. A. | PTA438N10 | 38 57 N | 123 44 W | 17 | $CO_2$, $CH_4$, $^{13}CO_2$ |
| Ragged Point | Barbados | RGP413NX0 | 13 10 N | 59 26 W | 45 | $CH_4$, $N_2O$, CFCs, $CCl_4$, $CHCl_3$, $CH_3CCl_3$ |
| Ragged Point | Barbados | RPB413N10 | 13 10 N | 59 26 W | 45 | $CO_2$, $CH_4$, CO, $H_2$, $^{13}CO_2$, $C^{18}O_2$ |
| Ragged Point | Barbados | RPB413N40 | 13 10 N | 59 26 W | 45 | $O_3$ |
| Sable Island | Canada | SBL443N00 | 43 56 N | 60 01 W | 5 | $CO_2$ |
| Saturna | Canada | SAT448N00 | 48 47 N | 123 08 W | 178 | $O_3$ |
| Shemya Island | U. S. A. | SHM452N10 | 52 43 N | 174 06 E | 40 | $CO_2$, $CH_4$, CO, $H_2$, $^{13}CO_2$, $C^{18}O_2$ |
| St. Croix | U. S. A. | AVI417N10 | 17 45 N | 64 45 W | 3 | $CO_2$, $CH_4$ |
| St. David's Head | United Kingdom | BME432N10 | 32 22 N | 64 39 W | 30 | $CO_2$, $CH_4$, CO, $H_2$, $^{13}CO_2$, $C^{18}O_2$ |
| Sutton | Canada | SUT445N00 | 45 05 N | 72 41 W | 243 | $O_3$ |
| Trinidad Head | U. S. A. | TRH441N00 | 41 03 N | 124 09 W | 120 | $CH_4$, $N_2O$, CFCs, $CCl_4$, $CHCl_3$, $CH_3CCl_3$ |
| Trinidad Head | U. S. A. | TRH441N10 | 41 03 N | 124 09 W | 120 | $CH_4$ |
| Trinidad Head | U. S. A. | TRH441N20 | 41 03 N | 124 09 W | 120 | CFCs, HCFCs, $SF_6$, $N_2O$, $CH_3CCl_3$ |
| Trinidad Head | U. S. A. | TRH441N40 | 41 03 N | 124 09 W | 120 | $O_3$ |
| Trinidad Head | U. S. A. | TRH441NX0 | 41 03 N | 124 09 W | 120 | HFCs |
| Tudor Hill | Bermuda, United Kingdom | BME432N40 | 32 22 N | 64 39 W | 30 | $O_3$ |
| Tudor Hill | United Kingdom | BMW432N10 | 32 16 N | 64 53 W | 30 | $CO_2$, $CH_4$, CO, $H_2$, $^{13}CO_2$, $C^{18}O_2$ |
| Wendover | U. S. A. | UTA439N10 | 39 54 N | 113 43 W | 1320 | $CO_2$, $CH_4$, CO, $H_2$, $^{13}CO_2$, $C^{18}O_2$ |
| **REGION V (South-West Pacific)** | | | | | | |
| Baring Head | New Zealand | BAR541S00 | 41 25 S | 174 52 E | 85 | $CH_4$, CO, $CO_2$, $N_2O$, $O_3$ |
| Baring Head | New Zealand | BAR541SA0 | 41 25 S | 174 52 E | 85 | CO |
| Bukit Koto Tabang | Indonesia | BKT500S00 | 0 12 S | 100 19 E | 864.5 | $NO_2$, $SO_2$ |
| Cape Ferguson | Australia | CFA519S30 | 19 17 S | 147 03 E | 2 | $CO_2$, $CH_4$, CO, $H_2$ |
| Cape Grim | Australia | CGO540S10 | 40 41 S | 144 41 E | 94 | $CO_2$, $CH_4$, CO, $H_2$, $^{13}CO_2$, $^{13}CH_4$, $C^{18}O_2$ |
| Cape Grim | Australia | CGO540S20 | 40 41 S | 144 41 E | 94 | CFCs, HCFCs, $CH_3CCl_3$, $C_2Cl_4$, $CH_2Cl_2$, $SF_6$, $N_2O$ |
| Cape Grim | Australia | CGO540SX0 | 40 41 S | 144 41 E | 94 | HFCs |
| Cape Grim | Australia | CGR540S00 | 40 41 S | 144 41 E | 94 | $CO_2$ |
| Cape Grim | Australia | CGR540S30 | 40 41 S | 144 41 E | 94 | $CO_2$, $CH_4$, CO, $^{13}CO_2$, $^{13}CH_4$, $H_2$ |
| Cape Grim | Australia | CGR540SX0 | 40 41 S | 144 41 E | 94 | $CH_4$, $N_2O$, CFCs, HFCs, HCFCs, $CCl_4$, $CHCl_3$, $CH_3CCl_3$, CO, $H_2$ |
| Cape Kumukahi | U. S. A. | KUM519N10 | 19 31 N | 154 49 W | 3 | $CO_2$, $CH_4$, CO, $H_2$, $^{13}CO_2$, $C^{18}O_2$ |
| Cape Kumukahi | U. S. A. | KUM519N20 | 19 31 N | 154 49 W | 3 | CFCs, HCFCs, $CH_3CCl_3$, $C_2Cl_4$, $CH_2Cl_2$, $SF_6$, $N_2O$ |
| Cape Kumukahi | U. S. A. | KUM519ND0 | 19 31 N | 154 49 W | 3 | HFCs |
| Cape Matatula | U. S. A. | MAT514SX0 | 14 15 S | 170 34 W | 42 | $CH_4$, $N_2O$, CFCs, $CCl_4$, $CHCl_3$, $CH_3CCl_3$ |
| Cape Matatula | American Samoa, U. S. A. | SMO514S40 | 14 15 S | 170 34 W | 42 | $O_3$ |
| Christmas Island | Kiribati | CHR501N10 | 1 42 N | 157 10 W | 3 | $CO_2$, $CH_4$, CO, $H_2$, $^{13}CO_2$, $C^{18}O_2$ |
| Guam | U. S. A. | GMI513N10 | 13 26 N | 144 47 E | 2 | $CO_2$, $CH_4$, CO, $H_2$, $^{13}CO_2$, $C^{18}O_2$ |

# LIST OF OBSERVING STATIONS (continued)

| Station | Country/Territory | Index Number | Location Latitude (° ') | Location Longitude (° ') | Altitude (m) | Parameter |
|---|---|---|---|---|---|---|
| Jakarta | Indonesia | JKR506S00 | 6 11 S | 106 50 E | 7 | $NO_2$, $SO_2$ |
| Kaitorete Spit | New Zealand | NZL543S10 | 43 50 S | 172 38 E | 3 | $CH_4$ |
| Lauder | New Zealand | LAU545S40 | 45 02 S | 169 40 E | 370 | $O_3$ |
| Macquarie Island | Australia | MQA554S30 | 54 29 S | 158 58 E | 12 | $CO_2$, $CH_4$, CO, $H_2$ |
| Mauna Loa | U. S. A. | MLO519N00 | 19 32 N | 155 35 W | 3397 | $CO_2$, $CH_4$ |
| Mauna Loa | U. S. A. | MLO519N10 | 19 32 N | 155 35 W | 3397 | $CO_2$, $CH_4$, CO, $H_2$, $^{13}CO_2$, $^{13}CH_4$, $C^{18}O_2$ |
| Mauna Loa | U. S. A. | MLO519N20 | 19 32 N | 155 35 W | 3397 | CFCs, HCFCs, HFCs, $CH_3CCl_3$, $C_2Cl_4$, $CH_2Cl_2$, $SF_6$, $N_2O$ |
| Mauna Loa | U. S. A. | MLO519N30 | 19 32 N | 155 35 W | 3397 | $CO_2$, $CH_4$, CO, $H_2$ |
| Mauna Loa | U. S. A. | MLO519N40 | 19 32 N | 155 35 W | 3397 | $O_3$ |
| Mauna Loa | U. S. A. | MLO519NX0 | 19 32 N | 155 35 W | 3397 | $N_2O$, CFCs, HFCs, $CCl_4$, $CH_3CCl_3$, $SF_6$, HCFCs |
| Sand Island | U. S. A. | MID528N10 | 28 13 N | 177 23 W | 4 | $CO_2$, $CH_4$, CO, $H_2$, $^{13}CO_2$, $C^{18}O_2$ |
| Tanah Rata | Malaysia | TAR504N00 | 4 28 N | 101 23 E | 1545 | $O_3$ |
| Tutuila | U. S. A. | SMO514S00 | 14 15 S | 170 34 W | 42 | $CO_2$ |
| Tutuila | U. S. A. | SMO514S10 | 14 14 S | 170 34 W | 42 | $CO_2$, $CH_4$, CO, $H_2$, $^{13}CO_2$, $^{13}CH_4$, $C^{18}O_2$ |
| Tutuila | U. S. A. | SMO514S20 | 14 15 S | 170 34 W | 42 | CFCs, HCFCs, $CH_3CCl_3$, $C_2Cl_4$, $CH_2Cl_2$, $SF_6$, $N_2O$ |
| Tutuila | U. S. A. | SMO514SX0 | 14 15 S | 170 34 W | 42 | $N_2O$, CFCs, HFCs, $CCl_4$, $CH_3CCl_3$, $SF_6$, HCFCs |
| **REGION VI (Europe)** | | | | | | |
| Adrigole | Ireland | ADR652NA0 | 52 N | 10 W | 50 | $N_2O$, CFCs, $CCl_4$, $CH_3CCl_3$ |
| Ähtäri | Finland | AHT662N00 | 62 35 N | 24 12 E | 180 | $NO_2$, $SO_2$, $O_3$ |
| Angra do Heroismo | Portugal | ANG638N00 | 38 40 N | 27 13 W | 74 | $O_3$ |
| Baltic Sea | Poland | BAL655N10 | 55 25 N | 17 04 E | 7 | $CO_2$, $CH_4$, CO, $H_2$, $^{13}CO_2$, $C^{18}O_2$ |
| Beja | Portugal | BEJ638N00 | 38 01 N | 7 52 W | 246 | $O_3$ |
| Black Sea | Romania | BSC644N10 | 44 10 N | 28 41 E | 3 | $CO_2$, $CH_4$, CO, $H_2$, $^{13}CO_2$, $C^{18}O_2$ |
| Bragança | Portugal | BRG641N00 | 41 48 N | 6 44 W | 690 | $SO_2$ |
| Brotjacklriegel | Germany | BRT648N00 | 48 49 N | 13 13 E | 1016 | $CO_2$, $O_3$ |
| Burgas | Bulgaria | BUR642N00 | 42 29 N | 27 29 E | 16 | $NO_2$, $SO_2$ |
| Castelo Branco | Portugal | CAS639N00 | 39 50 N | 7 28 W | 386 | $O_3$ |
| Danki | Russian Federation | DAK654N00 | 54 54 N | 37 48 E | 140 | $O_3$ |
| Deuselbach | Germany | DEU649N00 | 49 46 N | 7 03 E | 480 | $CO_2$, $O_3$, $CH_4$ |
| Dwejra Point | Malta | GOZ636N10 | 36 03 N | 14 11 E | 30 | $CO_2$, $CH_4$, CO, $H_2$, $^{13}CO_2$, $C^{18}O_2$ |
| Eskdalemuir | United Kingdom | EDM655N00 | 55 19 N | 3 12 W | 242 | $O_3$ |
| Fundata | Romania | FDT645N00 | 45 28 N | 25 18 E | 1371 | $NO_2$, $SO_2$ |
| Fundata | Romania | FDT645N20 | 45 28 N | 25 18 E | 1383.5 | $CO_2$, $NO_2$, $O_3$ |
| Giordan Lighthouse | Malta | GLH636N00 | 36 04 N | 14 13 E | 167 | $O_3$, CO |
| Hegyhatsal | Hungary | HUN646N10 | 46 57 N | 16 39 E | 344 | $CO_2$, $CH_4$, CO, $H_2$, $^{13}CO_2$, $C^{18}O_2$ |
| Heimaey | Iceland | ICE663N10 | 63 20 N | 20 17 W | 100 | $CO_2$, $CH_4$, CO, $H_2$, $^{13}CO_2$, $C^{18}O_2$ |
| Heimaey | Iceland | ICE663N40 | 63 24 N | 20 17 W | 100 | $O_3$ |
| Hohe Warte | Austria | HHE648N00 | 48 15 N | 16 22 E | 202 | NO, $NO_2$, $SO_2$ |
| Hohe Warte | Austria | HHE648N20 | 48 15 N | 16 22 E | 202 | NO, $NO_2$, $SO_2$ |
| Hohenpeissenberg | Germany | HPB647N00 | 47 48 N | 11 01 E | 985 | CO, NO, $NO_2$, NOx, NOy, $SO_2$, ROOH, $H_2O_2$, $O_3$, PAN |
| Hohenpeissenberg | Germany | HPB647N20 | 47 48 N | 11 01 E | 985 | VOCs |
| Hohenpeissenberg | Germany | HPB647N50 | 47 48 N | 11 01 E | 985 | $^{222}Rn$ |
| Iskrba | Slovenia | IRB645N00 | 45 34 N | 14 52 E | 520 | $SO_2$, $O_3$ |
| Ivan Sedlo | Bosnia and Herzegovina | IVN643N00 | 43 46 N | 18 02 E | 970 | $NO_2$, $SO_2$ |
| Jarczew | Poland | JCZ651N00 | 51 49 N | 21 59 E | 180 | $NO_2$, $SO_2$ |

# LIST OF OBSERVING STATIONS (continued)

| Station | Country/Territory | Index Number | Location Latitude (° ') | Location Longitude (° ') | Altitude (m) | Parameter |
|---|---|---|---|---|---|---|
| Jungfraujoch | Switzerland | JFJ646N00 | 46 33 N | 7 59 E | 3578 | CO, $O_3$, NO, $NO_2$, NOx, $SO_2$, |
| K-puszta | Hungary | KPS646N00 | 46 58 N | 19 33 E | 125 | $CO_2$, $NO_2$, $SO_2$, $O_3$ |
| Kamenicki Vis | Serbia and Montenegro | KAM643N00 | 43 24 N | 21 57 E | 813 | $NO_2$, $SO_2$ |
| Kloosterburen | Netherlands | KTB653N00 | 53 24 N | 6 25 E | 0 | CO, NO, NOx, $NO_2$, $SO_2$ |
| Kollumerwaard | Netherlands | KMW653N00 | 53 20 N | 6 17 E | 0 | $CO_2$, $CH_4$, CO, NO, NOx, $NO_2$, $SO_2$, $O_3$ |
| Kosetice | Czech Republic | KOS649N00 | 49 35 N | 15 05 E | 534 | $CH_4$, CO, NO, $NO_2$, $SO_2$, $O_3$ |
| Kovk | Slovenia | KVK646N00 | 46 07 N | 15 06 E | 600 | $O_3$ |
| Krvavec | Slovenia | KVV646N00 | 46 18 N | 14 32 E | 1720 | $O_3$ |
| La Cartuja | Spain | CAR637N00 | 37 12 N | 3 36 W | 720 | $NO_2$, $SO_2$ |
| Lampedusa | Italy | LMP635N00 | 35 31 N | 12 38 E | 45 | $CO_2$, $CH_4$, $N_2O$, CFCs |
| Lazaropole | The former Yugoslav Republic of Macedonia | LZP641N00 | 41 32 N | 20 42 E | 1320 | $NO_2$, $SO_2$ |
| Leba | Poland | LEB654N00 | 54 45 N | 17 32 E | 2 | $NO_2$, $SO_2$ |
| Lisboa / Gago Coutinho | Portugal | LIS638N00 | 38 46 N | 9 08 W | 105 | $O_3$ |
| Logroño | Spain | LOG642N00 | 42 27 N | 2 30 W | 370 | $NO_2$, $SO_2$ |
| Mace Head | Ireland | MCH653N20 | 53 20 N | 9 54 W | 25 | CFCs, HCFCs, $CH_3CCl_3$, $SF_6$, $N_2O$ |
| Mace Head | Ireland | MCH653NX0 | 53 20 N | 9 54 W | 25 | $CH_4$, $N_2O$, CFCs, HFCs, HCFCs, $CCl_4$, $CHCl_3$, $CH_3CCl_3$, CO, $H_2$ |
| Mace Head | Ireland | MHD653N10 | 53 20 N | 9 54 W | 25 | $CO_2$, $CH_4$, CO, $H_2$, $^{13}CO_2$, $C^{18}O_2$ |
| Mace Head | Ireland | MHD653N20 | 53 20 N | 9 54 W | 25 | $CO_2$ |
| Mace Head | Ireland | MHD653NX0 | 53 20 N | 9 54 W | 25 | HFCs |
| Mahón | Spain | MHN639N00 | 39 52 N | 4 19 E | 78 | $NO_2$, $SO_2$, $O_3$ |
| Monte Cimone | Italy | CMN644N00 | 44 11 N | 10 42 E | 2165 | $CO_2$, $O_3$ |
| Monte Velho | Portugal | MVH638N00 | 38 05 N | 8 48 W | 43 | $O_3$ |
| Neuglobsow | Germany | NGL653N00 | 53 10 N | 13 02 E | 65 | $CO_2$, $O_3$, $CH_4$ |
| Noia | Spain | NIA642N00 | 42 44 N | 8 55 W | 685 | $NO_2$, $SO_2$, $O_3$ |
| Ny-Alesund | Norway | ZEP678N10 | 78 54 N | 11 53 E | 474 | $CO_2$, $CH_4$, CO, $H_2$, $^{13}CO_2$, $C^{18}O_2$ |
| Ocean Station "C" | U. S. A. | STC654N10 | 54 00 N | 35 00 W | 6 | $CO_2$ |
| Ocean Station "M" | Norway | STM666N10 | 66 00 N | 2 00 E | 7 | $CO_2$, $CH_4$, CO, $H_2$, $^{13}CO_2$, $C^{18}O_2$ |
| Ocean Station Charlie | Russian Federation | STC652N00 | 52 45 N | 35 30 W | 5 | $CO_2$ |
| Oulanka | Finland | OUL666N00 | 66 19 N | 29 24 E | 310 | $NO_2$, $SO_2$, $O_3$ |
| Pallas-Sammaltunturi | Finland | PAL667N00 | 67 58 N | 24 07 E | 565 | $CO_2$, $O_3$ |
| Pallas-Sammaltunturi | Finland | PAL667N10 | 67 58 N | 24 07 E | 565 | $CH_4$ |
| Penhas Douradas | Portugal | PEN640N00 | 40 25 N | 7 33 W | 1380 | $O_3$ |
| Plateau Rosa | Italy | PLR645N00 | 45 56 N | 7 42 E | 3480 | $CO_2$, $CH_4$ |
| Pleven | Bulgaria | PLV643N00 | 43 25 N | 24 36 E | 64 | $NO_2$, $SO_2$ |
| Plovdiv | Bulgaria | PLD642N00 | 42 08 N | 24 45 E | 179 | $NO_2$, $SO_2$ |
| Puszcza Borecka/Diabla Gora | Poland | DIG654N00 | 54 09 N | 22 04 E | 157 | $CO_2$, $NO_2$, $O_3$, $SO_2$ |
| Roquetes | Spain | ROQ640N00 | 40 49 N | 0 29 E | 50 | $NO_2$, $SO_2$, $O_3$ |
| Rucava | Latvia | RCV656N00 | 56 10 N | 21 11 E | 18 | $NO_2$, $SO_2$, $O_3$ |
| San Pablo de los Montes | Spain | SPM639N00 | 39 33 N | 4 21 W | 917 | $NO_2$, $SO_2$, $O_3$ |
| Schauinsland | Germany | SSL647N00 | 47 55 N | 7 55 E | 1205 | $CO_2$, $O_3$, $CH_4$, $N_2O$, $SF_6$ |
| Sede Boker | Israel | WIS631N10 | 31 08 N | 34 53 E | 400 | $CO_2$, $CH_4$, CO, $H_2$, $^{13}CO_2$, $C^{18}O_2$ |
| Semenic | Romania | SEM645N00 | 45 07 N | 21 58 E | 1432 | $NO_2$, $SO_2$ |
| Shepelevo | Russian Federation | SHP659N00 | 59 58 N | 29 07 E | 4 | $O_3$ |
| Shetland | United Kingdom | SIS660N30 | 60 05 N | 1 15 W | 30 | $CO_2$, $CH_4$, CO, $H_2$ |
| Site J | Denmark | GRL666N00 | 66 30 N | 46 12 W | 2030 | $CH_4$ |
| Sniezka | Poland | SNZ650N00 | 50 44 N | 15 44 E | 1603 | $NO_2$, $SO_2$ |
| Sofia | Bulgaria | SOF642N00 | 42 39 N | 23 23 E | 586 | $NO_2$, $SO_2$ |
| Sonnblick | Austria | SNB647N00 | 47 03 N | 12 57 E | 3106 | $CO_2$, $O_3$, CO |
| Stephansplatz | Austria | STP648N00 | 48 13 N | 16 23 E | 171 | NO, $NO_2$, $SO_2$ |

# LIST OF OBSERVING STATIONS (continued)

| Station | Country/Territory | Index Number | Location Latitude (° ') | Location Longitude (° ') | Altitude (m) | Parameter |
|---|---|---|---|---|---|---|
| Stephansplatz | Austria | STP648N20 | 48 13 N | 16 23 E | 171 | NO, $NO_2$, $SO_2$ |
| Stîna de Vale | Romania | STN646N00 | 46 41 N | 22 37 E | 1116 | $NO_2$, $SO_2$ |
| Summit | Denmark | SUM672N10 | 72 35 N | 38 29 W | 3238 | $CH_4$, $CO_2$ |
| Summit | Greenland, Denmark | SUM672N40 | 72 35 N | 38 29 W | 3238 | $O_3$ |
| Suwalki | Poland | SWL654N00 | 54 08 N | 22 57 E | 184 | $NO_2$, $SO_2$ |
| Terceira Island | Portugal | AZR638N10 | 38 46 N | 27 23 W | 40 | $CO_2$, $CH_4$, CO, $H_2$, $^{13}CO_2$, $C^{18}O_2$ |
| Teriberka | Russian Federation | TER669N00 | 69 12 N | 35 06 E | 40 | $CO_2$, $CH_4$ |
| Utö | Finland | UTO659N00 | 59 47 N | 21 22 E | 7 | $NO_2$, $SO_2$, $O_3$ |
| Varna | Bulgaria | VRN643N00 | 43 12 N | 27 55 E | 41 | $NO_2$, $SO_2$ |
| Viana do Castelo | Portugal | VDC641N00 | 41 42 N | 8 48 W | 16 | $SO_2$ |
| Vindeln | Sweden | VDL664N00 | 64 15 N | 19 46 E | 271 | $O_3$ |
| Virolahti | Finland | VIR660N00 | 60 32 N | 27 40 E | 4 | $NO_2$, $SO_2$, $O_3$ |
| Waldhof | Germany | LGB652N00 | 52 48 N | 10 46 E | 74 | $CO_2$, $O_3$ |
| Wank Peak | Germany | WNK647N00 | 47 31 N | 11 09 E | 1780 | $CO_2$, NOx, $SO_2$ |
| Westerland | Germany | WST654N00 | 54 56 N | 8 19 E | 12 | $CO_2$, $O_3$ |
| Zabljak | Serbia and Montenegro | ZBL643N00 | 43 09 N | 19 08 E | 1450 | $NO_2$, $SO_2$ |
| Zavodnje | Slovenia | ZRN646N00 | 46 26 N | 15 00 E | 770 | $O_3$ |
| Zeppelinfjellet | Norway | ZEP678N00 | 78 54 N | 11 53 E | 475 | $CO_2$, $N_2O$, CFCs, $CCl_4$, $CH_3CCl_3$, $O_3$, $SO_2$ |
| Zingst | Germany | ZGT654N00 | 54 26 N | 12 44 E | 1 | $CO_2$, $O_3$, $CH_4$ |
| Zoseni | Latvia | ZSN657N00 | 57 08 N | 25 55 E | 183 | $NO_2$, $SO_2$ |
| Zugspitze | Germany | ZGP647N00 | 47 25 N | 10 59 E | 2960 | $CO_2$, $CH_4$, CO, NO, NOx, NOy, $O_3$ |
| Zugspitze | Germany | ZSP647N00 | 47 25 N | 10 59 E | 2960 | $CO_2$ |
| Zugspitze/Schneefernerhaus | Germany | SFH647NA0 | 47 25 N | 10 59 E | 2656 | $CH_4$, CO, $CO_2$, $N_2O$, NO, $NO_2$, NOy, $O_3$, $SF_6$ |
| Zugspitze/Schneefernerhaus | Germany | SFH647N00 | 47 25 N | 10 59 E | 2656 | $SO_2$ |
| **ANTARCTICA** | | | | | | |
| Arrival Heights | Antarctica / New Zealand | ARH778S00 | 77 48 S | 166 40 E | 184 | $CH_4$, CO, $N_2O$ |
| Arrival Heights | Antarctica / New Zealand | ARH778SA0 | 77 48 S | 166 40 E | 184 | CO |
| Halley Bay | United Kingdom | HBA775S10 | 75 35 S | 26 30 W | 10 | $CO_2$, $CH_4$, CO, $H_2$, $^{13}CO_2$, $C^{18}O_2$ |
| Jubany | Argentina | JBN762S00 | 62 14 S | 58 40 W | 15 | $CO_2$ |
| Mawson | Australia | MAA767S30 | 67 37 S | 62 52 E | 32 | $CO_2$, $CH_4$, CO, $H_2$ |
| McMurdo / Arrival Height | U. S. A. / New Zealand / Antarctica | MCM777S40 | 77 48 S | 166 46 E | 50 | $O_3$ |
| McMurdo Station | U. S. A. | MCM777S10 | 77 50 S | 166 36 E | 11 | $CH_4$ |
| Mizuho | Japan | MZH770S00 | 70 42 S | 44 18 E | 2230 | $CH_4$ |
| Neumayer | Germany | NMY770S00 | 70 39 S | 8 15 W | 42 | $O_3$ |
| Palmer Station | U. S. A. | PSA764S10 | 64 55 S | 64 00 W | 10 | $CO_2$, $CH_4$, CO, $H_2$, $^{13}CO_2$, $C^{18}O_2$ |
| Palmer Station | U. S. A. | PSA764S20 | 64 55 S | 64 00 W | 10 | CFCs, HCFCs, $CH_3CCl_3$, $SF_6$, $N_2O$ |
| Palmer Station | U. S. A. | PSA764SX0 | 64 55 S | 64 00 W | 10 | HFCs |
| South Pole | U. S. A. | SPO789S00 | 89 59 S | 24 48 W | 2810 | $CO_2$ |
| South Pole | U. S. A. | SPO789S10 | 89 59 S | 24 48 W | 2810 | $CO_2$, $CH_4$, CO, $H_2$, $^{13}CO_2$, $^{13}CH_4$, $C^{18}O_2$ |
| South Pole | U. S. A. | SPO789S20 | 89 59 S | 24 48 W | 2810 | CFCs, HCFCs, $CH_3CCl_3$, $C_2Cl_4$, $CH_2Cl_2$, $SF_6$, $N_2O$ |
| South Pole | U. S. A. | SPO789S30 | 89 59 S | 24 48 W | 2810 | $CO_2$, $CH_4$, CO, $H_2$ |
| South Pole | U. S. A. | SPO789S40 | 89 59 S | 24 48 W | 2810 | $O_3$ |

# LIST OF OBSERVING STATIONS (continued)

| Station | Country/Territory | Index Number | Location Latitude (° ') | Location Longitude (° ') | Altitude (m) | Parameter |
|---|---|---|---|---|---|---|
| South Pole | U. S. A. | SPO789SX0 | 89 59 S | 24 48 W | 2810 | $N_2O$, CFCs, HFCs, $CCl_4$, $CH_3CCl_3$, $SF_6$, HCFCs |
| Syowa Station | Japan | SYO769S00 | 69 00 S | 39 35 E | 29 | $CO_2$ |
| Syowa Station | Japan | SYO769S10 | 69 00 S | 39 35 E | 11 | $CO_2$, $CH_4$, CO, $H_2$, $^{13}CO_2$, $C^{18}O_2$ |
| Syowa Station | Japan | SYO769S20 | 69 00 S | 39 35 E | 29 | $O_3$ |
| **MOBILE STATION** | | | | | | |
| Aircraft (over Bass Strait and Cape Grim) | Australia | AIA999930 | | | | $CO_2$, $CH_4$, CO, $H_2$ |
| Akademik Korolev, R/V | U. S. A. | AKD999910 | | | | $CH_4$ |
| Alligator liberty, M/V | Japan | ALG999900 | | | | $CO_2$ |
| Discoverer 1983 & 1984, R/V | U. S. A. | DIS999910 | | | | $CH_4$ |
| Discoverer 1985, R/V | U. S. A. | DSC999910 | | | | $CH_4$ |
| Environmental observation and monitoring project | Japan | EOM999900 | | | | $CO_2$, $CH_4$ |
| HATS Ocean Projects | U. S. A. | HOP9999X0 | | | | HFCs |
| INSTAC-I (International Strato/Tropospheric Air Chemistry Project) | Japan | INS9999A0 | | | | $CO_2$, $CH_4$, $^{13}CO_2$ |
| John Biscoe, R/V | U. S. A. | JBS999910 | | | | $CH_4$ |
| Keifu Maru, R/V | Japan | KEF999900 | | | | $CO_2$ |
| Kofu Maru, R/V | Japan | KOF999900 | | | | $CO_2$ |
| Korolev, R/V | U. S. A. | KOR999910 | | | | $CH_4$ |
| Long Lines Expedition, R/V | U. S. A. | LLE999910 | | | | $CH_4$ |
| Mexico Naval H-02, R/V | U. S. A. | MXN999910 | | | | $CH_4$ |
| MRI Research, 1978-1986, R/V | Japan | MRI9999A0 | | | | $CH_4$ |
| MRI Research, Hakuho Maru, R/V | Japan | HKH999900 | | | | $CO_2$ |
| MRI Research, Kaiyo Maru, R/V | Japan | KIY999900 | | | | $CO_2$ |
| MRI Research, Mirai, R/V | Japan | MMR999900 | | | | $CO_2$ |
| MRI Research, Natushima, R/V | Japan | NTU999900 | | | | $CO_2$ |
| MRI Research, Ryofu Maru, R/V | Japan | RFM999900 | | | | $CO_2$ |
| MRI Research, Wellington Maru, R/V | Japan | WLT999900 | | | | $CO_2$ |
| Oceanographer, R/V | U. S. A. | OCE999910 | | | | $CH_4$ |
| Pacific Ocean | U. S. A. | POC9XXX10 | | | 8 | $CO_2$, $CH_4$, CO, $H_2$, $^{13}CO_2$, $C^{18}O_2$ |
| Polar Star, R/V | U. S. A. | PLS999910 | | | | $CH_4$ |
| Ryofu Maru, R/V | Japan | RYF999900 | | | | $CO_2$, $CH_4$, $N_2O$, CFCs |
| Ryofu Maru, R/V | Japan | RYF9999A0 | | | | $CO_2$, $CH_4$ |
| South China Sea | U. S. A. | SCS9XXX10 | | | 15 | $CO_2$, $CH_4$, CO, $H_2$, $^{13}CO_2$, $C^{18}O_2$ |
| Surveyor, R/V | U. S. A. | SUR999910 | | | | $CH_4$ |
| The Observation of Atmospheric Sulfur Hexafluoride Over Japan | Japan | OAS999900 | | | | $SF_6$ |

# LIST OF CONTRIBUTORS

| Station<br>Country/Territory | Name | Address |
|---|---|---|
| **REGION I (Africa)** | | |
| Assekrem<br>(Algeria) | Mimouni Mohamed | Office National de la Meteorologie<br>POBox 31 Tamanrasset 11000, Algeria |
| Amsterdam Island<br>(France) | M. Ramonet<br>P. Ciais<br>V. Kazan<br>L. Jourd'Heuil<br>S.G. Jennings | LSCE (Laboratoire des Sciences du Climat et de l'Environnement) UMR CEA-CNRS<br>LSCE - CEA Saclay - Orme des Merisiers - Bat.709<br>91191 Gif-sur-Yvette, France |
| Funchal<br>(Portugal) | Antonio Dias Baptista | Instituto de Meteorologia<br>Rua C, Aeroporto<br>1749-077 Lisboa, Portugal |
| Cape Point<br>(South Africa) | Casper Labuschagne<br>Ernst-Günther Brunke<br>and Gerrie Coetzee | South African Weather Service (Climate Division)<br>SAWS, c/o CSIR (Environmentek),<br>P.O. Box 320,<br>Stellenbosch 7599, South Africa. |
| Izaña<br>(Spain) | Ramon Ramos<br>Ramon Juega | Observatorio Atmosferico de Izana,<br>Instituto Nacional de Meteorologia, Spain<br>C/ La Marina, 20, atico<br>Apartado 880<br>38071 Santa Cruz de Tenerife, Spain |
| Izaña<br>(Spain) | Juanma Sancho<br>Ramon Ramos | Observatorio Atmosferico de Izana,<br>Instituto Nacional de Meteorologia, Spain<br>C/ La Marina, 20, atico<br>Apartado 880<br>38071 Santa Cruz de Tenerife, Spain |
| **REGION II (Asia)** | | |
| Mt. Waliguan<br>(China) | Wen Yupu<br>Zhang Xianchun | Chinese Academy of Meteorological Sciences<br>46 Zhongguancun Nandajie, Haidian,<br>Beijing 100081, P.R. of China |
| Hok Tsui<br>(Hong Kong, China) | Ka Se Lam | Department of Civil and Structural Engineering,<br>Hong Kong Polytechnic University<br>Hung Hom, Kowloon, Hong Kong |
| Takayama<br>(Japan) | Shohei Murayama<br>Susumu Yamamoto<br>Nobuko Saigusa and<br>Hiroaki Kondo | Research Institute for Environmental Management Technology<br>National Institute of Advanced Industrial Science and Technology (AIST)<br>AIST Tsukuba West, 16-1 Onogawa, Tsukuba, Ibaraki 305-8569, Japan |
| Tsukuba<br>(Japan) | M. Hirota<br>K. Shibata | Atmospheric Environment and Applied Meteorology Research Department, Meteorological Research Institute<br>1-1, Nagamine,<br>Tsukuba, Ibaraki 305-0052, Japan |

# LIST OF CONTRIBUTORS (continued)

| Station<br>Country/Territory | Name | Address |
|---|---|---|
| Minamitorishima<br>Ryori<br>Yonagunijima<br>(Japan) | Hideyuki SASAKI | Atmospheric Environment Division,<br>Observations Department,<br>Japan Meteorological Agency (JMA)<br>1-3-4 Otemachi, Chiyoda-ku,<br>Tokyo 100-8122, Japan |
| Tsukuba<br>(Japan) | H. Y. Inoue<br>H. Matsueda<br>M. Ishii | Geochemical Research Department, Meteorological Research Institute<br>1-1, Nagamine, Tsukuba,<br>Ibaraki 305-0052, Japan |
| Kisai<br>Mt. Dodaira<br>Urawa<br>(Japan) | Yosuke MUTO | Center for Environmental Science in Saitama<br>914 Kamitanadare, Kisai-machi, Kita-Saitama-gun,<br>Saitama 347-0115, Japan |
| Mikawa-Ichinomiya<br>(Japan) | Seiko Iwata | Aichi Environmental Research Center<br>7-6 Aza-Nagare, Tuji-machi, Kita-ku,<br>Nagoya, Aichi 462-0032, Japan |
| Cape Ochi-ishi<br>Hateruma<br>(Japan) | Hitoshi Mukai<br>Toshinobu Machida<br>Yukihiro Nojiri<br>Yasumi Fujinuma<br>Masayuki Katsumoto | Center for Global Environmental Research,<br>National Institute for Environmental Studies<br>16-2, Onogawa, Tsukuba-shi,<br>Ibaraki, 305-0053, Japan |
| Nagoya<br>(Japan) | K. Kitagawa<br>A. Matsunami | Research Center for Advanced Energy Conversion,<br>Nagoya University<br>Furo-cho, Chikusaku,<br>Nagoya 464-8603, Japan |
| Hamamatsu<br>(Japan) | Mitsuo TODA | Shizuoka University<br>3-5-1 Jyohoku,<br>Hamamatsu 432-8561, Japan |
| Memanbetsu<br>(Japan) | M. Hirota<br>H. Muramatsu | Meteorological Research Institute<br>Nagamine, Tsukuba, Ibaraki 305-0082, Japan |
| | F. Muromatsu<br>M. Hashimoto<br>T. Koike | Memanbetsu Magnetic Observatory<br>Memanbetsu, Hokkaido 099-2356, Japan |
| Tsukuba<br>(Japan) | Tosiro Kimura<br>Eiji Ogura<br>Takeo Ueno<br>Yuuzou Ikeda | Lower Aerological Observations Division, Aerological Observatory,<br>Japan Meteorological Agency (JMA)<br>Lower Aerological Observations Division, Aerological Observatory<br>1-2 Nagamine, Tsukuba, Ibaraki, 305-0052, Japan |
| Issyk-Kul<br>(Kyrgyzstan) | V. Semenov<br>V. Sinyakov<br>L. Sorokina<br>N. Ignatova | Laboratory of Geophysics, Institute of Fundamental sciences at the<br>Kyrgyz National University, Kyrgyzstan<br>Manas Street 101, Bishkek, 720033, Kyrgyz Republic |
| | V. Aref'ev<br>N. Kamenogradsky<br>F. Kashin | Institute of Experimental Meteorology SPA 'Typhoon', Russia<br>Lenin St. 82, Obninsk, Kaluga reg. 249020,<br>Russian Federation |

# LIST OF CONTRIBUTORS (continued)

| Station<br>Country/Territory | Name | Address |
|---|---|---|
| Gosan<br>(Rep. of Korea) | Jae-Cheol Nam<br>So-young Bang<br>Kyung-Ryul Kim<br>Mi-Kyung Park | Applied Meteorology Research Laboratory, Meteorological Research Institute (METRI), Korea Meteorological Administration (KMA)<br>460-18, Shindaebang-dong, Tongjak-gu,<br>Seoul 156-720, Rep. of Korea |
| Anmyeon-do<br>(Rep. of Korea) | Jeong-Sik Kim<br>Ki-Jun Park | Climate Policy Division, Climate Bureau, Korea Meteorology Administration<br>460-18, Shindaebang-dong, Dongjak-gu<br>Seoul 156-720, Republic of Korea |
| Bering Island<br>Kotelny Island<br>(Russian Federation) | A. Shashkov<br>N. Paramonova<br>V. Privalov<br>A. Reshetnikov | Main Geophysical Observatory (MGO)<br>Karbyshev Street 7,<br>St. Petersburg, 194021, Russian Federation |
| Kyzylcha<br>(Uzbekistan) | A. Shashkov<br>N. Paramonova<br>V. Privalov<br>A. Reshetnikov | Main Geophysical Observatory (MGO)<br>Karbyshev Street 7,<br>St. Petersburg, 194021, Russian Federation |
| **REGION III (South America)** | | |
| Ushuaia<br>(Argentina) | Miguel Pereyra<br>Sergio Luppo | Estacion VAG Ushuaia, Servicio Meteorológico Nacional<br>Subsecretaria de Planeamiento<br>Fagnano 486, Planta Alta<br>9410 Ushuaia, Tierra del Fuego, Argentina |
| Arembepe<br>(Brazil) | | |
| Huancayo<br>(Peru) | M. Ishituka | Observatorio de Huancayo, Instituto Geofisico del Peru<br>Apartado 46, Huancayo, Peru |
| **REGION IV (North and Central America)** | | |
| Alert<br>Cape St. James<br>Sable Island<br>(Canada) | V. Hudec<br>C.S. Wong | Meteorological Service of Canada (MSC)<br>4905 Dufferin Street,<br>Downsview, Ontario, Canada, M3H 5T4 |
| Chalk River<br>Chapais<br>Egbert<br>Esther<br>Experimental Lakes Area<br>Kejimkujik<br>Longwoods<br>Saturna<br>Sutton<br>(Canada) | | Environment Canada<br>Meteorological Service of Canada<br>Air Quality Research Branch<br>4905 Dufferin St.<br>Toronto, Ontario<br>CANADA M3H 5T4 |

# LIST OF CONTRIBUTORS (continued)

| Station<br>Country/Territory | Name | Address |
|---|---|---|
| La Palma<br>(Cuba) | Osvaldo Cuesta Santos | Institute of Meteorology,<br>Atmospheric Environment Research Center<br>Apdo. 17032,<br>Postal Code 11700, Havana 17, Cuba |
| Barrow<br>(U. S. A.) | Pieter P. Tans<br>Kirk Thoning<br>Lee Waterman<br>Thomas Mefford | Climate Monitoring and Diagnostics Laboratory (CMDL),<br>National Oceanic and Atmospheric Administration (NOAA)<br>325 Broadway, Boulder, CO 80303-3328, U.S.A. |
| **REGION V (South-West Pacific)** | | |
| Cape Grim<br>(Australia) | Paul Fraser | Commonwealth Scientific and<br>Industrial Research Organization (CSIRO)<br>CSIRO, Division of Atmospheric Research<br>107-121 Station Street,<br>Aspendale, Victoria 3195, Australia<br>Postal adress: PMB 1 Aspendale Vic 3195 |
| Bukit Koto Tabang<br>Jakarta<br>(Indonesia) | Tuti Mulyani | Bureau of Meteorology and Geophysics<br>Jalan Angkasa 1 No.2<br>Jakarta 10720, Indonesia |
| Tanah Rata<br>(Malaysia) | | Malaysian Meteorological Service |
| Baring Head<br>(New Zealand) | M.R. Manning<br>A.J. Gomez<br>G.W. Brailsford<br>S.E. Nichol | National Institute of Water & Atmospheric Research Ltd.<br>301 Evans Bay Parade, Greta Point<br>Private Bag 14-901,<br>Kilbirnie, Wellington, New Zealand |
| Mauna Loa<br>Tutuila<br>(U. S. A.) | Pieter P. Tans<br>Kirk Thoning<br>Lee Waterman<br>Thomas Mefford | Climate Monitoring and Diagnostics Laboratory (CMDL),<br>National Oceanic and Atmospheric Administration (NOAA)<br>325 Broadway, Boulder, CO 80303-3328, U.S.A. |
| **REGION VI (Europe)** | | |
| Hohe Warte<br>Stephansplatz<br>(Austria) | Wolfgang Spangl | Federal Environmental Agency<br>Spittelauer L?de 5<br>A-1090 Wien, Austria<br>wolfgang.spangl@umweltbundesamt.at |
| Sonnblick<br>(Austria) | Wolfgang Spangl | Federal Environment Agency Austria<br>Spittelauer Lande 5,<br>A-1090 Wien, Austria |
| Hohe Warte<br>Stephansplatz<br>(Austria) | Guenther Schermann | Municipal Department 22 - Environmental Protection<br>Air quality subdepartment,<br>City of Vienna<br>Ebendorferstrasse 4,<br>A-1082 Vienna, Austria |

# LIST OF CONTRIBUTORS (continued)

| Station<br>Country/Territory | Name | Address |
|---|---|---|
| Ivan Sedlo<br>(Bosnia and Herzegovina) | Enes Sarac | Meteoroloski zavod Bosne i Hercegovine<br>Bardakcije 12,<br>71000 Sarajevo, Bosnia and Herzegovina |
| Burgas<br>Pleven<br>Plovdiv<br>Sofia<br>Varna<br>(Bulgaria) | N. Valkov<br>E. Batchvarova | National Institute of Meteorology and Hydrology<br>66 Tzarigradsko chaussee,<br>1784 Sofia, Bulgaria |
| Kosetice<br>(Czech Republic ) | Milan Vana | Air Quality Protection Department, Czech Hydrometeorological Institute<br>Czech Hydrometeorological Institute, Kosetice Observatory,<br>394 22 Kosetice, Czech Republic |
| Site J<br>(Denmark) | S. Morimoto<br>G. Hashida | National Institute of Polar Research<br>Kaga 1-9-10, Itabashi-ku, Tokyo 173-8515, Japan |
| | S. Aoki<br>T. Nakazawa | Center for Atmospheric and Oceanic Studies, Graduate School of Science, Tohoku University<br>Sendai 980-8578, Japan |
| Pallas-Sammaltunturi<br>(Finland) | Dr. Tuula Aalto | Finnish Meteorological Institute<br>Sahaajankatu 20 E,<br>FIN-00880 Helsinki, Finland |
| Ähtäri<br>Oulanka<br>Pallas-Sammaltunturi<br>Utö<br>Virolahti<br>(Finland) | Jussi Paatero<br>Yrjö Viisanen | Finnish Meteorological Institute<br>Sahaajankatu 20 E,<br>FIN-00880 Helsinki, Finland |
| Hohenpeissenberg<br>(Germany) | U.Kaminski | Deutscher Wetterdienst (DWD)<br>Meteorologisches Observatorium Hohenpeissenberg<br>Albin-Schwaiger-Weg 10<br>D-82383 Hohenpeissenberg, Germany |
| Hohenpeissenberg<br>Zugspitze/Schneefernerhaus<br>(Germany) | S. Gilge | German Meteorological Service (DWD)<br>Meteorological Observatory Hohenpeissenberg<br>Albin-Schwaiger-Weg 10<br>D-82383 Hohenpeissenberg, Germany |
| Brotjacklriegel<br>Deuselbach<br>Neuglobsow<br>Schauinsland<br>Waldhof<br>Westerland<br>Zingst<br>Zugspitze<br>Zugspitze/Schneefernerhaus<br>(Germany) | R. Graul<br>K. Uhse<br>L. Ries<br>U. Treffert | Federal Environmental Agency<br>(Umweltbundesamt)<br>Federal Environmental Agency<br>Paul-Ehrlich Strasse 29,<br>D-63225 Langen, Germany |

# LIST OF CONTRIBUTORS (continued)

| Station<br>Country/Territory | Name | Address |
|---|---|---|
| Wank Peak<br>Zugspitze<br>(Germany) | H.E. Scheel<br>R. Sladkovic | Fraunhofer-Institute for Atmospheric Environmental Research, since 1.1.2002:<br>Forschungszentrum Karlsruhe, IMK-IFU<br>D-82467 Garmisch-Partenkirchen, Germany |
| Hohenpeissenberg<br>(Germany) | Christian Plass-Duelmer<br>Harald Berresheim | Deutscher Wetterdienst (DWD), Meteorologisches Observatorium Hohenpeissenberg<br>Albin-Schwaiger-Weg 10<br>D-82383 Hohenpeissenberg, Germany |
| K-puszta<br>(Hungary) | L. Horvath | Hungarian Meteorological Service<br>P.O. Box 39<br>H-1675 Budapest, Hungary |
| Mace Head<br>(Ireland) | M. Ramonet<br>P. Ciais<br>V. Kazan<br>L. Jourd'Heuil<br>S.G. Jennings | LSCE (Laboratoire des Sciences du Climat et de l'Environnement) UMR CEA-CNRS<br>LSCE - CEA Saclay - Orme des Merisiers - Bat.709<br>91191 Gif-sur-Yvette, France |
| Monte Cimone<br>(Italy) | Riccardo Santaguida<br>Francesco De Nile<br>Luigi Lauria | Italian Air Force Meteorological Service<br>C.A.M.M. Mt. CIMONE,<br>Via delle Ville 40,<br>41029-Sestola (MO), Italy |
| Lampedusa<br>(Italy) | P. Chamard<br>F. Artuso<br>L. De Silvestri<br>A. di Sarra<br>P. Grigioni<br>F. Monteleone<br>S. Piacentino | Italian National Agency for New Technology, Energy and the Environment (ENEA)<br>ENEA CLIM-OSS Via Anguillarese 301, 00060 S.<br>00060 Maria di Galeria, Rome, Italy |
| Plateau Rosa<br>(Italy) | Claudio Vannini | Italian Electrical Experimental Center (CESI)<br>Via Rubattino, 54,<br>20134 Milano, Italy |
| Monte Cimone<br>(Italy) | Paolo Bonasoni<br>Paolo Cristofanelli | National Research Council, Institute of Atmospheric Sciences and Climate, Mt. Cimone Station<br>Via Gobetti 101<br>40129 Bologna, Italy |
| Rucava<br>Zoseni<br>(Latvia) | Iraida Lyulko | Observation Network Department, Latvian Hydrometeorological Agency, Ministry of Environmental<br>165 Maskavas str.<br>LV-1019, Riga, Latvia |
| Giordan Lighthouse<br>(Malta) | Raymond Ellul<br>Martin Saliba | Atmospheric Research Unit / Physics Department /University of Malta<br>Msida MSD 06, Malta |
| Kloosterburen<br>Kollumerwaard<br>(Netherlands) | J.P. Beck | Air Research Laboratory,<br>National Institute of Public Health and the Environment<br>P.O. Box 1,<br>3720 BA Bilthoven, Netherlands |
| Zeppelinfjellet<br>(Norway) | Johan Strom | The Air Pollution Laboratory (ITMI), Stockholm University<br>SE-106 91 Stokholm, Sweden |

# LIST OF CONTRIBUTORS (continued)

| Station<br>Country/Territory | Name | Address |
|---|---|---|
| Zeppelinfjellet<br>(Norway) | Ove Hermansen | Norwegian Institute for Air Research (NILU)<br>P. O. Box 100 Instituttveien 18,<br>N-2027 Kjeller, Norway |
| Puszcza Borecka/Diabla Gora<br>(Poland) | Institute of Environmental Protection<br>Warsaw | Institute of Environmental Protection<br>Kolektorska 4<br>01-692 Warsaw, Poland |
| Jarczew<br>Leba<br>Sniezka<br>Suwalki<br>(Poland) | prof. dr eng. Henryk Slota | Laboratory of Atmospheric Chemistry, Institute of Meteorology and Water Management (IMWM)<br>Podlesna Street 61,<br>01-673 Warszawa, POLAND |
| Angra do Heroismo<br>Beja<br>Bragança<br>Castelo Branco<br>Lisboa / Gago Coutinho<br>Monte Velho<br>Penhas Douradas<br>Viana do Castelo<br>(Portugal) | Antonio Dias Baptista | Instituto de Meteorologia<br>Rua C, Aeroporto<br>1749-077 Lisboa, Portugal |
| Fundata<br>Semenic<br>Stîna de Vale<br>(Romania) | Daniela ZISU | National Research and Development Institute for Environmental Protection<br>Splaiul Independentei nr. 294, sector 6,<br>77703 Bucuresti Romania |
| Fundata<br>(Romania) | Adriana Nicodim<br>Florin Nicodim | National Meteorological Administration<br>Sos. Bucuresti-Ploiesti nr. 97,<br>71552 Bucharest, Romania |
| Ocean Station Charlie<br>Teriberka<br>(Russian Federation) | A. Shashkov<br>N. Paramonova<br>V. Privalov<br>A. Reshetnikov | Main Geophysical Observatory (MGO)<br>Karbyshev Street 7,<br>St. Petersburg, 194021, Russian Federation |
| Danki<br>Shepelevo<br>(Russian Federation) | | |
| Kamenicki Vis<br>Zabljak<br>(Serbia and Montenegro) | Tanja Vukovic | Republic Hydrometeorological Institute of Serbia<br><br>P. O. Box 604,<br>Bircaninova 6,<br>11001 Beograd, Serbia and Montenegro |
| Iskrba<br>Kovk<br>Krvavec<br>Zavodnje<br>(Slovenia) | Brigita Jesenovec | Ministry of Environment and Spatial Planning<br>Environmental Agency of the Republic of Slovenia (EARS)<br><br>Vojkova 1/b,<br>Sl-1000 Ljubljana, Slovenia |

# LIST OF CONTRIBUTORS (continued)

| Station<br>Country/Territory | Name | Address |
|---|---|---|
| La Cartuja<br>Logroño<br>Mahón<br>Noia<br>Roquetes<br>San Pablo de los Montes<br>(Spain) | J.M. Saenz<br>R.G. Marin | Instituto Nacional de Meteorologia,<br>Ministerio de Medio Ambiente<br>Leonardo Prieto Castro, 8,<br>28071 Madrid, Spain |
| Vindeln<br>(Sweden) | Karin Sjoberg | Swedish Environmental Research Institute (IVL)<br>P.O.Box 47086<br>S-402 58 Goteborg, Sweden |
| Jungfraujoch<br>(Switzerland) | Brigitte Buchmann | EMPA, Swiss Federal Laboratories for Materials Testing and Research<br>Air Pollution / Environmental Technology<br>Uberlandstrasse 129<br>CH-8600 Dubendorf, Switzerland |
| Lazaropole<br>(The former Yugoslav Republic of Macedonia) | Suzana Alcinova Monevska | Hydrometeorological Service<br>Skupi bb, 1000 Skopie,<br>The former Yugoslav Republic of Macedonia |
| Eskdalemuir<br>(United Kingdom) | Peter Kuria | Air and Environment Quality Division, DEFRA<br>4/F15, Ashdown House<br>123 Victoria Street<br>London, SW1E 3DE, United Kingdom |
| **ANTARCTICA** | | |
| Arrival Heights<br>(Antarctica / New Zealand) | M.R. Manning<br>A.J. Gomez<br>G.W. Brailsford<br>S.E. Nichol | National Institute of Water & Atmospheric Research Ltd.<br>301 Evans Bay Parade, Greta Point<br>Private Bag 14-901,<br>Kilbirnie, Wellington, New Zealand |
| Jubany<br>(Argentina) | L. Ciattaglia | Consiglio Nazionale delle Ricerche<br>Istituto di Scienze dell'Atmosfera e del Clima (CNR-ISAC)<br>Area della Ricerca di Roma Tor Vergata<br>via Fosso del Cavaliere, 100, 00133 Rome, Italy |
| | J. Araujo<br>H.Rodriguez | Direccion Nacional del Antartico<br>Instituto Antmgtico Argentino (DNA-IAA)<br>Cerrito 1248, 1010 Buenos Aires, Argentina |
| Neumayer<br>(Germany) | Rolf Weller | Alfred Wegener Institute<br>Am Handelshafen 12, 27570 Bremerhaven, Germany |
| | Uwe Kaminski | Deutscher Wetterdienst, Meteorologisches Observatorium, GAW Global station<br>Albin-Schwaiger-Weg 10, 82383 Hohenpeissenberg, Germany |

# LIST OF CONTRIBUTORS (continued)

| Station<br>Country/Territory | Name | Address |
|---|---|---|
| Syowa Station<br>(Japan) | S. Morimoto<br>G. Hashida | National Institute of Polar Research<br>Kaga 1-9-10, Itabashi-ku, Tokyo 173-8515, Japan |
| | S. Aoki<br>T. Nakazawa | Center for Atmospheric and Oceanic Studies, Graduate School of Science, Tohoku University<br>Sendai 980-8578, Japan |
| Mizuho<br>(Japan) | Takakiyo Nakazawa | Center for Atmospheric and Oceanic Studies, Graduate School of Science, Tohoku University<br>Aoba, Sendai 980-8578, Japan |
| Syowa Station<br>(Japan) | Yasuo Shudou | Office of Antarctic Observations,<br>Japan Meteorological Agency (JMA)<br>1-3-4 Otemachi, Chiyoda-ku,<br>Tokyo 100-8122, Japan |
| South Pole<br>(U. S. A.) | Pieter P. Tans<br>Kirk Thoning<br>Lee Waterman<br>Thomas Mefford | Climate Monitoring and Diagnostics Laboratory (CMDL),<br>National Oceanic and Atmospheric Administration (NOAA)<br>325 Broadway, Boulder, CO 80303-3328, U.S.A. |
| **MOBILE STATION** | | |
| Keifu Maru, R/V<br>Kofu Maru, R/V<br>Ryofu Maru, R/V<br>(Japan) | T. Miyao | Climate and Marine Department, Japan Meteorological Agency<br>1-3-4 Otemachi, Chiyoda-ku, Tokyo 100-8122, Japan |
| | H. Matsueda | Meteorological Research Institute<br>1-1 Nagamine, Tsukuba, Ibaraki 305-0052, Japan |
| | K. Saitou | Kobe Marine Observatory<br>1-4-3 Wakinohama-Kaigandori, Chuo-ku, Kobe 651-0073, Japan |
| MRI Research<br>1978-1986, R/V<br>Hakuho Maru, R/V<br>Kaiyo Maru, R/V<br>Natushima, R/V<br>Ryofu Maru, R/V<br>Wellington Maru, R/V<br>(Japan) | H. Matsueda<br>H. Yoshikawa | Geochemistry Research Department,<br>Meteorological Research Institute<br>Nagamine 1-1, Tsukuba,<br>Ibaraki 305-0052, Japan |
| Alligator liberty, M/V<br>(Japan) | S. Kato | Foundation for Promoting Perspnal Mobility and Ecological Transportation (Eco-Mo Foundation)<br>808, Syuwakioicho-TBR-Building, 5-7, Koujimachi,<br>Chiyodaku, Tokyo 102-0083, Japan |
| | J. Oyama | Pollutants Chemical Analysis Center, Marine Division, Climate and Marine Department,<br>Japan Meteorological Agency (JMA)<br>1-3-4 Otemachi, Chiyoda-ku, Tokyo 100-8122, Japan |

# LIST OF CONTRIBUTORS (continued)

| Station<br>Country/Territory | Name | Address |
|---|---|---|
| Environmental observation and monitoring project INSTAC-I (International Strato/Tropospheric Air Chemistry Project)<br>(Japan) | H. Matsueda<br>H. Yoshikawa<br>M. Ishii | Geochemical Research Department,<br>Meteorological Research Institute<br>Nagamine 1-1, Tsukuba,<br>Ibaraki 305-0052, Japan |
| The Observation of Atmospheric Sulfur Hexafluoride Over Japan<br>(Japan) | M. Hirota<br>H. Muramatsu | Meteorological Research Institute/JMA<br>1-1 Nagamine, Tsukuba,<br>Ibaraki 305-0052, Japan |
| MRI Research Mirai, R/V<br>(Japan) | Masao Ishii | Geochemistry Research Department, Meteorological Research Institute<br>Nagamine 1-1, Tsukuba,<br>Ibaraki 305-0052, Japan |

**NOAA/CMDL Flask Network**

| | | |
|---|---|---|
| Halley Bay<br>(United Kingdom / Antarctica) | T. J. Conway*<br>P. P. Tans*<br>($CO_2$) | (*) Climate Monitoring and Diagnostics Laboratory (CMDL), National Oceanic and Atmospheric Administration (NOAA), 325 Broadway, Boulder, CO 80305, U.S.A. |
| Tierra del Fuego<br>(Argentina) | Edward J. Dlugokencky*<br>Patricia M. Lang*<br>Kenneth A. Masarie* | (**) Institute of Arctic and Alpine Research (INSTAAR), Campus box 450, University of Colorado, Boulder, CO 80309-0450, U.S.A. |
| Cape Grim<br>(Australia) | ($CH_4$) | |
| Ragged Point<br>(Barbados) | Paul C. Novelli*<br>Kenneth A. Masarie*<br>(CO) | |
| Alert<br>Mould Bay<br>(Canada) | Paul C. Novelli*<br>($H_2$) | |
| Easter Island<br>(Chile) | James White**<br>Bruce Vaughn**<br>($^{13}CO_2$ and $C^{18}O_2$) | |
| Mt. Waliguan<br>(China) | John Miller*<br>James White**<br>($^{13}CH_4$) | |
| Summit<br>(Denmark) | | |
| Pallas-Sammaltunturi<br>(Finland) | | |
| Amsterdam Island<br>Crozet<br>(France) | | |
| Hegyhatsal<br>(Hungary) | | |
| Heimaey<br>(Iceland) | | |

# LIST OF CONTRIBUTORS (continued)

| Station<br>Country/Territory | Name | Address |
|---|---|---|
| Mace Head<br>(Ireland) | | |
| Sede Boker<br>(Israel) | | |
| Syowa Station<br>(Japan / Antarctica) | | |
| Plateau Assy<br>Sary Taukum<br>(Kazakhstan) | | |
| Christmas Island<br>(Kiribati) | | |
| Kaashidhoo<br>(Maldives) | | |
| Dwejra Point<br>(Malta) | | |
| Ulaan Uul<br>(Mongolia) | | |
| Gobabeb<br>(Namibia) | | |
| Kaitorete Spit<br>(New Zealand) | | |
| Ny-Alesund<br>Ocean Station "M"<br>(Norway) | | |
| Baltic Sea<br>(Poland) | | |
| Terceira Island<br>(Portugal) | | |
| Tae-ahn Peninsula<br>(Rep. of Korea) | | |
| Black Sea<br>(Romania) | | |
| Mahe Island<br>(Seychelles) | | |
| Tenerife<br>(Spain) | | |
| Akademik Korolev, R/V<br>Barrow<br>Cape Kumukahi<br>Cape Meares | | |

# LIST OF CONTRIBUTORS (continued)

| Station<br>Country/Territory | Name | Address |
|---|---|---|
| Cold Bay<br>Discoverer 1983 & 1984, R/V<br>Discoverer 1985, R/V<br>Grifton<br>Guam<br>John Biscoe, R/V<br>Key Biscayne<br>Kitt Peak<br>Korolev, R/V<br>La Jolla<br>Long Lines Expedition, R/V<br>Mauna Loa<br>Mexico Naval H-02, R/V<br>Moody<br>Niwot Ridge<br>Ocean Station "C"<br>Oceanographer, R/V<br>Olympic Peninsula<br>Pacific Ocean<br>Park Falls<br>Point Arena<br>Polar Star, R/V<br>Sand Island<br>Shemya Island<br>South China Sea<br>St. Croix<br>Surveyor, R/V<br>Trinidad Head<br>Tutuila<br>Wendover<br>(U. S. A.) | | |
| McMurdo Station<br>Palmer Station<br>South Pole<br>(U. S. A. / Antarctica) | | |
| Ascension Island<br>Bird Island<br>St. David's Head<br>Tudor Hill<br>(United Kingdom) | | |
| Assekrem<br>(Algeria) | | |

**NOAA/CMDL/HATS Network**

| | | |
|---|---|---|
| Cape Grim<br>(Australia) | James W. Elkins<br>James H. Butler<br>Thayne M. Thompson | Halocarbons and Other Atmosphere Trace Species Group (HATS)<br>/CMDL/NOAA<br>325 Broadway R/CMDL1 |
| Alert<br>(Canada) | Geoffrey S. Dutton<br>Stephen A. Montzka<br>Bradley D. Hall | Boulder, CO 80305, U.S.A. |
| Mace Head<br>(Ireland) | | |

# LIST OF CONTRIBUTORS (continued)

| Station<br>Country/Territory | Name | Address |
|---|---|---|
| Barrow<br>Cape Kumukahi<br>Grifton<br>Harvard Forest<br>HATS Ocean Projects<br>Mauna Loa<br>Niwot Ridge<br>Niwot Ridge C-1<br>Park Falls<br>Trinidad Head<br>Tutuila<br>(U. S. A.) | | |
| Palmer Station<br>South Pole<br>(U. S. A. / Antarctica) | | |
| **NOAA/CMDL Surface Ozone Network** | | |
| McMurdo / Arrival Height<br>(U. S. A. / New Zealand /<br>Antarctica) | Sam Oltmans | Climate Monitoring and Diagnostics Laboratory (CMDL)/NOAA<br>325 Broadway<br>Boulder, CO 80305-3328, U.S.A. |
| Ragged Point<br>(Barbados) | | |
| Tudor Hill<br>(Bermuda, United Kingdom) | | |
| Summit<br>(Greenland, Denmark) | | |
| Heimaey<br>(Iceland) | | |
| Lauder<br>(New Zealand) | | |
| Barrow<br>Mauna Loa<br>Niwot Ridge<br>Niwot Ridge (Saddle)<br>Trinidad Head<br>(U. S. A.) | | |
| South Pole<br>(U. S. A. / Antarctica) | | |
| Cape Matatula<br>(American Samoa, U. S. A.) | | |

# LIST OF CONTRIBUTORS (continued)

| Station<br>Country/Territory | Name | Address |
|---|---|---|
| **CSIRO Flask Network** | | |
| Aircraft (over Bass Strait and<br>Cape Grim)<br>Cape Ferguson<br>Cape Grim<br>Macquarie Island<br>(Australia) | Paul Steele<br>Paul Krummel<br>Ray Langenfelds<br>Roger Francey | Commonwealth Scientific and<br>Industrial Research Organisation (CSIRO)<br>CSIRO Atmospheric Research<br>107-121 Station Street,<br>Aspendale, Victoria 3195, Australia<br>Postal address: PMB 1, Aspendale, Victoria 3195, Australia |
| Mawson<br>(Australia / Antarctica) | | |
| Alert<br>Estevan Point<br>(Canada) | | |
| Mauna Loa<br>(U. S. A.) | | |
| South Pole<br>(U. S. A. / Antarctica) | | |
| Shetland<br>(United Kingdom) | | |
| **ALE/GAGE/AGAGE Network** | | |
| Cape Grim<br>(Australia)<br><br>Ragged Point<br>(Barbados) | R. Prinn | TEPCO Professor of Atmospheric Chemistry,<br>Director, Center for Global Change Science<br>Head, Dept. of Earth, Atmospheric & Planetary Sciences<br>MIT, Bldg. 54-1312, Cambridge, MA 02139-4307, U.S.A. |
| Adrigole<br>Mace Head<br>(Ireland) | D. Cunnold<br>R. H. J. Wang | School of Earth and Atmospheric Sciences,<br>Georgia Institute of Technology<br>30332-0340 Atlanta, GA, U.S.A. |
| Cape Matatula<br>Cape Meares | P. Fraser<br>L. P. Steele | CSIRO Atmospheric Research,<br>PMB #1 Aspendale Victoria 3195, Australia |
| Trinidad Head<br>(U. S. A.) | R. Weiss<br>P. Salameh | Scripps Institution of Oceanography,<br>University of California,<br>San Diego, La Jolla, California 92093-0244, U.S.A. |
| | P. Simmonds<br>S. O'Poherty | 39 Avon Castle Drive, Ringwood, Hants, BH24 2BB,<br>United Kingdom |

# GLOSSARY

**AGENCIES AND PROGRAMMES:**

| | |
|---|---|
| **AGAGE** | Advanced Global Atmospheric Gases Experiment |
| **ALE** | Atmospheric Lifetime Experiment |
| **AES** | Atmospheric Environment Service (Canada, presently MSC) |
| **CAMS** | Chinese Academy of Meteorological Sciences (China) |
| **CESI** | Italian Electrical Experimental Center (Italy) |
| **CFR** | Centre des Faibles Radioactivites (France) |
| **CHMI** | Czech Hydrometeorological Institute (Czech Republic) |
| **CMA** | China Meteorological Administration (China) |
| **CMDL** | Climate Monitoring and Diagnostics Laboratory (USA/NOAA) |
| **CNR** | Consiglio Nazionale delle Ricerche (Italy) |
| **CNRS** | Centre National de la Recherche Scientifique (France) |
| **CSIRO** | Commonwealth Scientific and Industrial Research Organisation (Australia) |
| **DNA-IAA** | Direccion Nacional del Antartico-Instituto Antartico Argentino (Argentina) |
| **DWD** | Deutscher Wetterdienst (German Meteorological Service, Germany) |
| **EMPA** | Swiss Federal Laboratories for Material Testing and Research (Switzerland) |
| **ENEA** | Italian National Agency for New Technology, Energy and the Environment (Italy) |
| **GAGE** | Global Atmospheric Gases Experiment |
| **GAW** | Global Atmosphere Watch (WMO) |
| **HATS** | Halocarbons and other Atmospheric Trace Species |
| **HMS** | Hungarian Meteorological Service (Hungary) |
| **IFU** | Institute of the Research of the Atmospheric Environment (Germany) |
| **IGP** | Instituto Geofísico del Perú (Peru) |
| **IMS** | Centro Aeronautico di Montagna, Italian Air Force Meteorological Service (Italy) |
| **INM** | Instituto Nacional de Meteorología (Spain) |
| **JMA** | Japan Meteorological Agency (Japan) |
| **KMA** | Korea Meteorological Administration (Republic of Korea) |
| **LSCE** | Laboratoire des Sciences du Climat et de l'Environnement (France) |
| **METRI** | Meteorological Research Institute (Republic of Korea /KMA) |
| **MGO** | Main Geophysical Observatory (Russian Federation) |
| **MISU** | Department of Meteorology, Stockholm University (Sweden) |
| **MRI** | Meteorological Research Institute (Japan/JMA) |
| **MSC** | Meteorological Service of Canada (Canada, formerly AES) |
| **NCEP** | National Centers for Environmental Prediction (USA/NOAA) |
| **NIES** | National Institute for Environmental Studies (Japan) |
| **NILU** | Norwegian Institute for Air Research (Norway) |
| **NIMH** | Institutul National de Meteorologie, Hidrologie si Gospodarirea Apelor (Romania) |
| **NIST** | National Institute of Standards and Technology (USA) |
| **NIWA** | National Institute of Water & Atmospheric Research (New Zealand) |
| **NOAA** | National Oceanic and Atmospheric Administration (USA) |
| **NCEP** | National Centers for Environmental Prediction (USA/NOAA) |
| **RIVM** | National Institute for Health and Environment (Netherlands) |
| **SAWS** | South African Weather Service (South Africa) |
| **SIO** | Scripps Institution of Oceanography, University of California at San Diego (USA) |

| | |
|---|---|
| **UBA** | Umweltbundesamt (Germany) |
| **WDCGG** | World Data Centre for Greenhouse Gases, operated by JMA, Japan (WMO) |
| **WMO** | World Meteorological Organization |
| **ZAMG** | Central Institute of Meteorology and Geodynamics (Austria) |

**ATMOSPHERIC SPECIES:**

| | |
|---|---|
| **$CCl_4$** | tetrachloromethane (carbon tetrachloride) |
| **CFC-11** | chlorofluorocarbon-11 (trichlorofluoromethane, $CCl_3F$) |
| **CFC-12** | chlorofluorocarbon-12 (dichlorodifluoromethane, $CCl_2F_2$) |
| **CFC-113** | chlorofluorocarbon-113 (1,1,2-trichlorotrifluoroethane, $CCl_2FCClF_2$) |
| **CFCs** | chlorofluorocarbons |
| **HCFC-141b** | hydrochlorofluorocarbon-141b (1,1-dichloro-1-fluoroethane, $CH_3CCl_2F$) |
| **HCFC-142b** | hydrochlorofluorocarbon-142b (1,1-difluoro-1-chloroethane, $CH_3CClF_2$) |
| **HCFCs** | hydrochlorofluorocarbons |
| **$CH_4$** | methane |
| **$CH_3CCl_3$** | trichloroethane (methyl chloroform) |
| **CO** | carbon monoxide |
| **$CO_2$** | carbon dioxide |
| **$N_2O$** | nitrous oxide |
| **NO** | nitrogen monoxide |
| **$NO_2$** | nitrogen dioxide |
| **$NO_X$** | nitrogen oxides |
| **$O_3$** | ozone |
| **$SO_2$** | sulphur dioxide |

**UNITS:**

| | |
|---|---|
| **ppb** | parts per billion |
| **ppm** | parts per million |
| **ppt** | parts per trillion |

**Others:**

| | |
|---|---|
| **ENSO** | El Niño-Southern Oscillation |
| **M/V** | merchant vessel |
| **R/V** | research vessel |
| **SOI** | Southern Oscillation Index |
| **SST** | Sea Surface Temperature |

# LIST OF WMO WDCGG PUBLICATIONS

## DATA REPORTING MANUAL:

| | | |
|---|---|---|
| WDCGG No. 1 | January | 1991 |

## WMO WDCGG DATA REPORT:

| | | | (period of data accepted) | | | | |
|---|---|---|---|---|---|---|---|
| WDCGG No. 2 Part A | October | 1992 | October | 1990 | ~ | August | 1992 |
| WDCGG No. 2 Part B | October | 1992 | October | 1990 | ~ | August | 1992 |
| WDCGG No. 3 | October | 1993 | September | 1992 | ~ | March | 1993 |
| WDCGG No. 5 | March | 1994 | April | 1993 | ~ | September | 1993 |
| WDCGG No. 6 | September | 1994 | September | 1993 | ~ | March | 1994 |
| WDCGG No. 7 | March | 1995 | April | 1994 | ~ | December | 1994 |
| WDCGG No. 9 | September | 1995 | January | 1995 | ~ | June | 1995 |
| WDCGG No.10 | March | 1996 | July | 1995 | ~ | December | 1995 |
| WDCGG No.11 | September | 1996 | January | 1996 | ~ | June | 1996 |
| WDCGG No.12 | March | 1997 | July | 1996 | ~ | November | 1996 |
| WDCGG No.14 | September | 1997 | December | 1996 | ~ | June | 1997 |
| WDCGG No.16 | March | 1998 | July | 1997 | ~ | December | 1997 |
| WDCGG No.17 | September | 1998 | January | 1998 | ~ | June | 1998 |
| WDCGG No.18 | March | 1999 | July | 1998 | ~ | December | 1998 |
| WDCGG No.20 | September | 1999 | January | 1999 | ~ | June | 1999 |
| WDCGG No.21 | March | 2000 | July | 1999 | ~ | December | 1999 |
| WDCGG No.23 | September | 2000 | January | 2000 | ~ | June | 2000 |
| WDCGG No.25 | March | 2001 | July | 2000 | ~ | December | 2000 |

## WMO WDCGG DATA CATALOGUE:

| | | |
|---|---|---|
| WDCGG No. 4 | December | 1993 |
| WDCGG No.13 | March | 1997 |
| WDCGG No.19 | March | 1999 |
| WDCGG No.24 | March | 2001 |

## WMO WDCGG DATA SUMMARY:

| | | |
|---|---|---|
| WDCGG No. 8 | October | 1995 |
| WDCGG No.15 | March | 1998 |
| WDCGG No.22 | March | 2000 |
| WDCGG No.26 | March | 2002 |
| WDCGG No.27 | March | 2003 |
| WDCGG No.28 | March | 2004 |
| WDCGG No.29 | March | 2005 |

## WMO WDCGG CD-ROM:

| | | | (period of data accepted) | | | | |
|---|---|---|---|---|---|---|---|
| CD-ROM No. 1 | March | 1995 | October | 1990 | ~ | December | 1994 |
| CD-ROM No. 2 | March | 1996 | October | 1990 | ~ | June | 1995 |
| CD-ROM No. 3 | March | 1997 | October | 1990 | ~ | June | 1996 |
| CD-ROM No. 4 | March | 1998 | October | 1990 | ~ | December | 1997 |
| CD-ROM No. 5 | March | 1999 | October | 1990 | ~ | December | 1998 |
| CD-ROM No. 6 | March | 2000 | October | 1990 | ~ | December | 1999 |
| CD-ROM No. 7 | March | 2001 | October | 1990 | ~ | December | 2000 |
| CD-ROM No. 8 | March | 2002 | October | 1990 | ~ | January | 2002 |
| CD-ROM No. 9 | March | 2003 | October | 1990 | ~ | December | 2002 |
| CD-ROM No.10 | March | 2004 | October | 1990 | ~ | December | 2003 |
| CD-ROM No.11 | March | 2005 | October | 1990 | ~ | December | 2004 |